Decentralized Interference Coordination for the Downlink of Fully Loaded Heterogeneous Wireless Networks

Von der Fakultät Informatik, Elektrotechnik und Informationstechnik
der Universität Stuttgart zur Erlangung der Würde eines
Doktor-Ingenieurs (Dr.-Ing.) genehmigte Abhandlung

Vorgelegt von

Zarah M. L. Bleicher

aus Stuttgart

Hauptberichter:	Prof. Dr.-Ing. J. Speidel
Mitberichter:	Prof. Dr.-Ing. A. Kirstädter
	Prof. Dr.-Ing. S. ten Brink
Tag der mündlichen Prüfung:	30. Juli 2019

Institut für Nachrichtenübertragung der Universität Stuttgart

2019

Acknowledgments

The thesis at hand is part of the outcomes of my research activities as a teaching and research assistant at the Institute of Telecommunications at the University of Stuttgart. First of all, I want to express my sincere gratitude to my advisor, Prof. Dr.-Ing. Joachim Speidel, for giving me the opportunity to work at his institute and pursue many interesting projects with the industry and international research institutes. I greatly appreciate his constant support and guidance even as an emeritus professor despite my long stay in Japan. Moreover, I want to thank him for his guidance in research as well as teaching, he is a perfect inspiring role model.

Also many thanks go to Prof. Dr.-Ing. Stephan ten Brink for providing such an open research and teaching environment, with open and interesting discussions. Further thanks for being the additional second reviewer. Furthermore, I would like to thank Prof. Dr.-Ing. Andreas Kirstädter who agreed on taking over the assessment of my thesis and his helpful advice.

During my work as a researcher at the Institute of Telecommunications I collaborated with the research division of the Deutsche Telekom AG. It was a very valuable collaboration and I want to address my special thanks to Dr.-Ing. Georg Kadel, Heinz Droste, Manfred Rosenberger, Dr.-Ing. Jakob Belschner and Paul Arnold for the numerous fruitful discussions online in our biweekly jour fixe on Wednesdays and face-to-face in Darmstadt, Bonn and Stuttgart. I learned a great deal from it and I am very happy to contribute therein to heterogeneous network deployments in future mobile communication networks.

Further, I want to thank all the colleagues I worked with on my journey towards my PhD. Thanks for the great time we spent together. Thanks for the kicker-time (“Druff”, “Kekse”, etc.), skiing trip, Karaoke nights, ice cream on hot summer days and all the technical but also non-technical discussions. Nabil, Marc, and Xiaojie, thanks a lot for proof-reading and the fruitful discussions, Emna for supervising my Study Thesis and giving me the first impression how working as a researcher looks like. Auch vielen Dank dem gesamten Support-Team. Ihr hattet immer ein offenes Ohr für mich. Thanks also to all my students and to the Flamingos, who contributed in many ways to the success of my research.

Warm thanks to my friends all over the globe for having a great time during school, my university studies and time as a research assistant. You gave me the wonderful work-life balance.

My very special gratitude goes to my parents Gabi und Franz. Thank you for being such great parents. You have always an open eye and ear and give me constant support whenever required. Thanks for always encouraging and supporting me to pursue my interests. There are for sure no words which can express this. Many many thanks to my parents-in-law, Birgit and Wilfried, for being like you are. Supporting me and giving me free time to work. Many thanks also to my sisters and their families for always being there for one another.

Ganz herzlich möchte ich meinen Kindern Maya, Tim und Lara danken. Danke, dass Ihr so tapfer seid, insbesondere in den Zeiten in denen ich sehr eingespannt in meine Arbeit war. Danke, dass Ihr mir die Welt aus Kinderaugen zeigt. Eure Phantasie und Sicht auf die Dinge ist einzigartig und lässt mich Einiges noch mal von einer ganz anderen Seite betrachten. Ihr seid toll. Ich liebe Euch.

Last but most important of all. A million thanks to the most special person in my life, Daniel. Without you, the finalization of this work would have certainly not been possible. Thanks for giving me the free time to write this dissertation and always bringing me back on track whenever necessary. You are the love of my life. Thanks for being exactly how you are.

October 2019
Zarah Maria Lena Bleicher

Contents

Acronyms

4G	4th generation of mobile cellular networks
5G	5th generation of mobile cellular networks
3GPP	third generation partnership project
ABS	almost blank subframe
AI	artificial intelligence
ARQ	automatic repeat request
AWGN	additive white Gaussian noise
BER	bit error rate
BLER	block error rate
BPSK	binary phase shift keying
BS	base station
CA	carrier aggregation
CC	component carrier
CDF	cumulative distribution function
COST	Co-Operative for Scientific and Technical Research
CQI	channel quality indicator
CRC	cyclic redundancy check
CP	cyclic prefix
CSG	closed subscriber group
CSI	channel state information
dc	direct current
DECT	Digital Enhanced Cordless Telecommunications
DL	downlink
DSL	Digital Subscriber Line
eICIC	enhanced inter-cell interference coordination
eNB	evolved NodeB
EPC	evolved packet core
E-UTRAN	evolved UMTS Terrestrial Radio Access, air interface of Long Term Evolution (LTE)
FBS	femto base station
FDD	frequency division duplex
FDM	frequency division multiplexing
FDMA	frequency division multiple access

feICIC	further enhanced inter-cell interference coordination
FFR	fractional frequency reuse
FFT	fast Fourier transform
FIFO	first in first out
FUE	user equipment connected to an FBS
GSM	Global System for Mobile Communications
HARQ	hybrid automatic repeat request
HBS	home base station
HFR	hard frequency reuse
HII	high interference indicator
ICIC	inter-cell interference coordination
IDFT	inverse discrete Fourier transform
IFFT	inverse fast Fourier transform
IFR	incremental frequency reuse
ILP	integer linear problem
IoE	internet of everything
IoT	internet of things
ISI	inter-symbol interference
ITU	International Telecommunication Union
L2S	link-to-system
LBS	low power BS
LDPC	low density parity check
LOS	line of sight
LTE	Long Term Evolution
LTE-A	Long Term Evolution-Advanced
LUE	user equipment connected to an LBS
MAC	medium access control
MBS	macro base station
MCS	modulation and coding scheme
MIESM	mutual information effective SINR mapping
MIMO	multiple input multiple output
MME	mobility management entity
MMSE	minimum mean squared error
NACK	negative acknowledge
NR	New Radio
MS	mobile station
MUE	user equipment connected to an MBS
MU-MIMO	multi user multiple input multiple output
NLOS	non line of sight
OFDM	orthogonal frequency division multiplex
OFDMA	orthogonal frequency division multiple access
OI	overload indicator

OSG	open subscriber group
PBS	pico base station
PFR	partial frequency reuse
PAPR	peak to average power ratio
PC	personal computer
PFS	proportional fair scheduler
PHY	physical layer
PL	path loss
PRB	physical resource block
PUE	user equipment connected to a PBS
QAM	quadrature amplitude modulation
QoS	quality of service
QPSK	quadrature phase-shift keying
RB	resource block
RE	resource element
RF	radio frequency
RLC	radio link control
RN	relay node
RNTP	relative narrowband transmit power
RR	round robin
RRH	remote radio head
RRM	radio resource management
RSS	received signal strength
SCM	spatial channel model
SC-FDMA	single-carrier frequency division multiple access
SDMA	space division multiple access
SFR	soft frequency reuse
SINR	signal-to-interference-plus-noise ratio
SISO	single-input single-output
SNR	signal-to-noise ratio
SU-MIMO	single user multiple input multiple output
TDD	time-division duplex
TTI	transmission time interval
UE	user equipment
UL	uplink
UMTS	Universal Mobile Telecommunications System
UPE	user plane entity
VR	virtual reality
WiFi	Wireless Fidelity
WiMAX	Worldwide Interoperability for Microwave Access
WLAN	Wireless Local Area Network
ZF	zero forcing

Notations And Symbols

z	scalar
$\mathbf{z}$	vector
$\mathbf{Z}$	matrix
$z_{\mu,\nu}$	entry at row μ and column ν of matrix $\mathbf{Z}$
c_0	speed of light
j	imaginary unit, $\mathrm{j} = \sqrt{-1}$
$\mathbb{B}$	set of binary numbers
$\mathbb{C}$	set of complex numbers
$\mathbb{Z}$	set of integer numbers
$.^*$	complex conjugate
$.^H$	Hermitian of a vector or matrix (conjugate transpose)
$.^{-1}$	inverse of a scalar or matrix
$.^T$	transpose of a vector or matrix
$\lvert\cdot\rvert$	absolute value
$\lfloor z \rfloor$	biggest integer smaller or equal to z
$\lvert\cdot\rvert^2$	squared norm
$\mathbb{E}[\cdot]$	expectation operator
$\emptyset$	empty set
ld	logarithm to base 2
log	logarithm to base 10
$\Re\{\cdot\}$	real part
α_{PFS}	fairness factor of the PFS
B_{al}	total allowed bandwidth in a cell
B_{RB}	bandwidth per resource block
B_{R}	bandwidth per resource for ICIC
B_{s}	bandwidth per subband
B_{tot}	total usable bandwidth
$b_{i,n}$	binary number, denotes if resource n is used by cell i or not
β	calibration factor
β_{PFS}	forgetting factor of the PFS

D_i	number of resources allowed for transmission in LBS cell i
d	distance between transmitter and receiver
d_{ISD}	inter-site-distance
F	frequency reuse factor
f	frequency
Δf	subcarrier spacing
f_c	carrier frequency
G_{rx}	receive antenna gain
G_{tx}	transmit antenna gain
γ	SINR
γ_{eff}	effective SINR
γ_{w}	wideband SINR
$\mathbf{H}$	channel matrix
I	interference
$I_{i,n}$	interference value at serving LBS i on resource n
I_{m}	interference margin
I_{b_m}	mutual information function
I_{th}	interference threshold
i	serving LBS
k	discrete time
κ	transmission time interval
L_{iw}	penetration loss of an indoor wall
L_{ow}	penetration loss of an outdoor wall
L_{p}	path loss
λ	wavelength
$M_{\mathrm{BS},\nu}$	number of antennas at BS ν
M_u	number of antennas at MS u
m	index of subcarrier
$\mathcal{M}$	set of scheduled MSs
N_{blocks}	number of blocks
N_{FFT}	size of FFT
N_{HBS}	number of HBSs
$N_{i,\max}$	number of available resources in LBS i
N_n	number of resource units within resource n
N_{MBS}	number of MBSs
N_{P}	number of different resource combinations
N_{RB}	number of resource blocks per total bandwidth
$N_{\mathrm{R,MBS}}$	number of resources exclusive for MBSs
N_{R}	number of subbands or resources in resource pool
N_{s}	number of subbands
N_{sc}	total number of subcarriers
$N_{\mathrm{sc,RB}}$	number of subcarriers per RB

N_{symbols}	number of OFDM symbols per RB
N_{u}	number of useful subcarriers
ν_u	index of serving BS of user u
n	index of resource
$\mathbf{n}$	noise vector
P_{d}	probability for apartment deployed with a femtocell
P_i	probability for switching of resources in LBS i
P_{m}	deviation probability margin for reselection of resources from candidate list
P_{N}	noise power
P_{rx}	receive power
P_{tx}	transmit power
p	frequency block number of (physical) RB
ψ	set of interferers
R_{b}	bit rate
r_n	one element of set of resource units within resource n
$\mathcal{R}_i$	set of resources in femtocell i as a subset of the resource pool
$\mathcal{R}_n$	set of resource units within resource n
$\mathcal{R}_{\text{Pool}}$	resource pool, set contains overall resources
ρ_{FCB}	number of femtocell blocks per MBS
ρ_{HBS}	number of HBSs per MBS
S_{eR}	size of the sum of all resources
$S_{\text{eR,LBS}}$	size of resources available for LBS
S_{R}	size of one resource
$\mathcal{S}$	set with all resource patterns built of all combinations of $\mathcal{R}_{\text{Pool}}$
$\mathfrak{s}$	resource pattern as a subset of $\mathcal{S}$
$\mathfrak{s}_i$	assignment of resource pattern in LBS i as a subset of $\mathcal{S}$
T_{f}	time duration of one frame
T_{g}	time of the guard interval
T_{s}	overall time duration of one OFDM symbol
T_{sf}	time duration of one subframe
T_{slot}	time duration of one slot
T_{su}	basic time unit
T_{u}	useful time of one OFDM symbol
t	time
$U_{i,n}$	utility value for cell i on resource n
u	user or MS u
Υ	throughput
$\mathbf{W}$	equalization matrix
$\mathbf{x}$	transmit signal vector

Abstract

The relentless evolution towards an overwhelming increase of mobile data traffic, where mobile phone subscribers demand the highest data rates and comprehensive coverage presents current and future mobile communication networks with demanding requirements. Previous homogeneous networks were mostly designed to optimize the sum capacity and peak data rates rather than take the individual user experience into account, and therefore failed to meet these requirements. Multi-layer networks, also known as heterogeneous networks, can improve the coverage and capacity of the cellular network and bring the network closer to the user. Moreover, the introduction of the smaller cells into the macro cellular network can improve the performance, especially in hotspots and indoors, which results in a better user experience.

Frequency spectrum is rare and valuable, thus solely adding further bandwidth does not meet the demand. However, when reusing the bandwidth, inter-cell interference from neighboring cells leads to performance degradations, in particular for users located at the cell edges. Within a multi-layer network, additional and even more dynamic interference is present, caused by different kinds of cells, like macro-, pico-, femtocells, and relays. Therefore, addressing the interference issue is essential.

This thesis examines suitable interference coordination algorithms and introduces an advanced interference coordination technique for heterogeneous networks. Whereas current techniques require significant communication between base stations, reduce the available bandwidth notably or do not consider interference between the small cells, the advanced technique is located in the small cells with only marginal information exchange. Its performance is investigated by means of computer simulations for fully loaded heterogeneous networks on the system layer. As a result, the proposed technique reduces the impact on the surrounding cells significantly, making in-home communication services attractive, leading to a tremendous advantage for service providers as well as the end-user.

Kurzfassung

Die Entwicklung hin zu einem überwältigenden Anstieg des mobilen Datenumsatzes ist unaufhaltsam. Dabei stellt der Anspruch mobiler Endnutzer an höchste Datenraten und eine umfassende Netzabdeckung aktuelle und zukünftige mobile Kommunikationsnetzwerke vor massive Herausforderungen. Da bisherige homogene Netzwerke darauf ausgelegt wurden die Gesamtkapazität und die Lastspitzen bestmöglich darzustellen, statt das individuelle Nutzererlebnis zu berücksichtigen, sind sie diesen Herausforderungen nicht gewachsen. Das Frequenzspektrum ist begrenzt und wertvoll und dem steigenden Bedarf an Kapazität kann nicht ausschließlich durch eine größere Bandbreite begegnet werden. Wenn allerdings wie heute üblich Bandbreite mehrfach belegt wird, entstehen speziell an den Randbereichen Interferenzen zwischen Zellen. Dies führt zu massiven Verlusten der Leistungsfähigkeit.

Multi-layer Netzwerke, auch bekannt als heterogene Netzwerke, können die Abdeckung und die Kapazität des Mobilnetzes verbessern und bringen damit das Netz näher an den Nutzer heran. Das Einbinden von kleineren Zellen in das übergeordnete Mobilfunknetz bringt außerdem eine deutliche Steigerung der Leistungsfähigkeit und damit vor allem an Hotspots und innerhalb von Gebäuden ein verbessertes Nutzererlebnis. In Multi-Layer-Netzwerken sind jedoch zusätzliche, sehr dynamische Interferenzen präsent, verursacht durch die unterschiedliche Art der Zellen, wie makro-, piko- oder femto-Zellen oder auch Relaisstationen. Daher ist es notwendig diese Interferenzen wirkungsvoll zu minimieren.

Kern dieser Arbeit ist die Entwicklung und Bewertung eines fortschrittlichen Interferenz-Koordinationsalgorithmus für heterogene Netze und dessen Vergleich mit dem Stand der Technik. Aktuelle Verfahren benötigen signifikanten Datenaustausch zwischen Basisstationen, schränken die nutzbare Bandbreite merkbar ein oder lassen die Interferenzen zwischen den kleinen Zellen außer Acht. Der vorgeschlagene Koordinationsalgorithmus muss im Gegensatz hierzu lediglich initialisiert werden, benötigt somit nur minimale Kommunikation mit dem Kernnetz und führt zu deutlich reduzierten Interferenzen auf beiden Layern. Die Makrozellen bleiben unangetastet, da dieser Koordinationsalgorithmus ausschließlich innerhalb der kleinen Zellen ausgeführt wird. Die Leistungsfähigkeit der fortschrittlichen Technik wird anhand von umfassenden Computersimulationen innerhalb heterogener Netzwerke auf der Systemebene nachgewiesen. Das Ergebnis der Simulationen zeigt deutlich, dass der vorgeschlagene Algorithmus den Einfluss der umgebenden Zellen signifikant reduziert, was in-house Kommunikationsdienstleistungen sehr attraktiv macht und dadurch einen enormen Vorteil für Service Provider und Endnutzer bietet.

Chapter 1

Introduction

The worldwide data traffic heads towards a tremendous amount. Cisco forecasts worldwide 1.5 mobile devices per capita and an overall traffic of more than half a zettabyte per year in 2021, where all of them demand to be able to communicate simultaneously all over the world [1]. Following the wireless trend, less desktop personal computers (PCs) with ethernet connection will be used, but notebooks, tablets, smartphones, wearables take over more and more of their tasks. Video conferences and video streaming is present in everyday life, now virtual reality (VR), artificial intelligence (AI), remote appliances as smart homes and autonomous cars drive head towards this trend. Machines and cars, industry robots amongst others become smarter with increased access to data and networks. Internet of Things (IoT), where physical objects are interconnected, and its progression internet of everything (IoE) build out of the cross-linkage of humans, devices, applications, processes, and things linked to each other online in real-time by an intelligent process, gains increasing prominence. Until 2020 more than 28 billion IoT-devices are estimated to be installed [2]. This leads to a world where nearly everything is part of the communication environment [3]. As a result, a huge data amount and demand has to be met by current and future wireless communication systems.

This demand on ever increasing transmission rates leads to a consequent search for new ways to address this. As the bandwidth and also frequency, time, and space processing are limited, the introduction of small cells into a cellular network can be used as a further parameter to enhance the performance of the network allowing frequency reuse.

Data is transmitted over the air interface from the base stations to the mobile terminals and vice versa. The system operators try to achieve a reuse factor of one, which means that the whole available spectrum is used in parallel in each cell. This dense reuse leads to interference especially at the edges of the cells. By introducing a second layer on top of the macro cellular layer, several small cells are placed inside, operating preferably on the same frequency band, not to waste precious resources. Their introduction increases the present interference augmenting the need for interference coordination techniques. Smart cars and part of the users are located outdoor, nevertheless a tremendous part is located inside buildings whereby the concrete of the walls attenuates the signal of outdoor base stations, further

encouraging this demand.

The history of communication dates back even long before the industrial age, where wireless transmission of data is conducted amongst others with the use of smoke signals, torch signals or flashing mirrors. Later these methods have been replaced by a telegraph network, which has been invented by Samuel Morse in 1838 and in a further step by the telephone. At the end of the 19th century Marconi exhibited the first radio transmission to about 29km distance in 1895 [4]. Since then radio transmission is more and more present in everyday live; on the one hand in radio and television broadcasting and on the other hand mobile telephony and data transmission in mobile communication cellular systems starting from 1G based on analog radio technology to 2G Global System for Mobile Communications (GSM) still present nowadays. At present 4th generation of mobile cellular networks (4G) Long Term Evolution-Advanced (LTE-A) is rolled out and 5th generation of mobile cellular networks (5G) gets off the starting blocks.

This work in hand gives a brief overview on the current interference coordination techniques for homogeneous and heterogeneous network deployments, shows their limits and provides the details of an advanced method which is well suited for an heterogeneous network deployment. Even though its analysis within this work uses 4G LTE-Advanced as a framework, it can also be applied within the upcoming 5G standard currently in process of specification by the third generation partnership project (3GPP) with the new air interface denoted as New Radio (NR) and to the best of one's knowledge for future generations of mobile communication networks.

The performance of the proposed technique for interference coordination is investigated within a heterogeneous network based on the selection of beneficial resources. In here, the resources are defined as subbands, a set of resource blocks. Furthermore, the interference coordination algorithm can be applied also to other situations, where interference has to be addressed, as it is not limited to this definition. A resource can be for example also a component carrier in a 5G network, a channel within a Wireless Fidelity (WiFi) network or in space dimension one stream of a multi user multiple input multiple output (MU-MIMO) network. In this regards, it can be adapted also to other homogeneous or heterogeneous network deployments operating in licensed or unlicensed bands.

The remainder of this thesis is organized as follows: Chapter 2 opens up the topic with an overview on background information. Chapter 3 provides the details of the developed advanced dynamic interference coordination technique with simulation results on the convergence behavior. Further results on the overall system performance are given in Chapter 4, followed by a brief conclusion.

The chapters in detail: Chapter 2 gives an overview on wireless communication systems. This comprises the physical layer (PHY) with the channel model, modulation technique as well as the medium access control (MAC) layer including scheduling of resources. Moreover it introduces the concept of heterogeneous networks where in addition to the macro base stations (MBSs) additional small cells are introduced, which provide a powerful concept to

increase data rates by offloading traffic to the smaller base stations, reducing the distances between transmitter and receiver as well as providing better indoor coverage. Section 2.4 outlines the principle of interference coordination, first for homogeneous and in a second step for heterogeneous networks. It provides a study of current interference coordination techniques, classifies them, and shows their limitations.

Chapter 3 proposes an advanced method for dynamic interference coordination located in the small cell. Unlike most of the common techniques, it does not require continuous signaling between the network nodes. Instead, it just relies on a preset configuration together with a minimum of data, which can be shared during set up of a new small cell. The restriction on the resources is limited to a small amount of the bandwidth in the small cell only. The MBSs are even untouched regarding functionality and bandwidth limitations. The improvement of the developed and enhanced simultaneous probabilistic method over the initial sequential deterministic approach is evaluated in terms of its convergence behavior, as well as its applicability to realistic deployment scenarios by means of simulations. The required time to reach a beneficial interference situation depends on the number of small cells in the network. For the sequential deterministic technique it rises sharply when the number of cells is enlarged. Instead, the simultaneous probabilistic method exhibits only a slight increase when the density of small cells in the network is enlarged. In addition, a central global optimizer is introduced. It renders the possibility to validate the near to optimum interference level after convergence of the proposed scheme.

Chapter 4 shows the results of intensive system-level simulations. The performance of the advanced interference coordination technique for different small cell densities is evaluated in terms of the user throughput for indoor and outdoor users connected to the macrocell and femtocell. Hereby, not only the average user throughput, which is commonly addressed, but also the throughput of the users at the edges of the cells, which experience high levels of interference, is taken into account. The investigation of a deployment scenario without interference coordination shows the necessity to take measures to protect users in critical situations. This is especially true for the users of the macrocell that are located indoors. Without countermeasures, their throughput rate can be very low and even no transmission is possible. The results presented within this chapter demonstrate the capability of the proposed technique to encounter critical interference situations, thus making co-channel macro and femto-cell deployments possible and attractive.

Chapter 5 concludes this thesis, summarizes the major achievements, and provides an outlook of possible topics for future research.

Chapter 2

Wireless Communication Systems

Nowadays, wireless communication systems are present everywhere. Their aim is to get data from a transmitter to a receiver wirelessly with the help of a wired backhaul. The cellular network comprises a set of base stations with comprehensive coverage, conducted by the network operators, small cell base stations superimposed by network operators or end users and mobile terminals. As the spectrum is valuable their goal is to apply a close to full usage of the available bandwidth in every cell, so interference is present and has to be addressed. Figure 2.1 depicts an overview of a cellular network with one center cell colored in yellow and one ring in light blue color. Each cell contains three sectors.

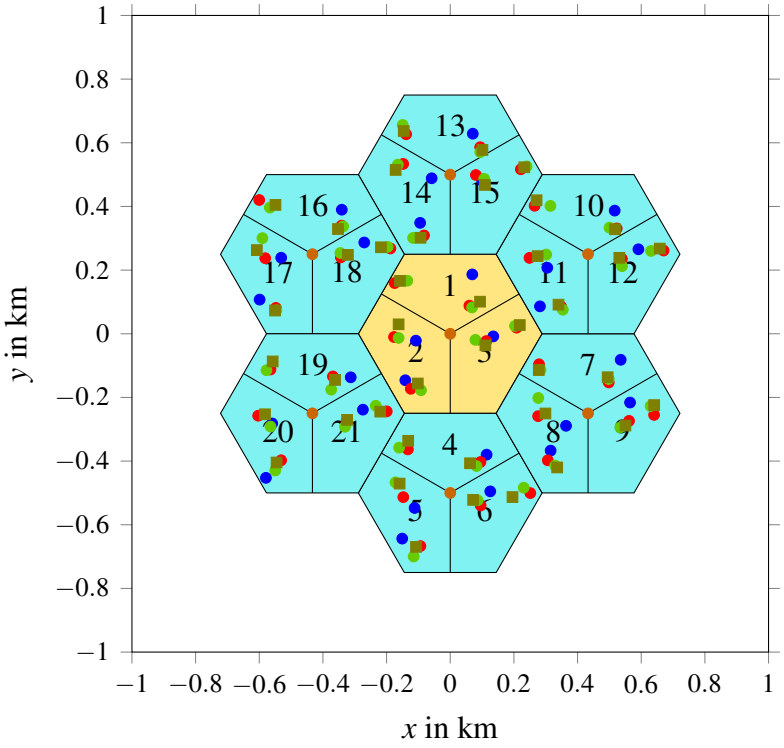

Figure 2.1: Overview on cellular network with macro and femtocells with mobile stations

Every cell consists of three sectors and contains three co-located MBSs in its center. Each MBS supplies one of the sectors. The position of the MBSs is given by an orange circle. The base stations of the femtocell are depicted with a dark green square and the user terminals with circles. Red gives the indoor and blue the outdoor users of the macrocell. The green bullets give the position of the indoor femtocell users.

The presented interference coordination technique is analyzed within a cellular mobile communication environment which operates in licensed spectrum. Anyhow, it could be transferred and integrated also in deployments with overlapping Wireless Local Area Network (WLAN) cells served by WiFi access points. These operate in license free spectrum.

2.1 Fundamentals

Current mobile communication standards as LTE-A in 4G and 5G use binary phase shift keying (BPSK), quadrature phase-shift keying (QPSK), 16-quadrature amplitude modulation (QAM), 64-QAM or even higher modulation techniques up to 1024-QAM [5]. Worldwide Interoperability for Microwave Access (WiMAX) has been treated during the work phase as well as LTE-A which is considered within this thesis. A mobile communication scenario with MBSs superimposed by femto base stations (FBSs) also referred to as home base stations (HBSs) is treated. Orthogonal frequency division multiple access (OFDMA) is used as multiple access technique for the downlink (DL) whereas single-carrier frequency division multiple access (SC-FDMA) is used in uplink (UL). The signal-to-interference-plus-noise ratio (SINR) is an essential quality indicator and is discussed in detail in Subsection 2.4.1. The decision when and where each mobile station (MS) gets data is done in the scheduler implemented in the evolved NodeB (eNB) also referred to as MBS and is based on circular round robin or proportional fair decisions, which is described in Subsubsection 2.2.3.1.

2.1.1 Quadrature Amplitude Modulation

Nowadays QAM is a widely used bandwidth efficient modulation technique using the orthogonality of sine and cosine. Hence two real signals $x_1(t)$, $x_2(t)$, with continuous time t band-limited with $f_{\max}$ can be transmitted in parallel $x(t) = x_1(t) + \mathrm{j}\,x_2(t)$ within the same frequency range in bandpass $f_c - f_{\max}, \ldots, f_c + f_{\max}$ with carrier frequency $f_c = \frac{\omega_c}{2\pi}$. Unlike $X_1(\omega)$, $X_2(\omega)$ the combined signal results in a non-symmetric spectrum $X(\omega)$. The real bandpass signal $u(t) = \sqrt{2}\Re\left\{x(t)\mathrm{e}^{j\omega_c t}\right\}$, with complex envelope $x(t)$ and complex carrier $\mathrm{e}^{j\omega_c t}$, contains the in-phase component $x_{\mathrm{I}}(t) = x_{\mathrm{re}} = x_1(t)$ and quadrature-component $x_{\mathrm{Q}}(t) = x_{\mathrm{im}}(t) = x_2(t)$. For digital transmission one restricts transmission to discrete-time k and discrete-valued symbols s_k. Figure 2.2 shows the constellation diagrams for QAM transmission from four up to 256-QAM, depicted without normalization. For a modulation scheme of four, pairs of bits are grouped and mapped to four complex symbols $s_k = \pm s_{\mathrm{re}} \pm \mathrm{j}\,s_{\mathrm{im}} = \frac{1}{\sqrt{2}}(\pm 1 \pm \mathrm{j})$ depicted in Figure 2.2a without factor $\frac{1}{\sqrt{2}}$. When one goes to

higher modulation schemes more data can be transmitted simultaneously but on the other side the robustness is decreased due to the limited transmission power which results in a tighter constellation grid. As a consequence, more transmission errors can occur.

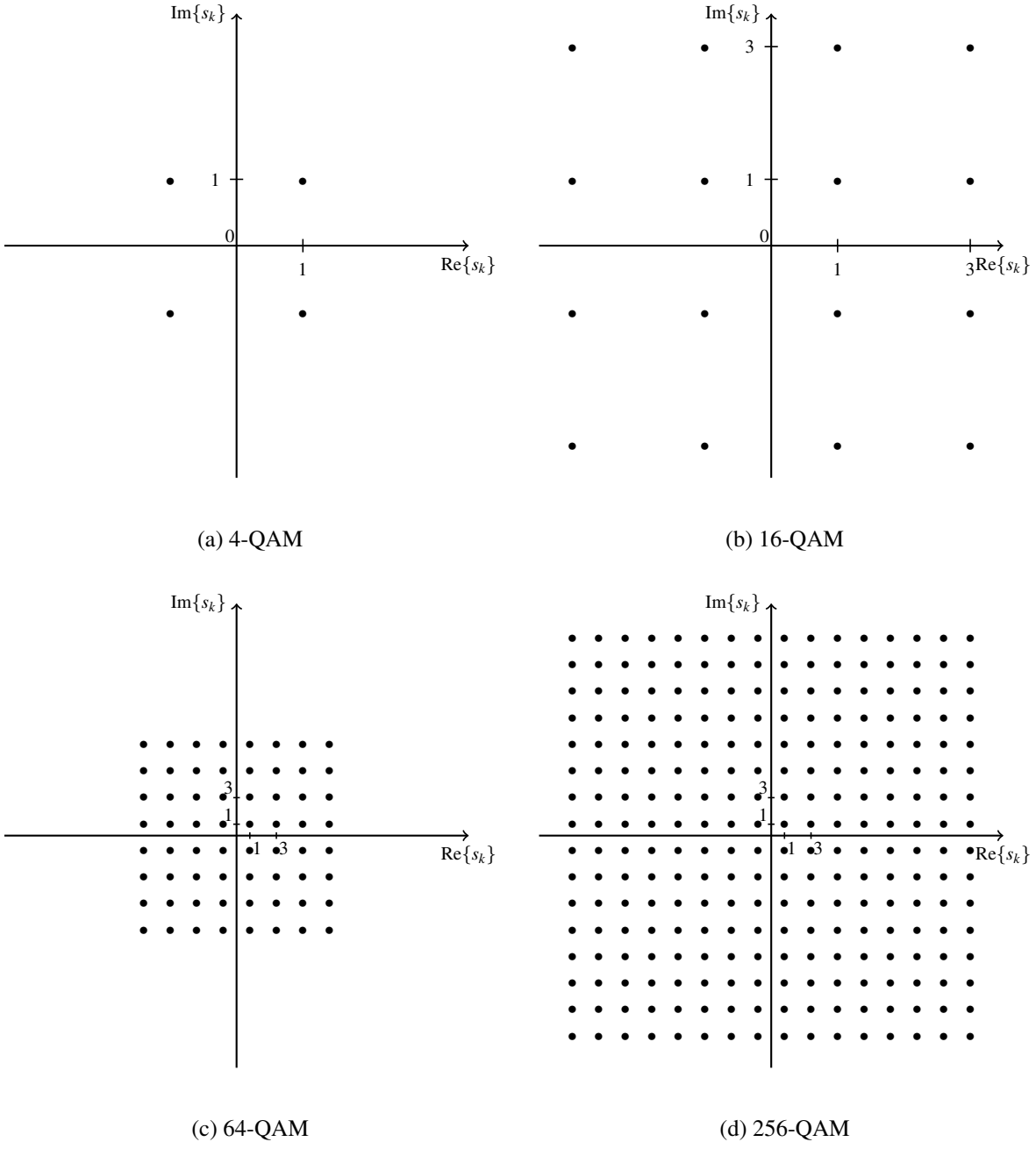

(a) 4-QAM

(b) 16-QAM

(c) 64-QAM

(d) 256-QAM

Figure 2.2: QAM constellation diagrams

2.1.2 Orthogonal Frequency Division Multiplex System

Orthogonal frequency division multiplex (OFDM) is a multi-carrier transmission technique based on frequency division multiplexing (FDM). In order to separate different signals, the

individual subcarriers are orthogonal to each other: To minimize the amount of spectrum used, a tight layout where the maximum of the signal at one subcarrier lies at the first null of the adjacent subcarrier is used. Its implementation is realized with an inverse fast Fourier transform (IFFT) at the transmitter and a fast Fourier transform (FFT) at the receiver. To encounter inter-symbol interference (ISI) due to the channel delay spread a guard interval is added to each OFDM symbol [6] [7]. Figure 2.3 shows one OFDM signal in frequency domain and several OFDM symbols in time domain separated by the guard interval.

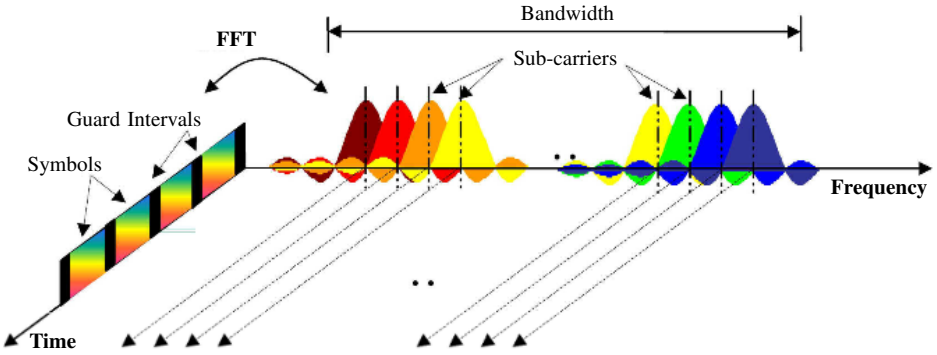

Figure 2.3: Exemplary time-frequency representation of an orthogonal frequency division multiplex signal [7]

Within LTE the guard interval is realized as a cyclic prefix (CP) transmitted prior to each OFDM symbol. The CP used in order to minimize the impact of ISI has to be dimensioned as a trade off between achievable throughput versus robustness. The overall OFDM symbol duration computes to the sum of guard interval time and useful OFDM symbol time as

$$T_\mathrm{s} = T_\mathrm{g} + T_\mathrm{u}. \tag{2.1}$$

Independent QAM symbols from Section 2.1.1 can be transmitted on the orthogonal subcarriers. The discrete OFDM symbol in frequency domain contains N_u useful orthogonal subcarriers. The time domain signal can be gained by using an inverse discrete Fourier transform (IDFT). The complex QAM symbol in subcarrier m and OFDM symbol l is $s_{m,l}$. The direct current (dc) carrier is not used and a guard band on the outer subcarriers is applied.

$$s_{m,l} = \begin{cases} 0 & |m| > \frac{N_\mathrm{u}}{2} \rightarrow \text{guard band} \\ 0 & m = 0 \rightarrow \text{dc-carrier} \\ \text{QAM symbol} & \text{else} \rightarrow \text{used subcarrier} \end{cases} \tag{2.2}$$

The OFDM symbol in frequency domain can be transformed to time-domain with the IFFT,

$$x_l(k) = \frac{1}{\sqrt{N_\mathrm{FFT}}} \sum_{m=-N_\mathrm{FFT}/2}^{N_\mathrm{FFT}/2-1} s_{m,l} \cdot \mathrm{e}^{\mathrm{j}2\pi \frac{m \cdot k}{N_\mathrm{FFT}}} = \frac{1}{\sqrt{N_\mathrm{FFT}}} \sum_{m=-N_\mathrm{u}/2}^{N_\mathrm{u}/2} s_{m,l} \cdot \mathrm{e}^{\mathrm{j}2\pi \frac{m \cdot k}{N_\mathrm{FFT}}}, \tag{2.3}$$

with the discrete time k, and whereas the size of the FFT N_{FFT} has to be selected larger than the number of useable subcarriers N_{u} . More details on the FFT size and the number of used subcarriers for the available bandwidths within an OFDM based system as LTE-A are given in Table 2.1 of Section 2.2.2.1. The subcarriers are spaced by $\Delta f = \frac{1}{T_{\mathrm{u}}}$. This leads to a brickstone-like spectrum with adjacent subcarriers at discrete frequencies $f_m = m \cdot \Delta f$. Each subcarrier, which can be individually chosen to the present radio channel, occupies only a small bandwidth resulting in a long OFDM symbol duration $T_{\mathrm{u}} = N_{\mathrm{sc}} T_{\mathrm{singlecarrier}}$ when the same coded data rate R_{b} is maintained. $T_{\mathrm{singlecarrier}}$ gives the time for a corresponding single carrier transmission and N_{sc} the total number of subcarriers. By modulation with radio frequency carrier $\mathrm{e}^{\mathrm{j}2\pi f_c t}$, the baseband signal is shifted to the desired carrier frequency f_c.

2.1.3 Channel Model

The wireless channel is a challenging medium. It changes with time and frequency when users or the surroundings move and is affected by interference, fading, and noise. In order to design and evaluate mobile communication systems in terms of the key performance indicators (KPIs), a realistic model is crucial. Therefore, the investigation of the propagation characteristics of a mobile communication channel for the small- and large-scale fading characteristic as well as the study of the path loss is relevant [4]. The free space model derived from Friis-transmission equation [8] gives the ratio between transmit power P_{tx} and receive power P_{rx} as

$$P_{\mathrm{rx}} = P_{\mathrm{tx}} G_{\mathrm{tx}} G_{\mathrm{rx}} \left(\frac{\lambda}{4\pi d} \right)^2, \tag{2.4}$$

with the transmit and receive antenna gain G_{tx} and G_{rx}, respectively, path loss exponent 2, distance between transmitter and receiver d, and wavelength $\lambda = \frac{c_0}{f_c}$. c_0 denotes the speed of light. The power at the receiver decreases proportional with the square of the carrier frequency f_c and distance to the transmitter. The path loss in decibel assuming isotropic radiation as the difference of transmit and receive power computes to $L_{\mathrm{p}}\Big|_{\mathrm{dB}} = P_{\mathrm{rx}}\Big|_{\mathrm{dBm}} - P_{\mathrm{tx}}\Big|_{\mathrm{dBm}} = 20\log\left(\frac{\lambda}{4\pi d}\right) = 20\log\left(\frac{c_0}{4\pi d f_c}\right) < 0$. For propagation environments with more obstacles the path loss exponent increases. Due to the presence of different kind of obstacles, electromagnetic waves are reflected, diffracted, and scattered on houses resulting in multi-path propagation. The received power fluctuates over time around a mean value determined by the path loss, even in cases where the positions of the transmitter and receiver are fixed. These variations are referred to as: (i) large-scale fading, also known as shadow fading caused by the geometric characteristics of the surrounding, where the received power in linear scale can be modeled by log-normal distribution. (ii) Small-scale fading caused by the superposition of the multi-path components which can be modeled with Rayleigh distribution for non line of sight (NLOS) and a Rice distribution for line of sight (LOS) propagation. Co-Operative for Scientific and Technical Research (COST) 231 model based on the Hata urban propagation model combines empirical and deterministic models for estimating the path loss [9].

The spatial channel model (SCM) from 3GPP is based on ray-modeling technique [10]. The signal at the receiver side is a summary of the constructive and destructive individual signal paths which result from multi-path propagation. Within the femtocell scenario the path loss is particularly important and the developed techniques are independent from multi-antenna techniques, thus in here one concentrates on the extended path loss model for indoor-outdoor modeling. With the introduction of small cells as a femto- and picocell an extended version of the pathloss model for heterogeneous deployments is used. A detailed examination is shown in the appendix Section A.2.

2.2 Orthogonal Frequency Division Multiple Access based Cellular Network

In current mobile communication systems, as LTE-A and 5G, directions from the base station to the mobile stations and vice versa are separated in downlink and uplink. They use time-division duplex (TDD) and frequency division duplex (FDD) modes to distinguish downlink and uplink transmission. With FDD the base station and mobile station can transmit and receive at the same time but in different frequency bands whereas in TDD mode they use the same frequency band but downlink and uplink are seperated by the time intervals.

OFDMA is a widely used technique, also foreseen as a part of next generation mobile communication systems 5G. LTE-A will be one representative of 5G. In order to address the simultaneous demand of data from mobile subscribers, LTE is based on OFDMA in DL direction and SC-FDMA, which is a modified version of OFDMA in UL direction. OFDMA is a multiple access technique based on OFDM. In LTE several bandwidths from 1.4 to 20 MHz are defined [11] [5]. The resource allocation is dynamic with the use of different scheduling techniques as explained in more detail in Subsubsection 2.2.3.1. With the use of space division multiple access (SDMA) a group of users is multiplexed simultaneously on the same physical resources (frequency and time) with beamforming and spatial multiplexing techniques which make use of the space dimension.The first version of LTE is standardized in Release 8. From Release 10 significant enhancements have been introduced and since then are defined as LTE-A which is a 4G technology and it is also included in 5G. One significant aspect of LTE-A is the aggregation of different carriers which leads to significantly higher peak data rates. Multiple antenna techniques are used to increase the maximum achievable data rate. LTE-A supports multiple input multiple output (MIMO) up to antenna configurations of 8×8 for single user multiple input multiple output (SU-MIMO).

The introduction of Heterogeneous Networks is one main approach to increase data rates and the coverage within the network. Here several small cells are installed within the range of a MBS. The small cells can be picocells, femtocells, and relays.

2.2.1 System Architecture

The system architecture of LTE is similar to previous standards as GSM and Universal Mobile Telecommunications System (UMTS) but with a reduced amount of network components in order to increase efficiency [12]. The system architecture of LTE is depicted in Figure 2.4. It divides into radio and core network [13] [14]. The air interface is defined completely new compared to the previous standards. Within the framework of LTE-A it is called evolved UMTS Terrestrial Radio Access, air interface of LTE (E-UTRAN) and comprises a flat topology with the evolved packet core (EPC) as the architecture of the core network. The EPC is connected via the S1-interface to the MBSs, also denoted as eNB [15]. S1 is the logical interface between the base stations ("eNBs") and the mobility management entity (MME) function and user plane entity (UPE) located in the EPC. The MBSs are connected by the logical interface X2. The X2-interface is a point to point connection for direct data exchange between neighboring base stations. The MBS is not only responsible for the air interface with transmission and reception of data but also routing and mobility functions as well as the allocation of resources in time and frequency, i.e. scheduling.

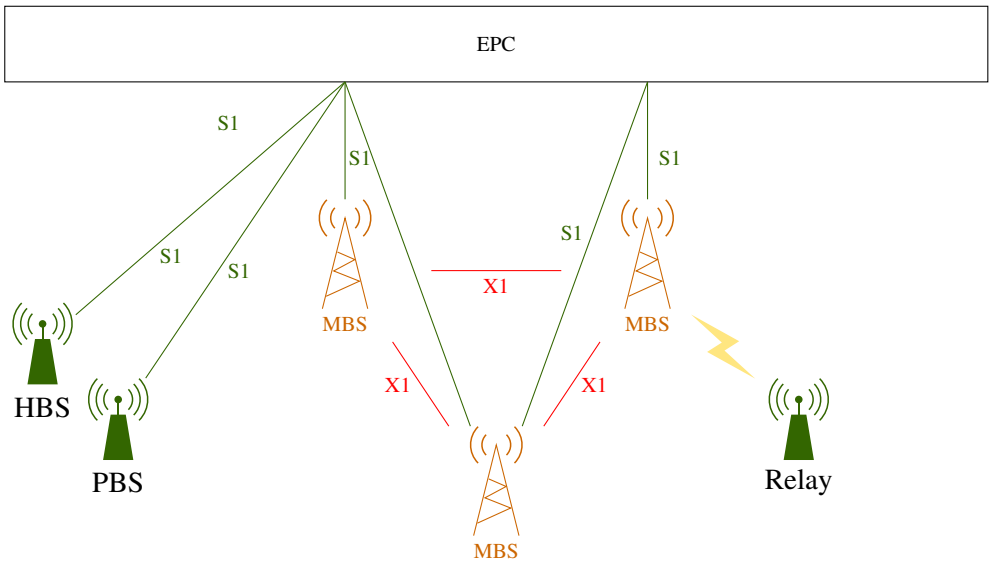

Figure 2.4: System architecture with air interface and interfaces between nodes

The E-UTRAN as the air interface of LTE is divided into a radio network layer and a transport network layer. The characteristics and specifications on the system layer of the wireless transmission are managed by the radio resource management (RRM) [16]. This comprises the multi-link aspect between multiple users and cells. Altogether system performance with spectral efficiency, cell edge and average user throughput are key parameters. The RRM should take care of these to get an overall optimum performance of the network taking also fairness aspects into account. It includes admission control, so which user is granted access to a specific base station, power control as well as resource control where the overall available resources are regulated.

2.2.2 Physical Layer

The uplink and downlink transmissions are separated with TDD by time or FDD by frequency and protected by a guard interval. In TDD the time slots can be of different size. FDD uses a paired spectrum. On each subcarrier modulation schemes from QPSK, 16-QAM over 64-QAM up to 256-QAM are deployed and even 1024-QAM is envisaged. The modulation mapper converts binary digits (bits) to complex-valued modulation symbols resulting in one up to 10-tuplets of bits [17].

2.2.2.1 Orthogonal Frequency Division Multiple Access

For a single carrier system the whole modulated (by amplitude, phase, frequency or combinations out of it) signal is transmitted at one carrier frequency. For multi-carrier transmission systems the data stream is modulated on different subcarriers. So in order to overcome the limits of the bandwidth size, compared to previous standards, LTE-A in 4G as well as 5G New Radio (NR) use OFDMA as transmission scheme for the downlink. On the basis of OFDM a fast data stream is divided into a lot of slow data streams which are transmitted in parallel over sub-channels of size 1.25kHz, 7.5kHz and 15kHz in LTE (-A) and even up to 240kHz in NR [18]. The number of subcarriers and thus the size of the IFFT, FFT as well as the number of resource blocks (RBs) (illustrated in Figure 2.8) depends on the used bandwidth according to Table 2.1 for $\Delta f = 15$kHz.

Table 2.1: Overview on the subcarrier size and number of available RBs in relation to channel bandwidth

Bandwidth [MHz]	FFT size	Number of used subcarriers	Number of RBs	Symbol rate $\left[\frac{1}{\mu s}\right]$
1.4	128	72	6	1.92
3	256	180	15	3.84
5	512	300	25	7.68
10	1024	600	50	15.36
20	2048	1200	100	30.72

The amount of data transmitted simultaneously can be increased when several channels are combined. This is explained in more detail in Subsubsection 2.2.3.8. The symbol time with OFDMA, for a subcarrier spacing of $\Delta f = 15$kHz (which is used throughout this thesis) results in useful OFDM symbol time of $T_u = 66.667\mu s$. It is much higher than the one of an individual subcarrier which makes it, together with the cyclic prefix, much more robust to multipath fading. The normal CP time is $T_{CP} = T_g = 4.7\mu s$ and for the first OFDM symbol 5.2µs. Several subcarriers are grouped to an RB which can be scheduled to different mobile terminals. An example for a distributed user assignment with four users is shown in Figure 2.5. When a user is scheduled, scrambled over the entire bandwidth, frequency diversity

results in a diversity gain. When the quality of each channel is known at the transmitter, users can be assigned resource blocks of good quality taking advantage of multi-user diversity.

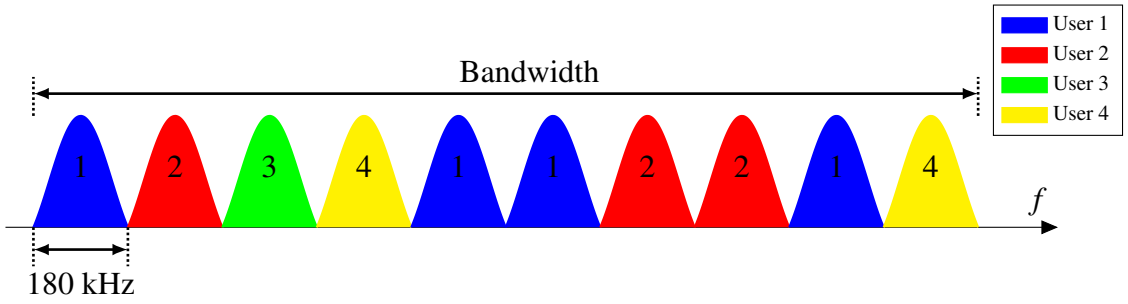

Figure 2.5: Exemplary user assignment in distributed orthogonal frequency division multiple access

2.2.2.2 Single Carrier Frequency Division Multiple Access

The battery power of mobile terminals is limited. OFDMA is less power efficient due to its high peak to average power ratio (PAPR). Thus a modified version of OFDMA is used in uplink direction. In addition to the IFFT for OFDMA, an additional FFT is introduced in front of the IFFT in order to spread each bit over all subcarriers assigned to one user. This leads to a single carrier frequency division multiple access (FDMA) signal with lower PAPR. Figure 2.6 shows an example of a user assignment with four users.

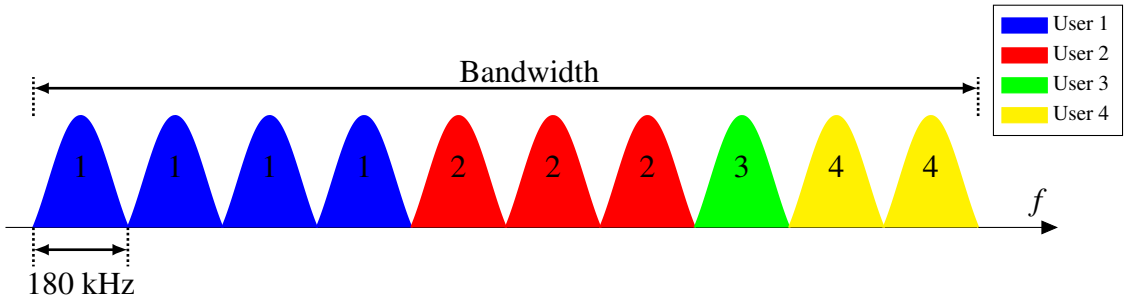

Figure 2.6: Exemplary user assignment in single-carrier frequency division multiple access

2.2.2.3 Frame Structure

The physical channels are mapped to a two dimensional area in the time-frequency plane [10]. An FDD OFDMA frame consists of 20 slots of duration $T_{\text{slot}} = 0.5\text{ms}$, which corresponds to a total frame length of 10 subframes equal to $T_{\text{f}} = 10\text{ms}$. Two consecutive slots form a subframe of $T_{\text{sf}} = 1\text{ms}$ illustrated in Figure 2.7 according to the standards definition [17]. $T_{\text{su}} = 1/\left(2048\Delta f\right)$ gives the basic time unit. Transmission or resource allocation works on subframe basis which is equal to the transmission time interval (TTI). In uplink

direction timing advance is introduced in order to guarantee that all frames of the individual users arrive simultaneously at the base station.

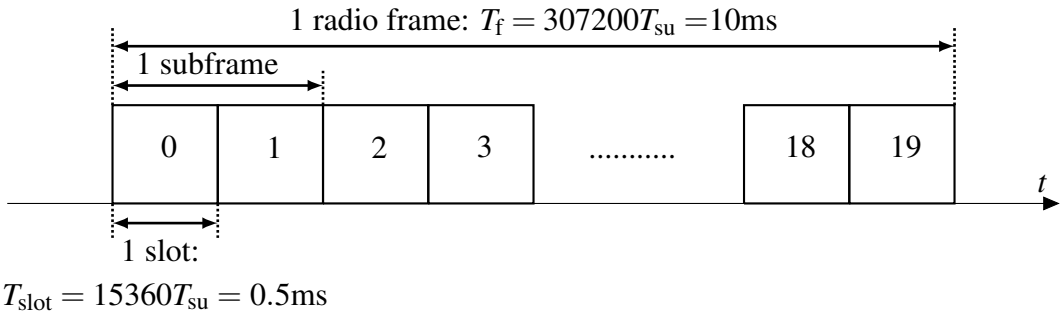

Figure 2.7: Orthogonal frequency division multiple access frame structure in frequency division duplex mode

The structure of the radio resource grid is shown in Figure 2.8, following the LTE standard [17]. The resource grid consists of $N_{RB} \cdot N_{sc,RB}$ subcarriers and $N_{symbols}$ OFDM symbols.

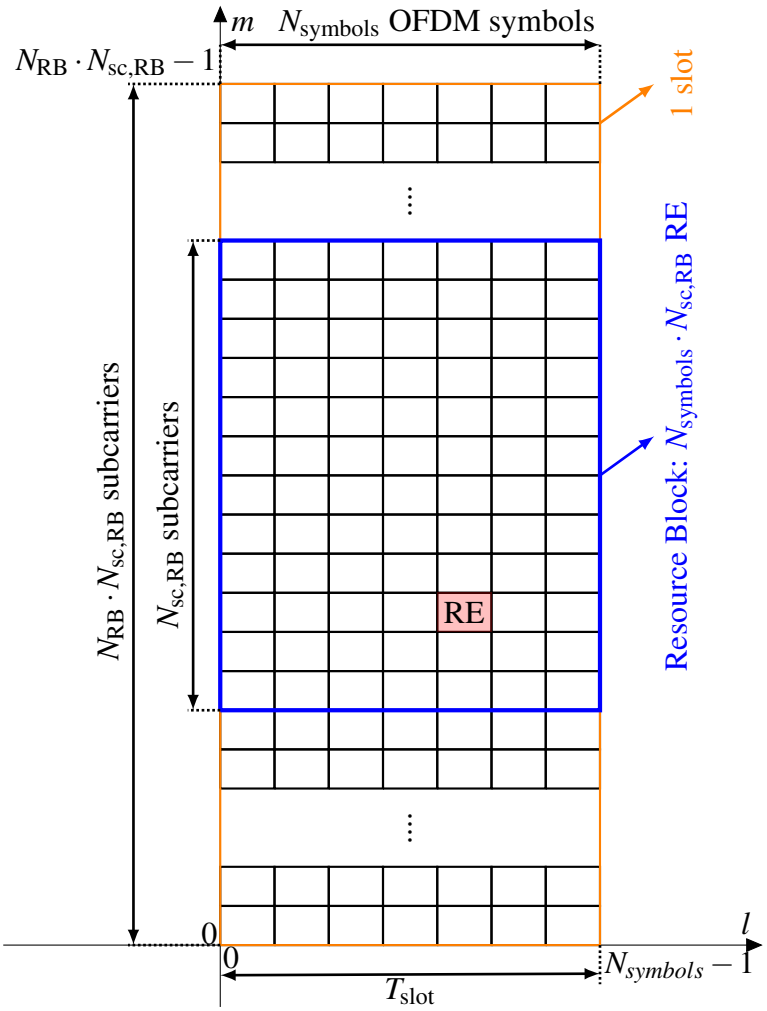

Figure 2.8: Orthogonal frequency division multiple access radio resource grid for the downlink in frequency division duplex mode

The abbreviation resource element (RE) denotes the smallest unit of resource which is of size one OFDM symbol in time and one subcarrier in frequency direction. For normal CP and a subcarrier spacing of $\Delta f = 15\text{kHz}$, $N_{\text{sc,RB}} = 12$ subcarriers in frequency domain and $N_{\text{symbols}} = 7$ OFDMA symbols or one slot in time domain are grouped to form an RB of size $(180\text{kHz} \times 1\text{slot})$. This results in a total of 50 RBs for 10MHz bandwidth and 100 RBs for 20MHz. Each user in the network can receive an integer multiple of RBs. In DL direction they do not have to be adjacent whereas in UL consecutive RBs are required. In order to address low latency applications for 5G NR a shorter TTI, which consists only of two OFDMA symbols instead of 14 OFDMA symbols, is supported. The decision of the scheduler (for more details please refer to Subsubsection 2.2.3.1) can be changed each TTI of length 1ms. Within each RB symbols for data transmission and reference symbols are allotted.

2.2.2.4 Reference Signals, Control Channels, and Channel Coding

Reference signals are needed for network search, differentiation of cells, and channel quality estimation. They are used to gain information on the signal power and to gain even an estimate of the channel. The positions of the distributed signals are given by a predefined pattern. On the first and sixth subframe synchronization signals are transmitted on the inner 72 subcarriers. Every seventh OFDMA symbol in time and sixth subcarrier in frequency contains reference data. For one and two antennas, four and eight REs per RB are used for channel estimation, respectively, whereas for more than two antenna elements only two REs per additional antenna and RB are reserved [12] [17].

Downlink control channel information contains data on the allocated resources, power control information, hybrid automatic repeat request (HARQ) information which defines the data as retransmission or new information, modulation and coding scheme (MCS), number of parallel datastreams, and precoding information [12].

Channel coding on the LTE DL is done with a cyclic redundancy check (CRC) sequence of length 24 bit added to the transport block where short blocks are filled up to a minimum block size and longer are truncated. Turbo coding is used for data channels and tail biting convolutional codes are used for control channels, and the blocks are interleaved. 5G uses low density parity check (LDPC) for data channels and polar codes for control channels [19] [20].

2.2.2.5 Space Division with the Cellular Principle and Multiple Input Multiple Output Transmission

The spatial dimension can be exploited on the one hand with the introduction of cellular networks and reusing the available resources of time, frequency, and power only at suitable distances. The spatial separation with the reuse of the same frequency resources is applied for example in 2nd generation GSM. On the other hand within a MIMO system, which refers to

a system with more than one antenna at the transmitter and receiver, several data streams can be transmitted simultaneously. Thus, the system capacity can be increased tremendously by introducing the additional dimension of space now from another perspective [21], [22]. This dimension comes on top of time and frequency. In critical transmission situations transmit diversity can be exploited by transmission of redundant information at the antennas to make the transmission more robust. Spatial multiplexing receivers can be e.g. zero forcing (ZF), minimum mean squared error (MMSE) or successive interference cancellation (SIC) [23]. Massive MIMO uses an array of many antennas at the network side and a small number at the mobile device to form multiple beams to spatially reuse the available resources [24] [25]. With a huge number of subscribers, users have to be assembled in clusters, their movement has to be tracked and the interference of surrounding base stations has to be addressed. Using TDD mode, the channel can be estimated at the base station due to the reciprocity property.

2.2.3 Medium Access Control Layer

This section presents the details of the MAC layer located on top of the PHY layer, treated within the previous sections. Based herein is a substantial part to guarantee reliable and fast wireless data transmission. The essential topics for the success of current and future mobile communication systems are the RRM, scheduling of resources, adaptation to the link quality as well as the HARQ protocol, all discussed in more detail within the next subsections.

2.2.3.1 Scheduling of Radio Resources

Data transmission in LTE is controlled by the network. Scheduling takes place in the eNBs. With this the allocation of resources can be adapted quickly to changing conditions at the air interface, the quality of service (QoS) constraints of each individual user can be monitored and steered and overload situations can be controlled [11]. Scheduling describes the procedure of dividing the available resources in time and frequency dimension and assigning them to the individual users in an optimal way. The definition of "optimal" can be made due to different perspectives. Different schedulers can use various types of resource allocation: uniform resource allocation among all users (round robin (RR)), sequential resource allocation (first in first out (FIFO)), scheduling to maximize the overall system throughput (max rate), and fair resource allocation among all users (proportional fair). Goal of a scheduler should be to aim for a balance between QoS of the individual user and the overall system performance. In the following a short description of the different schedulers is given:

Round robin Resources are allocated sequentially to each user independently of the channel conditions. Hence, each user gets the same amount of resources. The overall throughput within a cell deviates from the optimum and the throughput of a user depends on the average radio conditions.

FIFO Resources are allocated to the users based on the order of the allocation requests.

Max rate The maximum rate scheduler is channel dependent as the resources are allocated according to a channel quality parameter. One condition could be the selection of the user with the highest SINR. In this way the time and frequency selective nature of the channel is exploited and the data rate maximized. On the other hand users with a low channel quality parameter are skipped or experience poor or even zero throughput and excessive delay.

Proportional fair The proportional fair scheduler provides a balance between scheduling at good channel conditions and fairness. This results in a higher cell throughput than the round robin technique but still maintaining commitment of the users experiencing poor channel conditions. The users are scheduled based on channel state information (CSI) measurements or channel quality indicator (CQI) reports. This results in a situation where users are scheduled on beneficial resources which provide good channel conditions. Thereby a high throughput is achieved. The utility value takes also into account the amount of allocated resources in the past, to maintain the fairness criteria, thus the users are scheduled when their instantaneous channel quality is high compared to its average. The time duration of one TTI is equal to $T_{\mathrm{sf}} = 1\mathrm{ms}$. The long-term average throughput is computed recursively as

$$\Upsilon_u(\kappa+1) = \begin{cases} \beta_{\mathrm{PFS}}\Upsilon_u(\kappa) & u \notin \mathcal{M}(\kappa) \\ \beta_{\mathrm{PFS}}\Upsilon_u(\kappa) + (1-\beta_{\mathrm{PFS}})R_u(\kappa) & u \in \mathcal{M}(\kappa) \end{cases}, \tag{2.5}$$

with the current aggregated throughput $R_u(\kappa)$ of user u during TTI κ, forgetting factor β_{PFS} for windowing aspects, and $\mathcal{M}$ indicating the set of scheduled MS [26] [27]. The scheduling metric on each individual RB p for user u during TTI κ is the ratio of instantaneously possible and long-term throughput, with adjusting parameter α_{PFS} for the fairness criteria:

$$M_{\mathrm{PFS},u,p}(\kappa) = \frac{R_{u,p}(\kappa)}{\Upsilon_u^{\alpha_{\mathrm{PFS}}}(\kappa)}. \tag{2.6}$$

The user with the highest scheduling metric on RB p is eligible to transmit on this RB during TTI κ.

In conclusion, modern communication networks use channel dependent scheduling in order to encounter the special channel characteristics [28] and realize an optimal resource utilization.

An exemplary scheduling decision is shown in Figure 2.9, where the different users are separated by color. Dependent of the decision of the scheduler one user equipment (UE) also denoted as MS can have a different number of RBs assigned whereas each one can have a different MCS.

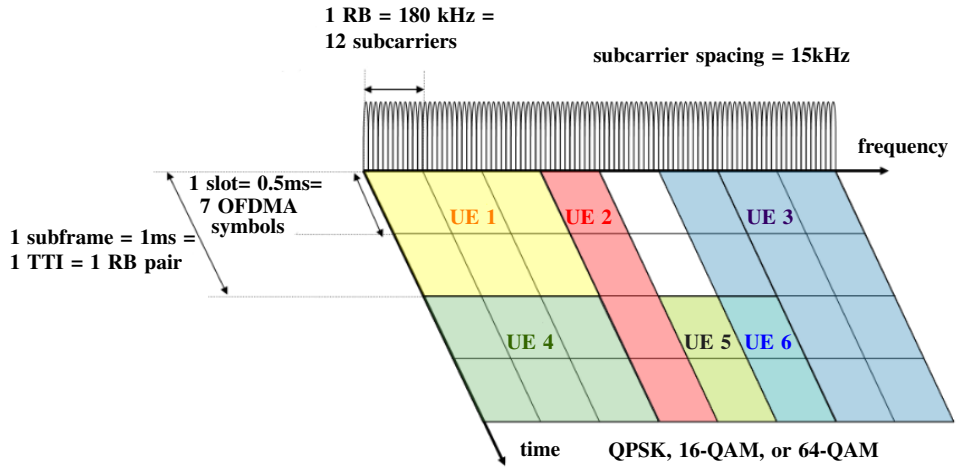

Figure 2.9: Exemplary user assignment with time-frequency multiplexing of an OFDMA signal (exemplary for normal CP) adapted from [6]

2.2.3.2 Hybrid Automatic Repeat Request

Channel decoding may fail and result in incorrect data, so erroneous data has to be detected and incorrect data discarded. Hence, in order to get more reliable data transmission the retransmission protocol HARQ located on the MAC layer is introduced. HARQ combines channel coding and automatic repeat request (ARQ). When a UE detects an RB to be incorrectly received it can request a retransmission by sending negative acknowledge (NACK) on the UL. In FDD mode, with in total 8 HARQ processes, the message transmitted corresponds to the DL packet received four subframes before [6]. In reaction, the identified erroneous data blocks are retransmitted. HARQ can be divided into a simple type 1 version where erroneous data is discarded and the retransmitted block is treated independently or a hybrid type 2 scheme, where the initial transmission is retained and combined with the retransmission [29] [11]. Type 2 includes also incremental redundancy, an adaptive error correction technique. The ARQ protocol on the radio link control (RLC) on top of this scheme is introduced in order to account for missing data.

2.2.3.3 Channel Quality Parameters

In order to react to different channel situations the transmission of a channel quality report is essential. The data transmitted to and between base stations (BSs) is the channel state information (CSI). It comprises the following information:

Channel quality indicator (CQI) (Wideband or subband wide) The UE sends the information of the preferred MCS to the BS.

Precoding matrix indicator (PMI) Indicates the index within the codebook table which corresponds to the preferred precoding matrix determined at the receiver according to

a certain criterion based on the estimated channel. These are needed when precoding at the transmitter is used as for schemes as MU-MIMO and closed loop spatial multiplexing.

Rank indicator (RI) (Wideband) Gives the number of useful transmission layers for spatial multiplexing.

The reporting of the channel feedback information as CSI may be periodic or aperiodic.

2.2.3.4 Link Adaptation

Link Adaptation adjusts the transmission parameters for the individual users to the present channel conditions. The desirable MCS is selected in order to maintain QoS criterias while realizing high throughput rates. Dependent on the signal-to-noise ratio (SNR) on the individual RBs a set of modulation scheme and code rate is selected. An overview on the different modulation schemes is presented in Section 2.1.1. Higher order modulations provide higher data rates and are used when a good link with adequately high SNR is available. In case of inferior channels, the MBS decides on a more robust lower modulation scheme as QPSK due to its fewer sensitivity to interference, noise, and estimation errors of the channel. The available coding schemes for the particular modulation schemes are $\{1/9, 1/6, 0.21, 1/4, 1/3, 0.42, 1/2, 0.58, 2/3, 0.73\}$ for QPSK, $\{0.43, 0.46, 1/2, 0.54, 0.58, 0.61, 2/3, 0.73, 4/5\}$ for 16-QAM, and $\{0.58, 0.62, 2/3, 0.70, 0.74, 4/5, 0.85, 0.9\}$ for 64-QAM [30]. In order to address the time variation of the channel, especially critical for uplink transmission, an additional outer loop link adaptation is introduced [31].

2.2.3.5 Link to System Mapping

In order to encounter the huge amount of data to be simulated, an abstraction level, including physical as well as system level aspects, has to be introduced. To address the complex and computationally complex simulations a link-to-system (L2S) level interface connects the two levels. The system level contains all connections between all kinds of BSs to the MSs and vice versa, whereas the link level considers the link-pair of transmitter and receiver. Measures on the link level are bit error rate (BER) and block error rate (BLER), whereas on the system level they are throughput of the cells and the system [32]. The L2S-level simulation mapping is performed through the use of look-up-tables. The tables are gained by performing link-level simulations. They contain the information on the BLER as a function of the SINR. The SINR of each subcarrier is determined. Subsequently, the value of the individual subcarriers is mapped to an effective SINR whereof the corresponding BLER can be gained. Figure 2.10 depicts the procedure of the mapping between link and system level according to [33].

In the literature, several methods which take into account the capacity effective, exponential effective, logarithmic, and mutual information effective SINR are presented [32]. An

attractive method for the L2S-level mapping is the mutual information effective SINR mapping (MIESM) as it supports a mapping with different modulation and coding schemes and due to its high accuracy.

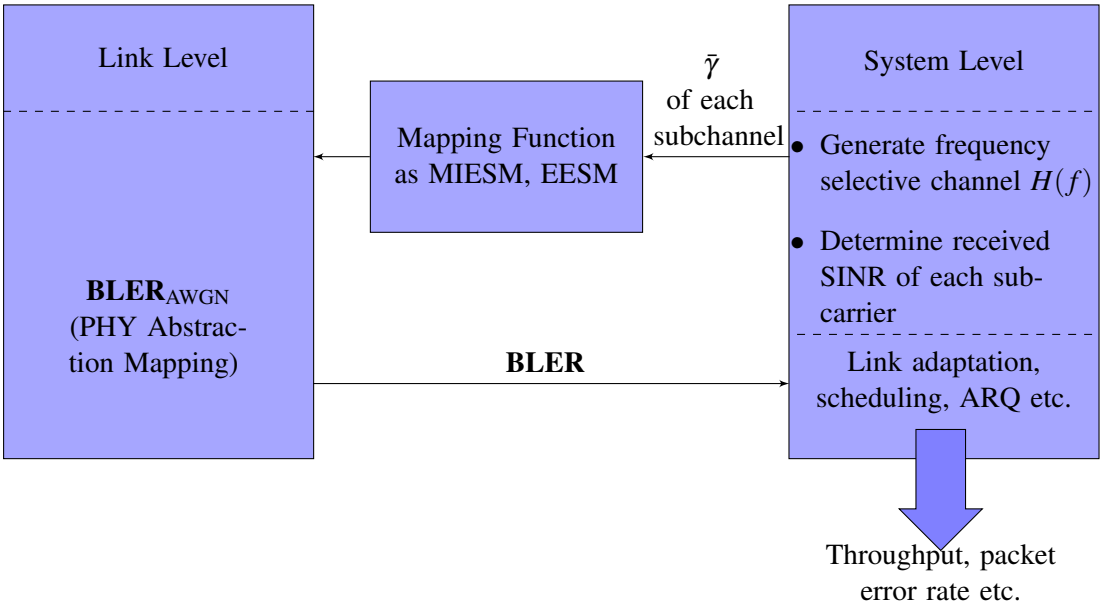

Figure 2.10: Procedure of the link-to-system-level mapping

The effective SINR γ_{eff} is calculated based on a non-linear mapping function with the use of the mutual information function I_{b_m} which considers the specific modulation, b_m the complex QAM-symbol, the reference b_{ref} as the average number of transmitted bits per resource, a calibration factor β, γ_m the SINR of subcarrier m, and the number of subcarriers per transport block N_{blocks} [33]:

$$\gamma_{\text{eff}} = \beta I_{b_{\text{ref}}}^{-1}\left(\frac{1}{N_{\text{blocks}}}\sum_{m=1}^{N_{\text{blocks}}} I_{b_m}\left(\frac{\gamma_m}{\beta}\right)\right) \tag{2.7}$$

The calibration factor β is chosen to minimize the root mean square error between γ_{eff} and the static SNR leading to the same BLER. The mutual information depends on the modulation alphabet size 2^{b_m} (with b_m bit per QAM symbol) and an expectation term. This results in curves which map the SNR for the individual MCS to the mutual information. The SNR is defined as the ratio of mean QAM symbol energy E_s to noise power density N_0. While for low SNR they follow the Shannon capacity, they saturate at b_m in the high SNR regime. The saturation due to the limited QAM symbol alphabet is shown in Figure 2.11 whereas Gray labeling is assumed [32] [34].

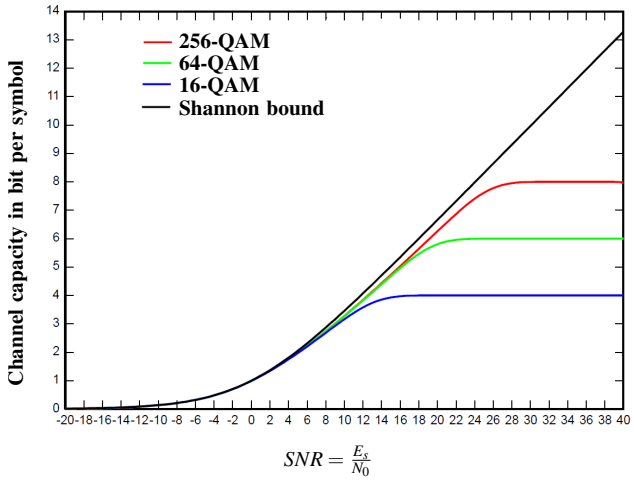

Figure 2.11: Capacity of complex-valued AWGN channel with different QAM input constellations [34]

2.2.3.6 Coordinated Multipoint

Coordinated multipoint (CoMP) is a method for cooperation between cells of homogeneous and heterogeneous deployments in order to improve the network performance [35]. Geographically separated base stations transmit and receive data in a coordinated way. It comprises joint transmission and reception as well as inter-cell coordinated scheduling. A central network element coordinates the radio frequency transmission at the spread antenna locations [12]. Especially the data rates for the cell edge users can be increased due to the reduced interference situation.

2.2.3.7 Handover

While some users of a cellular system might reside at one location others move with pedestrian speed or travel in cars and highspeed trains. Due to the limited coverage of one cell a handover procedure has to be integrated. In case the signal from the neighboring cell is higher than the one from the associated cell a seamless handover is favored in order to constantly maintain the QoS. A handover can be controlled by the network as well as requested by the UE. In case the serving BS and the requested BS are directly connected by the logical X2-interface, the handover decisions are negotiated between these two cells. Otherwise, the EPC is involved in the handover procedure. Classical handover scenarios are on the macrocell layer from one MBS to another. With the introduction of an additional layer, further unsymmetrical inter-layer handover scenarios such as from MBS to HBS and HBS to MBS as well as inter femtocell-layer handovers from HBS to HBS come in addition. Within these multi-layer scenarios further aspects, as the unsymmetrical power levels, increasing handover rates as well as the admission control due to limitations such as closed subscriber group (CSG), have to be addressed.

2.2.3.8 Carrier Aggregation

To reach the requirements of the radio communication sector of the International Telecommunication Union (ITU) the concept of carrier aggregation (CA) was introduced. To guarantee backward compatibility it has been decided not to increase the overall system bandwidth of maximum 20MHz but to add several channels intra-band (consecutively or discontinuously) and also inter-band at different frequency ranges and aggregate them. With this also fragmented spectrum can be exploited. One individual channel is denoted as a component carrier (CC). With CA the usable bandwidth can be increased dependent on the LTE Release from five CC in Release 12 up to 32 CC in Release 13 by aggregating multiple carrier components. This results in a maximum available bandwidth of 100MHz in Release 12 to 640MHz in Release 13 [12] [36]. Figure 2.12 depicts an example of FDD carrier aggregation where legacy Release 8 and 9 UEs get only one of the component carriers and LTE-A UEs can transmit on several CCs simultaneously. The UEs from previous releases are denoted by R8/R9 UE. Their restriction on only one CC is illustrated with their blue and red color. The blue colored UE is only eligible to use CC 1 printed with the same color and the red colored UE transmits on CC three. Different an LTE-A UE can use several up to all available CCs. The aggregation of CCs can be different for DL and UL transmission. As the CCs can be adjacent or spread over the frequency, different scenarios have to be discussed. In case they are co-located they span similar coverage areas. Contrary, when the CCs are non-contiguous in different frequency band areas the coverage area can differ significantly which has to be addressed. Mobility and handover aspects need to be based on the CC with lower frequency, as this results in a wider coverage area due to lower path loss.

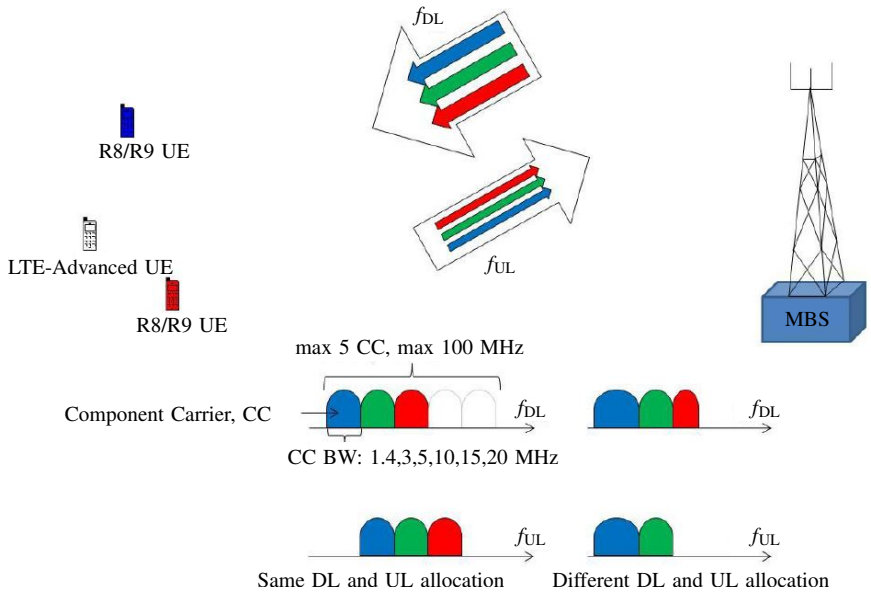

Figure 2.12: Overview on carrier aggregation adapted from [36]

Carrier aggregation can be also thought of together with different beams of sectorization and separate component carriers for macrocells and small cells. Nevertheless, this reduces the overall available resources when pre-assigning the bandwidth completely.

2.3 Heterogeneous Networks

The trend in mobile communication systems heads to an overwhelming increase in the number of base stations, with the vision of more base stations than user terminals, in the next one to two decades [37]. Reasons to this are as follows: Radio resources in a mobile communication network are limited and the number of mobile broadband data subscribers is increasing. Therefore operators have to plan the network carefully. In a traditional network the positions of the macro base stations are carefully planned to achieve a coverage close to 100% and low inter-cell interference. To master the increasing demand operators (i) increase capacity, by adding radio spectrum, (ii) are using multi-antenna techniques, and (iii) implement more efficient modulation and coding schemes. Nevertheless these actions taken on their own are not sufficient in congested places, as well as at the cell edges. To cope with this, the introduction of small cells to the macro-cellular network is promising [38]. The highly loaded macro layer can handover part of its users, e.g. stationary users with high data rate demands, to the small cell layer and herewith improve the overall user experience. As more than 80% of the traffic originates or terminates indoor [39] and the coverage indoors with a traditional cellular network is not sufficient, small cells can help to improve coverage where needed and increase the capacity at the bottlenecks. Figure 2.13 shows an area covered by a macrocell overlayed by several femtocells, clustered in enterprise scenarios and scattered in detached houses [40].

Figure 2.13: Overview of an heterogeneous network with macrocell and femtocells

Within a heterogeneous network in addition to the MBSs further BSs with lower transmit power, the so called “low-power” base stations (LBS), are placed. They serve to supply small and smallest areas with enhanced data transmission demands, as well as areas without coverage, the so called white-spots and to enhance indoor coverage. Within heterogeneous networks, new base stations can be placed successively, based on the demand, to enhance

transmission capacities. This leads to a change of the interference situation each time a new base station is placed, replaced or shut down. Further, the interference situation in heterogeneous networks is highly changeable, due to the following reasons: To begin, the low transmit power leads to a low coverage area of a cell. Further, the number of users in low power cells changes significantly, leading to rapidly changing cell loads and thus resulting in a significantly and quickly changing interference situation for the surrounding cells. Special to HBSs is that consumers can even switch them on and off and change the BS position based on their own demand. [41] shows the efficiency of different deployment locations of femtocells, where an appropriate location can almost double the coverage and enhance the average received data rate significantly. In case of femtocells, which are user deployed, this might be difficult to address, however for picocells this can be taken into account.

Portable low power BSs (LBSs) are used for short time usage, for example for football games, open air concerts, or in case of a disaster. Small cells can even be mobile, integrated in trains or vehicles. Table 2.2 gives an overview on different cell types from the MBS, over different LBSs, relays, and remote radio heads (RRHs) [42]. The range of the transmit power P_{tx} for the individual cells, together with their backhaul connection, the typical access mode, and cell size at typical LTE frequencies are given.

Table 2.2: Overview on different cell types within a heterogeneous network

Cell type	Typ. access mode	P_{tx} of BS	Cell size	Backhaul conn. of BS
Macrocell	open	46dBm	few km	S1 interface
Picocell	open	$23-30$dBm	$<$300m	X2 interface
Femtocell	closed	$<$23dBm	$<$50m	Internet IP (recent Rel 3GPP: X2)
Relay	open	30dBm	300m	Wireless
RRH	open	46dBm	few km	Fiber

The access policy of the several cell types varies. Whereas macrocells, picocells, relays, and RRHs are of open access, femtocells can be of closed or hybrid access type. If users are in the list of a CSG they are granted access. In an open subscriber group (OSG) all users are allowed to connect. Table 2.3 gives an overview on different access policies. An open access concept would improve the overall capacity, avoids femtocells to behave as interferers, but increases the number of handovers. This method can be commercially challenging for femtocells since the owner of a cell pays for equipment and backhaul connection. In contrast to this, closed subscriber groups, special to femtocells, just allow users on the CSG list to connect leading to a critical interference situation, where interference coordination has to be taken into account. In hybrid access mode all users have access to the BS. While users on the CSG list have full access to the resources, other users just get a portion of it.

Table 2.3: Overview on different access policies

Access Type	Method	Goal	Drawback
Closed	Only users belonging to CSG are granted access	Increase data rate of registered users	Users not on list experience high interference
Open	All users can connect (OSG)	Interference free supply	Throughput could collapse if too many users are connected. Increased number of handovers.
Hybrid	User belonging to CSG have full access. Non-subscriber just for control signals and a percentage of the resources for data transfer.	Loss of connections can be reduced and overall network throughput can be increased.	Difficult as owner of cell provides backbone connection.

2.3.1 Relays

Relays are set by the network operator and behave as common LTE cells. Compared to these, they are of lower cost, transmit with lower power, and do not have a wired or microwave backhaul, but use the air interface to an MBS as backhaul connection [43]. Relaying of data uses the same channel as the connection from MBS to the MS. The relay node (RN) forwards the received data to the user terminals. With this the range of a macrocell can be extended and white spots can be supplied without the need of installation of a microwave or wired connection.

Figure 2.14 gives an overview on different deployment scenarios of relays, which ranges from stationary, over nomadic to mobile use cases. The quality of service in the network can be improved as well as the capacity. On the other hand the interference in the network is increased and network complexity is increased. This has to be addressed carefully to prevent potential performance degradations.

Relays can be divided into the group of transparent and non-transparent relays. Relays of several types from type 1 to type 3 can be distinguished [44]. While layer 1 relays, also known as repeaters, just amplify and forward the received signal, type 2 and 3 relays perform suppression of noise by processing data by decoding and encoding, before forwarding it to the UE [45]. Decoding and encoding data increases the delay, but is especially helpful in interference limited scenarios.

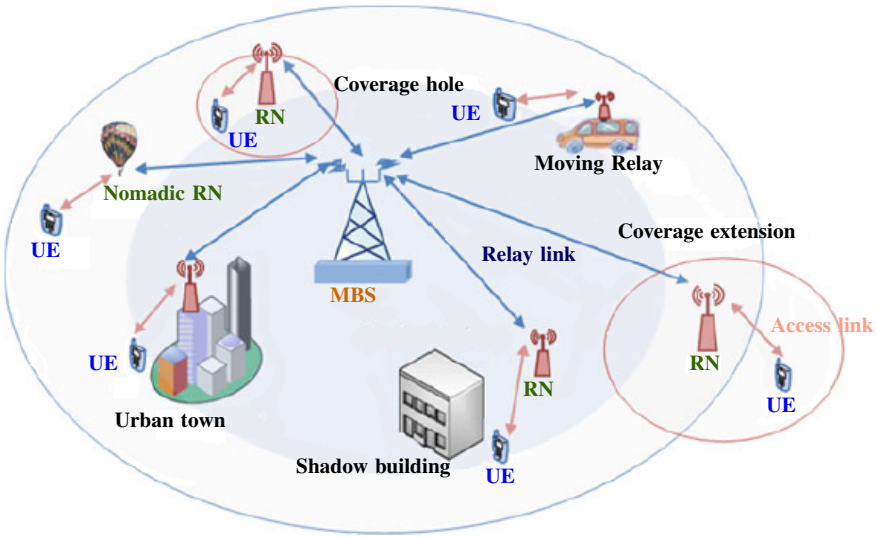

Figure 2.14: Different scenarios of relays adapted from [43]

2.3.2 Picocells

A picocell or low power node is served by an LBS, which is similar to an MBS, but transmits with lower power. It is planned and installed by the network operator and can be used to close coverage holes in the macrocellular network, as well as to increase the capacity in areas of high demand, the so called "hot-spots". This can be permanently, e.g. in city centers, shopping malls, sport stadiums, train stations, office buildings, or just temporarily for a concert, market, festival. Likewise macrocells, the picocell is also of open access, hence as long as the capacity limits are not exceeded, all users can be granted access.

In an heterogeneous network the MBS transmits with high transmit power and the pico base station (PBS) with much lower power, thus spanning a wider area in DL direction. In contrast to this, for the UL this does not hold, as the UEs connected to the different cells have the same maximum transmit power independent of the cell being associated with. This leads to asymmetric cell sizes resulting in different handover boundaries for DL and UL direction. By introducing cell range expansion, shown in Figure 2.15 adapted from [46], more users can be attached to the PBS leading to a beneficial traffic offload from the MBSs to the PBSs.

Usually a UE connects to the cell with the highest received signal strength (RSS) [47]. With range expansion, a UE which is located in an overlapping region of both cell types can now be associated with the PBS, even if it receives the PBS with lower signal power. With this approach the PBSs can increase their coverage area and thereby support the traffic burdened macrocell. The introduction of interference coordination schemes can improve the overall system performance and increase in particular the throughput of the user equipment connected to a PBS (PUE) [48].

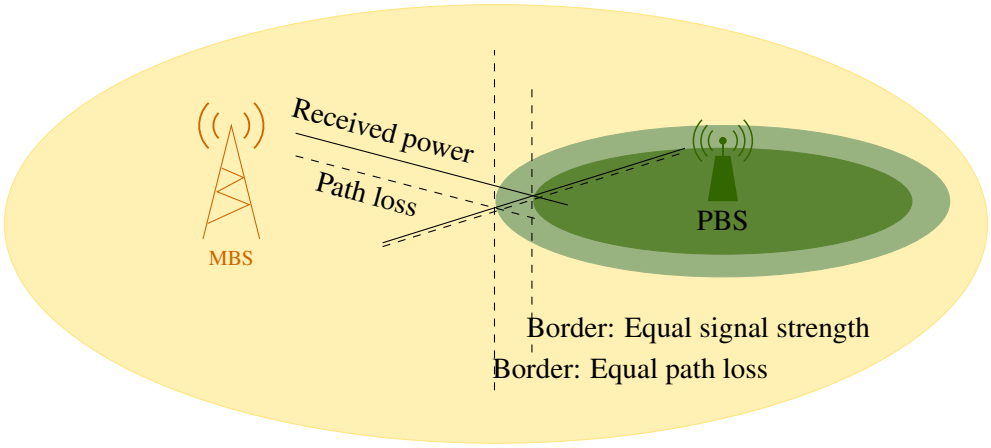

Figure 2.15: Heterogeneous deployment of macrocell and picocell with range extension

2.3.3 Femtocells

An LBS, serving a femtocell, is a low cost base station set, paid and used by the consumer for home usage [49]. The low transmit power with typical values in the range of $10-100$mW results in a short range of about $10-50$m. Femtocells are usually configured as CSG, and LBSs are placed mainly indoor to serve stationary or low-mobility users.

The connection to the backbone is via the Digital Subscriber Line (DSL), cable or fiber connection of the owner of the cell. Recent 3GPP releases introduce femtocells with X2 interface with the possibility of direct base station communication [50]. The femtocell is a small cell which serves only a small amount of users.

Goal of the femtocell is to improve the indoor coverage, as well as to provide higher capacity, and offload the traffic from the macrocell. An advantage is that users could replace their Digital Enhanced Cordless Telecommunications (DECT) phone and need to own and maintain just one device with all information on it. Further, the closer distance to the base station reduces the battery consumption of the mobile device.

Due to the limited available spectrum a deployment scenario where the BSs of different layers will share the bandwidth is preferable. Challenges are: (i) the HBSs are set by the owner, which will most probably result in a suboptimal position and (ii) the concept of the closed subscriber groups. With this some users are not granted access in the femtocell, even if this is the connection with the highest received power, leading to situations where the sometimes quite poor received indoor signal is further weakened.

Figure 2.16 shows critical interference scenarios especially related to the introduction of CSGs. In here MBSs are printed in orange and user equipment connected to an MBSs (MUEs) in blue. The femtocell base station (depicted as LBS) as well as the small cell users (user equipment connected to an LBS (LUE)) are colored in green. The useful signal paths are given by a black solid line whereas the interference with a red dashed line.

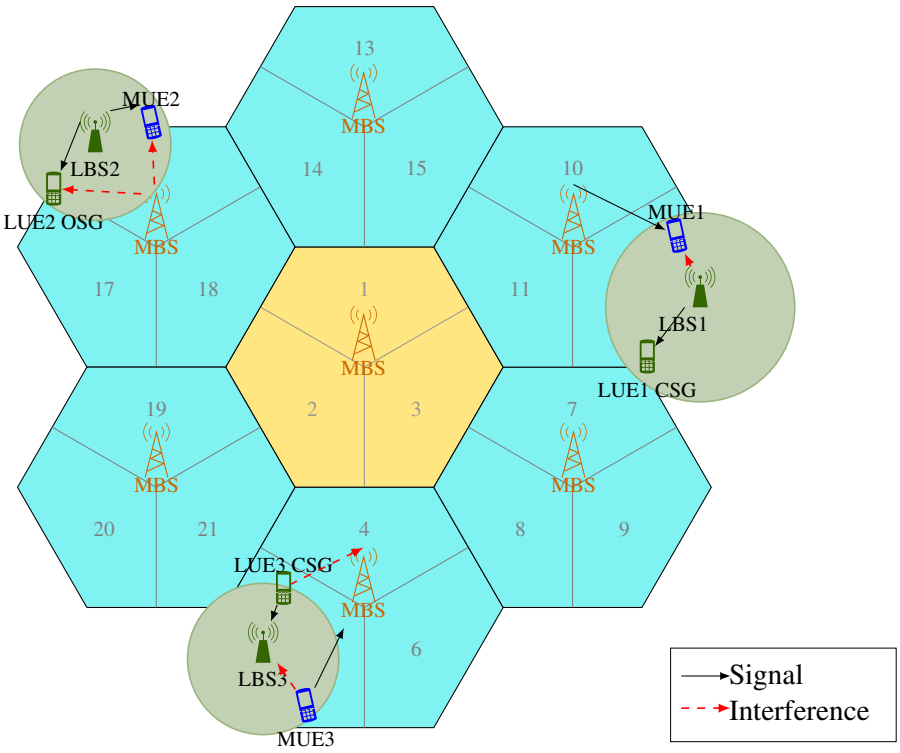

Figure 2.16: Interference in heterogeneous networks with macrocells overlayed by a femtocell layer

LBS one and three supply a femtocell with the CSG concept, where only users on the list can access. LBS three offers open access with an OSG. First, considering the downlink with transmission from the BSs to the UEs, MUE 1 is in the range of an HBS but cannot be handed over thus suffers from high interference. Differently, MUE 2 can be handed over to the femtocell in its vicinity in case this offers a more beneficial situation.

On the other side, considering uplink direction from an UE to the basestation, another UE, as for example LUE 3, handed over to the femtocell can introduce high interference at the MBS.

Fast moving UEs should not be handed over to an HBS, as the time in the cell would be really short. If a fast moving UE passes by several HBSs, the extreme interference situation could occur for a long time. So the introduction of interference coordination techniques is necessary.

2.4 Principle of Interference Coordination in Homogeneous and Heterogeneous Networks

Transmission in wireless communication systems is affected by several kinds of interference. Interference reduces the useful received power which leads to reduced transmission quality and reduced transmission rates. The main issue in OFDMA mobile communication systems is inter-cell interference from neighboring cells when the same frequency band is used. This leads to performance degradation especially at the cell edges. To guarantee efficient communication with good quality between base stations and user terminals, interference has to be removed or at least lowered. The principle of interference coordination is introduced since LTE Release 8. This section gives an overview on the basics of the interference situation in mobile communication systems. Important aspects are to identify the most critical interference situations and find solutions adapted to it. First interference coordination techniques in homogeneous networks are shown, followed by techniques applicable to heterogeneous networks with macrocell and small cells.

2.4.1 Basics of the Interference Situation

The type and amount of interference depends on the specific technology. LTE uses OFDMA in DL and SC-FDMA in UL direction where resources are allocated on RB basis. In homogeneous networks with macrocells only, due to the orthogonality of the assignable resources to the individual users in one cell (in time, frequency, and space) only inter-cell interference is present. Inter-cell interference arises from the fact of the usage of a frequency reuse factor of one (i.e. each cell uses the whole bandwidth). [51] gives an overview on techniques combating interferences in MIMO systems. With the introduction of small cells additional interference is introduced into the network, called inter-layer or inter-cell-interference. In particular, users located at the cell-edge suffer from severe interference. The different types of interference are:

A Intra-cell-interference

- **A1** Intra-user-interference: Inter-symbol-interference and inter-carrier-interference
- **A2** Inter-user-interference (UL/DL)

B Inter-cell interference

- **B1** Inter-user-interference (UL)
- **B2** Inter-base station-interference (DL)

Within an OFDMA system with synchronization between the cells, inter-symbol and inter-carrier interference is not relevant. Figure 2.17 depicts an overview on the different types of

inter-cell interferences which can occur in the downlink of an heterogeneous mobile communication network as LTE.

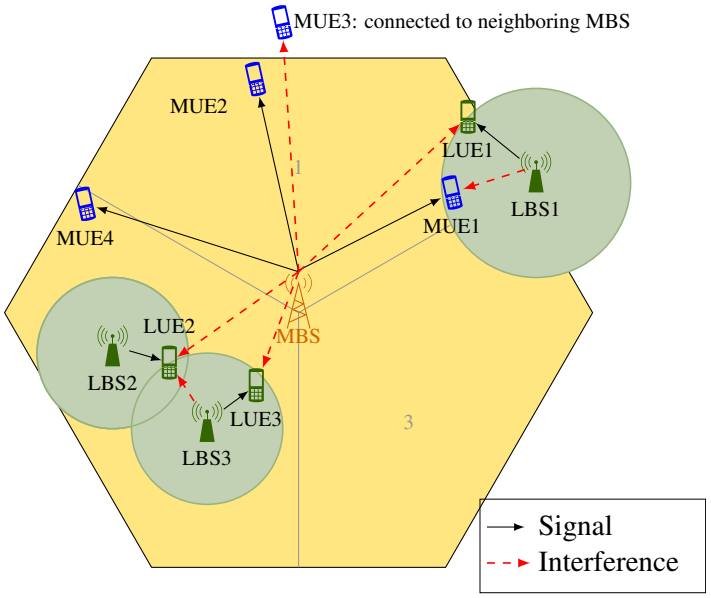

Figure 2.17: Overview on the critical interference situations in downlink of a heterogeneous networks with macrocell and small cells

As can be seen, intra-layer inter-cell interference on the macro layer affecting MUE 3 (which is connected to the neighboring MBS) is present, due to transmission of MUE 2. Inter-cell interference beyond layers is shown for LUE 1, 2, and 3 which receive interfering signals from the MBS.

Most critical for heterogeneous networks with HBSs due to the CSG concept is the inter-cell interference, when HBSs with CSGs are present, between and across layers. On the one hand inter-small cell interference for LUE 2 from LBS 3 is critical and on the other hand especially relevant MUE 1 experiences interference from LBS 1. Both UEs might not be able to switch to their interfering LBS.

In the uplink, critical interference situations are the interference of an MUE in close proximity to an LBS which obstructs the transmission of the LUEs to their serving LBS and the uplink transmission of an LUE in short distance to an MUE. This impact is even more severe if this MUE is not on the corresponding CSG-list, thus not able to connect with the BS of the interferer. Further, inter-small cell interference caused by uplink transmission from a LUE to its assigned LBS is introduced to close-by small cells.

In the following, the downlink of a cellular system is considered. OFDMA is used, thus the channel within one subcarrier can be assumed to be flat and one complex coefficient per transmitter and receiver pair describes the channel on one subcarrier. The number of macrocells is N_{MBS} and the number of small cells or femtocells is N_{HBS}. The index $\nu = (1,\ldots,N_{\mathrm{MBS}},N_{\mathrm{MBS}}+1,\ldots,N_{\mathrm{MBS}}+N_{\mathrm{HBS}})$ corresponds to one BS. One element thereof ν_u denotes the serving BS of user u, which can be either a MBS or a HBS.

The received signal at user u at time instance k after equalization of the received signal $\mathbf{r}_u$ with the equalization matrix $\mathbf{W}_u$ computes to

$$\begin{aligned}\mathbf{y}_u(k) = \mathbf{W}_u(k)\mathbf{r}_u(k) = &\underbrace{\mathbf{W}_u(k)\mathbf{H}_{u,\nu_u}(k)\mathbf{P}_{\nu_u}(k)\mathbf{x}_{\nu_u}(k)}_{\text{signal}} \\ &+\underbrace{\mathbf{W}_u(k)\sum_{\nu=1,\nu\neq\nu_u}^{N_{\text{MBS}}}\mathbf{H}_{u,\nu}(k)\mathbf{P}_\nu(k)\mathbf{x}_\nu(k)}_{\text{macro interference}} \\ &+\underbrace{\mathbf{W}_u(k)\sum_{\nu=N_{\text{MBS}}+1,\nu\neq\nu_u}^{N_{\text{MBS}}+N_{\text{HBS}}}\mathbf{H}_{u,\nu}(k)\mathbf{P}_\nu(k)\mathbf{x}_\nu(k)}_{\text{femto interference}} + \mathbf{W}_u(k)\mathbf{n}_u(k). \end{aligned} \tag{2.8}$$

$\mathbf{H}_{u,\nu} \in \mathbb{C}^{(M_u \times M_{\text{BS},\nu})}$ describes the MIMO channel matrix from BS ν to user u, where M_u denotes the number of antennas at the u-th user and $M_{\text{BS},\nu}$ the number of antennas at the BS ν. $\mathbf{P}_\nu$ is the diagonal transmit power matrix of size $(M_{\text{BS},\nu} \times M_{\text{BS},\nu})$ with limited total transmit power $\text{trace}(\mathbf{P}_\nu \mathbf{P}_\nu^T) \leq P_{\text{tx}}$, where P_{tx} is the maximum transmit power and $\mathbf{x}_\nu$ denotes the transmit signal vector $(M_{\text{BS},\nu} \times 1)$ of BS ν. $\mathbf{n}_u \in \mathbb{C}^{(M_u \times 1)}$ is the zero mean additive white Gaussian noise (AWGN) noise vector at user u. With the discrete time left out, the inter-cell signal-to-interference and noise ratio at user u computes to

$$\gamma_u = \frac{\mathbf{W}_u\mathbf{H}_{u,\nu_u}\mathbf{P}_{\nu_u}\mathbb{E}\left[\mathbf{x}_{\nu_u}\mathbf{x}_{\nu_u}^H\right]\mathbf{P}_{\nu_u}^H\mathbf{H}_{u,\nu_u}^H\mathbf{W}_u^H}{\mathbf{W}_u\left(\mathbf{R}_{\text{int fem}} + \mathbf{R}_{\text{int mac}} + \mathbf{R}_{\text{noise}}\right)\mathbf{W}_u^H}, \tag{2.9}$$

with the covariance matrices of the femtocell interference $\mathbf{R}_{\text{int fem}}$, the macrocell interference $\mathbf{R}_{\text{int mac}}$, and noise $\mathbf{R}_{\text{noise}}$, respectively. The aim of interference coordination is to find a robust solution which adapts to different scenarios. The inter-cell-interference can be lowered by coordinating the usage of available resources. This can be done by means of usage of only sub-parts of the overall spectrum in each cell. Lower interference leads to higher capacity per resource but lower available resources lead to lower capacity. Hence, a trade off between interference and higher amount of available resources has to be found. In LTE overlapping or collision of resource blocks leads to signal distortion. Interferences lead to signal degradation and can cause that the received signal cannot be demodulated correctly or just a small throughput to guarantee correct demodulation is possible. This can be seen with the definition of the SINR $\gamma_{u,\nu_u,p}$ of user u assigned to BS ν_u on RB p. For single-input single-output (SISO) transmission and receiver u on RB p we get:

$$\gamma_{u,\nu_u,p} = \frac{P_{S,\nu_u,p}\left|h_{u,\nu_u,p}\right|^2}{\sum_{\nu\in\psi} P_{S,\nu,p}\left|h_{u,\nu,p}\right|^2 + P_N} = \frac{P_{S,\nu_u,p}\left|h_{u,\nu_u,p}\right|^2}{\sum_{\nu=1,\nu\neq\nu_u}^{N_{\text{HBS}}+N_{\text{MBS}}} P_{S,\nu,p}\left|h_{u,\nu,p}\right|^2 + P_N}, \tag{2.10}$$

with the transmit power $P_{S,\nu_u,p}$ of BS ν_u on (physical) RB p and being $h_{u,\nu_u,p}$ the channel

between BS v_u and MS u and $h_{u,v,p}$ the channel between BS v and MS u on RB p, whereas MS u is connected to BS v_u. The set of interferers is given by ψ and the noise power is $P_{\mathrm{N}} = N_0 B_{\mathrm{RB}}$ with noise power density N_0 over the bandwidth of one RB. The task of interference coordination consists of reducing the interference from other cells in order to increase the SINR to improve the user and therewith the overall system throughput. The channel capacity for user u computes to

$$C_u = \sum_{p=1}^{N_{\mathrm{RB}}} B_{\mathrm{RB}} \mathrm{ld}(1 + \gamma_{u,v_u,p}), \tag{2.11}$$

with the bandwidth per resource block B_{RB} and the number of resource blocks N_{RB}, if all resource blocks N_{RB} are assigned. The upper bound on the achievable rate for user u is a truncated function due to modulation and coding of the channel capacity. The total rate computes as the sum of the rates per individual resource block and increases with better SINR but is limited by the selected modulation and coding scheme. A balance between increased coordination which can increase the performance of the network but also increases the backhaul traffic and the latency has to be found. Static or adaptive algorithms which restrict the usage of resources reduce the degree of freedom on the one hand, but reduce interference on the other hand. Optimizing the overall system throughput by tuning the usage of resources might result highly unfair where the QoS constraints might not be given. As a result a trade-off between maximizing the overall network performance under consideration of fairness for weak users is necessary.

2.4.2 Interference Coordination between Macrocells

In a macro-cellular network the transmit power of the base stations in each cell is similar. One cell can be divided into the cell center and the cell edge. In contrast to the center of the cell, the interference situation at the edges of the cell is critical and has to be paid attention by the applied interference management. Interference management can be divided into interference cancellation, randomization, and coordination or avoidance. With interference cancellation, interference suppression is performed at the user terminals and employs multiple receive antennas. The idea with interference randomization is to randomize interference signals by means of cell-specific scrambling and interleaving using a scrambling code and an interleaving sequence to whiten the interference. Frequency hopping of different kinds is also proposed with it. Interference coordination applies restrictions to the resource management in a coordinated way between base stations. Restrictions may be in usage of time/frequency resources, code parameter, spatial resources or restrictions on the transmit power level at certain time/frequency resources. [52], [53], [54], [55] give an overview on inter-cell interference coordination (ICIC) in macrocell networks. Basically the techniques can be divided into static techniques like hard frequency reuse (HFR), partial frequency reuse (PFR), soft frequency reuse (SFR), and incremental frequency reuse (IFR) [56] and dynamic techniques like adaptive power control or a central coordinator.

Static ICIC techniques based on the reuse factor use different frequency reuse patterns which describe the maximum allowed amount of frequency sets. With HFR (this method has already been used in GSM) a static reuse factor F describes the cluster size of base stations which use disjunctive frequency parts [57]. The reuse factor is defined as the quotient of the overall bandwidth B_{tot} and the usable bandwidth which is allowed in the cell B_{al}.

$$F = \frac{B_{\text{tot}}}{B_{\text{al}}} \tag{2.12}$$

A reuse factor of $F = 3$ depicted in Figure 2.18 tells, that three adjacent cells A, B, and C use non overlapping frequency parts Δf_1, Δf_2, and Δf_3, respectively, which leads to a structure where neighboring cells do not use the same frequency.

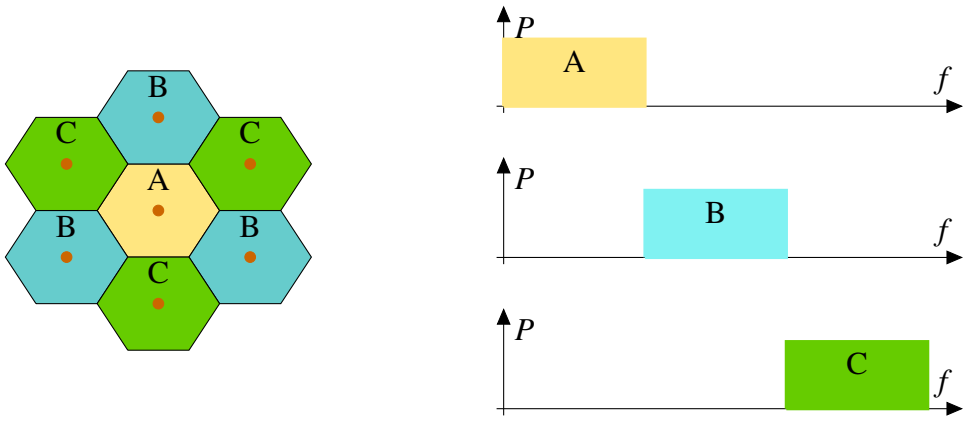

(a) Cellular Layout (b) Fixed reuse 3

Figure 2.18: Example of hard frequency reuse with fixed reuse factor 3

With fractional frequency reuse (FFR) (in literature also referred to as PFR), the overall bandwidth is divided into two parts, as can be seen in Figure 2.19a. One uses an HFR approach, the other allows a reuse factor of one in this subpart. The HFR part can be given to the cell edge users to reduce the impact of interference in the neighboring cells whereas the other part is given to the cell center users. Such a configuration tries to provide the cell edge users a better interference situation but reduces the impact on the other users with a too restrictive reuse pattern. A power control can be introduced with different power levels at the particular frequency parts.

A third method SFR, an extension of the reuse $F = 1$ scenario, divides the available bandwidth into several parts. An exemplary version with three parts is given in Figure 2.19b. The idea behind is to provide the cell edge users with a scenario similar to reuse $F = 3$ but not to restrict the other part completely. So one part can be used with high transmit power by one cell whereas the other cells can transmit with reduced power. As a result, each cell uses the whole bandwidth but with different power levels.

3GPP LTE provides different indicators which can be exchanged between base stations via the X2 interface [58] [59]. These are on the DL relative narrowband transmit power (RNTP)

which reactively or proactively informs neighboring cells if for a specific RB of DL transmission the transmit power is below a defined threshold and gives information on the RB with users of critical interference situations requesting the neighboring cell to avoid them (transmitted every 200ms).

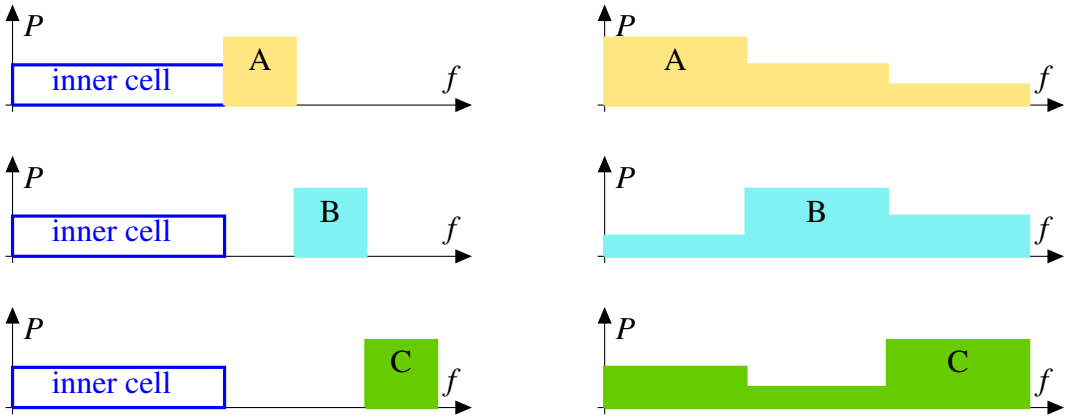

(a) Partial frequency reuse (b) Soft frequency reuse

Figure 2.19: Comparison of inter cell interference coordination in homogeneous networks

On the uplink the proactive high interference indicator (HII) informs the neighboring cells on planned UL transmission of its cell edge users which can result in high interference for them in order to request the neighbors not to schedule their own cell edge user on the specified RBs. This results in a reduced level of interference in both cells. Further the reactive overload indicator (OI) is used to exchange interference plus noise power measurements between base stations. The addressee of the indicator message can decide to change its resource assignment accordingly in order to resolve critical situations (transmitted every 20ms as the HII). Adaptive techniques are adaptive power control in each base station and techniques with a central controller.
ICIC can be on the one hand proactive, preventing interferences a priori, independently if interference actually occurs or not. On the other hand it can be reactive, adapting to occurred interference trying to eliminate or avoid further interference.

2.4.3 Interference Coordination between Different Cell Hierarchies

In heterogeneous networks not only the transmit signals within one layer can interfere with each other, but also signals with those of another layer. When BSs of different layers are transmitting simultaneously in the same frequency band interference is a major issue limiting the network performance [60]. In a multi-layer network the different access methods as open, close, and hybrid access introduced in Section 2.3 have to be taken into account. Methods of spectrum allocation within a multi-layer network are categorized in Table 2.4 [61] [49] and an exemplary resource assignment with lowered interference situation for a part of the users is depicted in Figure 2.20 according to [49].

Table 2.4: Overview on the allocation of spectrum within a network with macro-cells and small cells

Dedicated Channel Assignment	Partial Co-channel Assignment	Co-channel Assignment
Partitioned spectrum usage: licensed spectrum divided into separate portions → Lower cross-layer interference, but reduced available amount of spectrum	Spectrum usage mode chosen, depending on the trade-off between larger bandwidth and cross-layer interference	Shared spectrum: Co-channel frequency reuse → More available amount of spectrum, but higher cross-layer interference

On the left hand side of Figure 2.20 the heterogeneous network with one MBS and 4 LBS, where each supplies a small cell, is shown. The sub-channel allocation for all users UE $1,\ldots,7$ is drawn at the right hand side of Figure 2.20 where a gray shaded square indicates the usage of the corresponding sub-channel for the considered UE. White squares indicate transmission free resources. The MBS assigns all sub-channels to its connected users MUE 5 to MUE 7. The orthogonal resource assignment for the users of the macrocell is an exemplary result of the scheduler. For example MUE 7 is scheduled on sub-channel one and two.

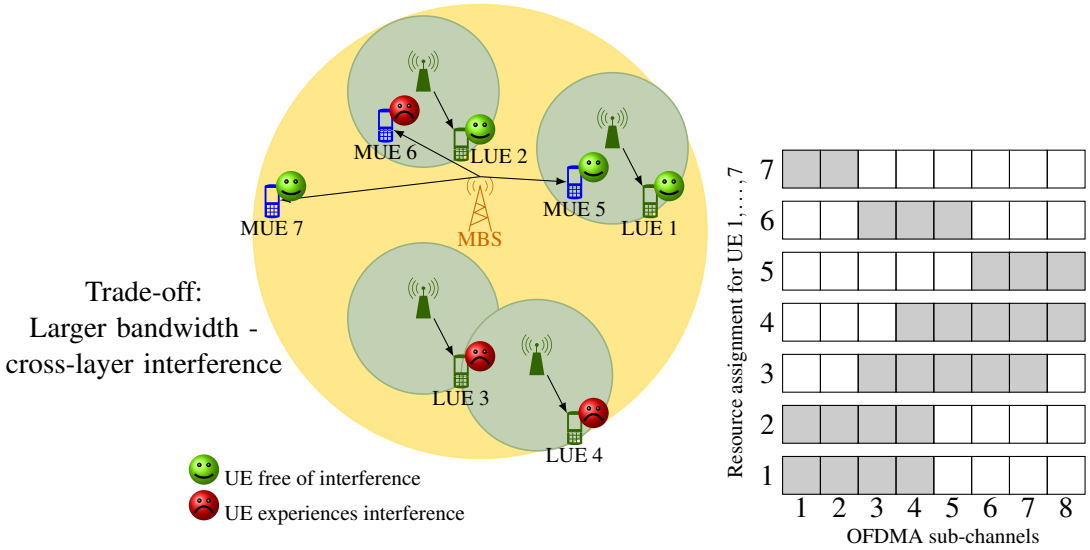

Figure 2.20: Overview on an exemplary allocation of spectrum within a network with macrocell and small cells

The setting in Figure 2.20 offers a beneficial situation for LUE 1 and 2 as well as MUE 5 and 7 indicated by the happy faces. Nevertheless, some users as MUE 6 and LUE 3 are still highly interfered. Thus, dynamic interference coordination techniques which adapt to the present interference situation are required.

The goal of interference coordination is to reduce interferences or lower the impact of interference. The easiest approach is to use different frequency bands for each layer. Thus,

the available spectrum can be assigned completely orthogonal into separated portions as denoted by dedicated channel assignment. The cross-layer interference is removed but this leads to significant lower data rates per layer as the reduced spectrum for transmission cannot be compensated by the better SINR. Partial co-channel assignment chooses the mode as a trade-off between larger bandwidth and interference across layers. In co-channel assignment mode the total available spectrum is shared. In here critical interference situations occur and have to be addressed by the network. For pico base stations set up by the network operator this can be optimized in the planning phase and communication and coordination can be foreseen. Differently, femtocells are set up by the customer. Due to the high number of cells and the uncertainty of number and position of the small cells in the network planning phase in a heterogeneous network, self-configuration and self-optimization is an important aspect. The HBS has to sense the environment and tune its own parameters (for a PBS this is optional). The self-configuration and self-optimization procedure can be divided into two parts. First, in the sensing phase each LBS has to learn about the state of the network, the channel conditions and has to establish knowledge of the surrounding MBS and LBSs and on their spectrum allocation. This can be done via network listening, exchange of information between LBS and MBSs over a direct link, broadcast messages or by measurement reports of the LUE. In the second phase, the LBS parameters have to be tuned. Self-configuration initializes the inceptive parameter settings based on the information gained in the sensing phase. Self-optimization adapts and optimizes the parameter settings dynamically on-line to changing environments and traffic-demands.

Considering ICIC in heterogeneous networks, one approach for PBS scenarios is to adapt the transmit power in the MBSs [62]. This increases the throughput in picocell hotspot scenarios and increases the benefit of cell range extended picocells. However in HBS scenarios, where some users of the MBS cannot be handed over to the small cell, this leads to a performance loss in the macrocell layer. An FFR based approach for ICIC with minimal but still necessary signaling overhead is introduced in [63]. It divides the spectrum in seven uneven parts and allocates these to predefined locations of the macrocell, again under consideration of an inner cell region. Within each of the six sectors of the macrocell not the whole spectrum is available. [64] proposes a similar FFR method, where users are divided according to their position to inner and outer cell location, to address interference between macrocells and femtocells. It is a static approach which has to be predefined and again some limits are set on the resources of the macrocells. Both FFR based schemes require the MBS to be adapted and be part of the interference coordination.

[65] considers an ICIC technique with almost blank subframe (ABS) offsetting based on multistage bargaining, where the bargaining situation is divided into two stages. Bargaining represents a situation with conflicting interests. In here, the blanking rate for the macrocells can be reduced but still the macrocell spectrum is reduced which is critical in combination with CSG femtocells. In LTE-A starting from Release 10, enhanced inter-cell interference coordination (eICIC) based on frequency, power, and time strategies is introduced in order to face the demand of new techniques. The first two are taken from previous releases whereas the time strategy is evolved. The idea behind is to protect the transmission by partially blank-

ing subframes which leads to a nearly interference free situation in the protected cell. For the tranquilized subframes the ABSs are used which contain no data and hardly any control information. In order to protect legacy standards further enhanced inter-cell interference coordination (feICIC) handles also the control channel limitations and introduces inter-cell interference cancellation on the receiver side [66]. Nevertheless, still communication between LBSs and MBSs is needed and pre-configuration of the ABS set is required.

Current research considers coordination of resources by means of a certain degree of the restriction of the resources in the small cells and macrocells, requiring some kind of communication up to even full knowledge of the present interference situation. Optimizing the overall network in a central controller would result in intensive computations and signaling which is hardly possible in real time and demanding backhaul capacity requirements. The advanced technique proposed in this thesis and described in the following offers a method which is located in the small cells, requiring only marginal data transfer for the initial setting and does not further demand the macrocell to adapt.

Chapter 3

Dynamic Interference Coordination Technique for Heterogeneous Networks

In a wireless cellular communication system with several base stations interference is present and is tremendous especially at the borders between the cells. As the interference situation is highly changeable in heterogeneous networks, dynamic interference coordination techniques are required. In particular, if the number of cells is high and existing MBSs should be used without changes, only dynamic approaches, without a significant amount of communication, are useful. The advanced interference coordination technique developed and evaluated in this thesis adapts to the interference situation dynamically. Furthermore, the implementation and intensive investigations by means of system-level simulations are an integral part of this work. As the algorithm is performed only in the LBS, the MBSs do not have to be adapted.

This chapter (i) introduces the advanced interference coordination technique, (ii) describes its concept in Section 3.1, (iii) depicts the sequential deterministic and the simultaneous probabilistic algorithm in Section 3.3.1 and Section 3.3.2, respectively, and (iv) gives an application scenario in Section 3.4. The advantageous fast adaptation to the interference situation is shown in Section 3.6. Section 3.7 summarizes the findings on the proposed dynamic interference coordination technique given within this chapter.

The interference coordination techniques determine the present interference situation for the current user assignment which is also part of current research [47]. Current research pays much attention to the interference situation between small cells and macrocells. Techniques which reduce the bandwidth in the macrocell in order to present the small cells a very good channel can be applied to picocell settings but especially in CSG femtocell scenarios, where the macrocell users can not be handed over to the interfering small cell, this is not acceptable. Further literature suggests techniques which require inter-cell communication. Even though the logical X2 interface can be used, further complexity and latency is introduced in the network. Methods which require full knowledge of the present channel in the macrocell as well as the small cells lead to intensive computations which is hardly possible in real time. Additionally, the backhaul capacity restrictions are not met. The presented advanced interference coordination method in this work does not need communication between the

cells and requires only marginal contribution of the MBS [67] [68] [69]. The first of the two approaches requires a table to determine the order to change the resource assignment and synchronized cells are advantageous. The second approach just requires the information of the overall available patterns in the small cells and leaves the MBS completely unchanged compared to the homogeneous setting.

3.1 Concept

The interference avoidance scheme reduces the impact of the small cells on the macrocellular network and other surrounding cells by restricting some resources of the small cell. Small cells as the hypernym for the cells as picocells, femtocells, and relays are served by an LBS and overlay the macrocell layer. Thereby they provide a dynamic coverage range to close coverage holes or gain higher throughput. Offloading of traffic and power saving aspects due to the shorter distances between transmitter and receiver is a key factor especially in dense urban scenarios. While in the first-mentioned case with coverage holes, interference is no issue, in the latter case with dense deployment scenarios, the interference situation has to be analyzed and measures to encounter this have to be taken. Consequently, a method which considers these aspects has been developed. Therein, the overall amount of resources is divided into a certain amount of sub-resources, further called resources.

The target of this advanced algorithm is to control the interference between the LBSs and to minimize the interference for macro users caused by LBSs, by using a subset of the overall resources in each small cell. In order to keep the small cells being able to be used without fundamental changes in the specification, the macrocells are unaltered and can use all resources. Consequently, the core functionality is located inside the small cells. The reuse of resources, when applied to the frequency the spectral reuse, is autonomous for each LBS. The total available pool of resources $\mathcal{R}_{\text{Pool}}$ is divided into resources which are indicated by their number

$$\mathcal{R}_{\text{Pool}} = \{1, 2, \ldots, n, \ldots N_{\text{R}}\}, \tag{3.1}$$

where N_{R} stands for the total number of available resources.

A resource is defined over the physical variables time, frequency, transmit power, and space, when applied to a heterogeneous mobile network. The entirety of all resources forms the pool of resources. When applied to the frequency dimension, the overall resources are given by the system bandwidth B_{tot}. Assuming resources of the same extent leads to the size for one resource of $S_{\text{R}} = \frac{S_{\text{eR}}}{N_{\text{R}}}$, where S_{eR} gives the overall size of the resources. A subset of the overall available resources could be exclusively used by the MBS to guarantee a minimum performance for cell-edge users in the macrocell. The number of resources for exclusive MBS usage is denoted by $N_{\text{R,MBS}}$. The introduction of the exclusive resources would lead to a slight reduction of the potential available resources for the LBSs. The sum of the size of all available resources of the LBSs is $S_{\text{eR,LBS}} = S_{\text{eR}} - N_{\text{R,MBS}} \frac{S_{\text{eR}}}{N_{\text{R}}}$.

Using (partially) disjunct sets of resources for LBSs minimizes the interference between the LBSs. The characteristics of this dynamic decentralized technique are as follows: The knowledge of the interference situation at the LBS is required. This information can be gained with (i) a DL receiver or (ii) measurement reports at the UEs which are transmitted to the LBS. A DL receiver is co-located with the LBS and measures the interference from the surrounding BSs during downlink transmission. The approach is distributed, located in each LBS. No communication is needed between LBS and MBS or neighboring LBSs. The transmit power in the LBS is fixed, in case the transmit power itself is not part of a resource. The resource allocation is based on a non-cooperative game where the players compete and act in a selfish way. The selection of resources by each LBS individually is the result. The basic principle of the inter-cell interference coordination (ICIC) algorithm is the allocation of resources based on Game Theory. It models a decision situation in which multiple players decide about their resource allocation. The strategic interdependence between the decisions of the players is given.

Considering a heterogeneous mobile communication network with macro and small cells operating within one component carrier, the advanced interference coordination algorithm works as follows: The overall available resources are divided into N_R parts (when applied to the spectrum where resource patterns in the frequency domain are used $N_\mathrm{R} = N_\mathrm{s}$, whereas N_s defines the total number of available subbands). The sum over all resources N_R forms the pool of resources $\mathcal{R}_\mathrm{Pool}$, with $|\mathcal{R}_\mathrm{Pool}| = N_\mathrm{R}$. The resources can, but do not have to, be of same size.

The set which indicates the available resources in LBS i is a subset of the resource pool: $\mathcal{R}_i \subseteq \mathcal{R}_\mathrm{Pool}$. The number of resources available for the LBS i is $|\mathcal{R}_i| = N_{i,\max} \leq N_\mathrm{R}$ which is limited by the total resources.

The amount of resources D_i which the LBS i is allowed to use for transmission is $D_i \leq N_{i,\max}$ and has to be determined as a balance between user data requests and interference level in the surrounding.

A resource pattern $\mathfrak{s}$ is a combination of the available resources. It comprises at least one resource and at the maximum all resources N_R. Built thereof, $\mathcal{S}$ is a list which contains all possible resource patterns $\mathfrak{s}$. The selected resource pattern in LBS i $\mathfrak{s}_i$, with altogether $D_i = |\mathfrak{s}_i|$ resources, is one element of the resource pattern list $\mathcal{S}$. If all N_R resources are assigned, the number of usable resources is equal to the number of elements of the resource pool, consequently $D_i = |\mathcal{R}_\mathrm{Pool}|$ and $\mathfrak{s}_i = \mathcal{R}_\mathrm{Pool}$.

The MBSs do not participate in the resource allocation game but are eligible to use all available resources. As a result, their resource pattern is $\mathfrak{s}|_\mathrm{MBS} = \mathcal{R}_\mathrm{Pool}$. This guarantees that a MBS does not experience a reduction of the resources which is for example equivalent to bandwidth, especially relevant if just a few or just one LBS are active in its service area. In order to protect the users connected to the MBS, one or more resources can be exclusively assigned to the MBS where no LBS can transmit. Within these protected resources the user of the MBS can connect to their BS without interference from all small cells.

LBS i selects one resource or in an extension to the algorithm several resources with the obligation to minimize its own interference based on the utility values $U_{i,n}$ described in detail within Section 3.2. The pattern of the selected resources is $\mathfrak{s}_i \in \mathbb{S}$. The selection of resources is done without signaling between different BSs which results in a non-cooperative approach.

The procedure of the algorithm can be either sequential, where only one LBS is active and decides on the updated resource allocation per round or simultaneously probabilistic, where all LBSs decide in parallel according to a certain probability whether to update their resource allocation or not. Both algorithms use multiple rounds but the simultaneous probabilistic approach shows a faster convergence behavior for realistic deployments, which is shown in Section 3.6 in detail.

3.2 Utility Function

The utility value for each resource $n \in \mathcal{R}_i$, of LBS i, is a measure for the average overall throughput on this resource n in the LBS i. In case $D_i = N_{i,\max} = N_\mathrm{R}$ all resources are available and the assignment of resources can directly be done. In all other cases, the assignment will be based on the utility values. Each resource consists of a certain number of resource units which denote the smallest unit. The set of resource units within resource n is $\mathcal{R}_n$, whereas one element thereof is denoted by $r_n \in \mathcal{R}_n$. The utility value for LBS i on resource n is

$$U_{i,n} = N_n \mathbb{E}\left[U_{i,r_n}\right] = N_n \bar{U}_{i,r_n}, \tag{3.2}$$

with the number of resource units within resource n as $N_n = |\mathcal{R}_n|$, the expectation $\mathbb{E}[\cdot]$, and U_{i,r_n} the utility value of a resource unit r_n [67]. The average utility over all resource units within resource n in cell i is denoted as $\bar{U}_{i,r_n}$. For the average utility value from (3.2) three definitions $\bar{U}_{i,r_n,1}$, $\bar{U}_{i,r_n,2}$, and $\bar{U}_{i,r_n,3}$ are given in the following based on (i) channel capacity, (ii) SINR, and (iii) average power of the interference, respectively. Considering the utility value based on channel capacity, the average utility of a resource unit computes as

$$\bar{U}_{i,r_n,1} = C_{i,r_n} = B_{r_n,n} \mathrm{ld}\left(1+\gamma_\mathrm{eff}\right) \left[\frac{\mathrm{bit}}{\mathrm{s}}\right], \tag{3.3}$$

with the bandwidth of a resource unit $B_{r_n,n}$ and the effective SINR of an equivalent AWGN-channel γ_eff. For continuous usage the average throughput of a resource unit corresponds to the channel capacity. Assuming $B_{r_n,n}$ is identical for all resources and $\gamma_\mathrm{eff} \gg 1$, a utility value based on the SINR can be expressed as a function of the average receive power $\bar{P}_\mathrm{rx}$, the interference power I, and noise power N approximately:

$$\bar{U}_{i,r_n,2} = 10\log\left(\frac{\bar{P}_\mathrm{rx}}{I+N}\right) = 10\log\left(\bar{P}_\mathrm{rx}\right) - 10\log\left(I+N\right)[\mathrm{dB}]. \tag{3.4}$$

The utility value based on an average interference power can be utilized, if the average receive power for all resource units of all resources n is identical

$$\bar{U}_{i,r_n,3} = -10\log(I)\,[\mathrm{dBm}], \tag{3.5}$$

with $I \gg N$ and where the receive power is determined by the product of transmit power and channel gain. All definitions from (3.3) - (3.5) use local interference information. In downlink this can be gained by measurements of a downlink receiver or measurement reports of the users which are fed back to the serving base station. For further analysis the definition of the utility according to (3.5) is used. The information of continuous measurements is used to determine up to date utility-values for step three in Figure 3.1 further explained in Section 3.3.

The LBS serving a small cell gains the information on the average interference on all resources n of the network by a downlink receiver or by measurement reports from the connected UEs, as described before. Each small cell i senses the environment of surrounding macro and small cells j, assuming normalized equal transmit power per resource pattern, on each physical resource n. Then the total interference suffered by cell i is

$$I_{i,n} \sim \sum_{j=1, j\neq i}^{N_{\mathrm{MBS}}+N_{\mathrm{HBS}}} |h_{i,j,n}|^2 b_{j,n}, \tag{3.6}$$

where $b_{j,n} = 1$ denotes that resource n is used by cell j and $b_{j,n} = 0$ if it is not used and thereby adds no interference. The channel gain between cell j and considered small cell i on resource n is given by $|h_{i,j,n}|^2$.

The utility for LBS i depends on the negative interference situation within the own newly selected resources

$$\mathrm{U}_i(\mathbf{b}_i, \mathbf{b}_{-i}) = -\sum_{n=1}^{N_{\mathrm{R}}} b_{i,n} I_{i,n}. \tag{3.7}$$

where $\mathbf{b}_i = (b_{i,1}, \ldots, b_{i,n}, \ldots, b_{i,N_{\mathrm{R}}})$ is the resource allocation vector of LBS i. One element $b_{i,n}$ denotes that resource n is used by cell i with $b_{i,n} = 1$ or that it is not used and thereby adds no interference with $b_{i,n} = 0$. $\mathbf{b}_{-i}$ is the resource allocation of all macro and small cells other than the considered small cell i. It is defined as $\mathbf{b}_{-i} = (\mathbf{b}_1, \mathbf{b}_2, \ldots, \mathbf{b}_{i-1}, \mathbf{b}_{i+1}, \ldots, \mathbf{b}_{N_{\mathrm{MBS}}+N_{\mathrm{HBS}}})$ where $\mathbf{b}_i$ is excluded.

As a summary, the utility for LBS i is a function of its resource allocation vector $\mathbf{b}_i$ and the resource allocation vector $\mathbf{b}_{-i}$ of all interfering BSs together.

A non cooperative game, within the framework of game theory, shows a situation where each individual player (a so called decision maker) encounters a strategic interdependent situation at the moment the players have to decide on their next actions [69]. The decisions are based on the utility U which in here contains the current interference situation. Result of the method is the resource allocation vector $\mathbf{b}_i$ which maximizes the utility and thereby minimizes the interference value. Assumption for the moment is, that each small

cell demands a fixed number of resources $D_i = D$. Thus, for selecting $D > 0$ also the trivial solution of not scheduling any resources which would lead to an interference free case is avoided. It follows that the sum over the entries of the resources allocation vector $\mathbf{b}_i$ is equal to D: $\sum_{n=1}^{N_R} b_{i,n} = D$. The utility function U_i maps the decisions of the own as well as of the surrounding cells to a real value. The procedure is non-coordinative as all small cells try to reduce their interference situation and thereby also their interference impact on the other cells which results in using different resources in close by cells. [69] shows that games based on sequential deterministic decisions result in the Nash equilibrium as a stable state but require a serialization mechanism to prevent two cells to adapt simultaneously.

The linear wideband SINR γ_w is the power of the receive signal P_{rx} divided by the sum of the received powers of the interfering signals $P_{rx,\nu}$ plus noise:

$$\gamma_w = \frac{P_{rx}}{\sum\limits_{\forall \nu \in \psi} P_{rx,\nu} + P_N}, \tag{3.8}$$

with the set of interferers ψ. And in dB $\gamma_w|_{dB} = 10\log(\gamma_w)$.

In order to loosen the constraint of limiting more resources in the small cells than required, an interference factor threshold I_{th} is introduced, which can optionally be applied for example in low density scenarios. The small cell continuously scans its environment by the DL receiver. When the detected interference I gets below a predefined threshold I_{th}

$$I < I_{th}, \tag{3.9}$$

all resources can be assigned without restrictions, or to be more conservative power control techniques with reduced power can be applied. The power control techniques are not further investigated within this work as a lot of research has been already done [70] [71] [72].

3.3 Principle of the Inter-Cell Interference-Coordination Algorithm

The procedure of the algorithm can be either sequential, described in Section 3.3.1, where only one LBS is active and decides on the updated resource allocation per round or simultaneously probabilistic where all LBSs decide in parallel according to a certain probability whether to update their resource allocation. Both algorithms use multiple rounds, but the simultaneous probabilistic approach shows a faster convergence behavior for situations where a lot of LBSs are closely located. Section 3.6 shows this in detail.

The step-by-step procedure of the advanced interference coordination algorithm is given in Figure 3.1. The algorithm is located in each LBS without any communication between the cells. Starting point is when an LBS is reset or installed at a new location, periodically after some pre-configured time or when requested by a higher layer entity as the RRM in order to

investigate the current status of the interference situation. It can stop after the configuration of the new resource pattern or continue in order to be able to react on subsequent changes of the interference situation.

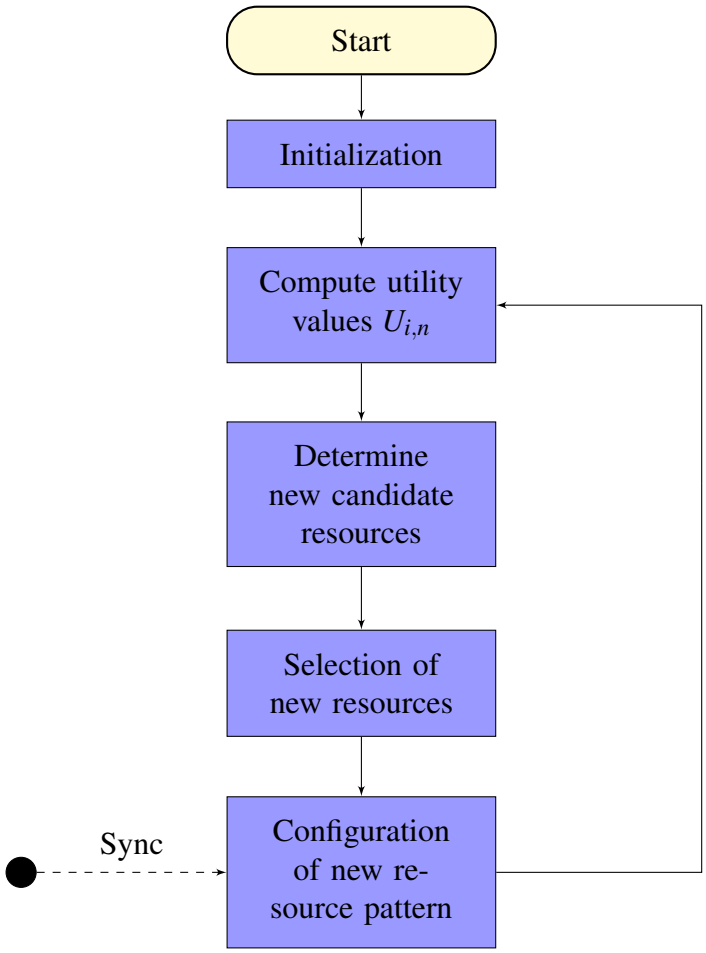

Figure 3.1: Schematic flow of advanced inter-cell interference-coordination algorithm

Before the start is triggered, first the required parameters have to be present. The definition of the resource set as a subset of the resource pool is given in Section 3.1. The overall allowed number of resources D_i from the available resources is required. The number can be preconfigured or determined as a function of the determined average SINR. In case $\mathfrak{s}_i = \mathcal{R}_{\text{Pool}}$ the determination is obsolete and all resources can directly be configured for transmission.

After the initialization step, the utility values $U_{i,n}$ for the individual resources are determined with the information about the interference from the downlink receiver or by measurement reports as described in detail in Section 3.2.

When the utility values are in place, the resource candidates can be determined according to (i) the sequential deterministic method based on selecting resources with highest utility value or (ii) the simultaneous probabilistic approach based on the selection of resources with

preselection of probable candidates. Details on the two methods are shown in Section 3.3.1 and Section 3.3.2.

When appropriate resources are determined the new resources are selected and subsequently configured to reflect the current interference situation. The trigger for the reconfiguration of the new determined resource pattern can be periodic and synchronized for all base stations. Information on the reconfiguration time index can be signaled by the MBS or the RRM under consideration of a realistic representation of the interference situation and accuracy of the utility-value computations.

The MBSs do not participate in the resource allocation procedure, but are eligible to use all available resources. This guarantees that an MBS does not experience a reduction of the bandwidth if just a few or just one LBS is active in the MBS service area. The actual usage of the determined resource pattern can be triggered by the MBS or the RRM and is denoted by Sync within Figure 3.1.

The algorithm defines those resources for transmission in each small cell which are least interfered. This is done based on sequential deterministic and simultaneous probabilistic decisions [69], extended to the small cell scenario.

Henceforth, a resource is equivalent to a subband and at least one subband is going to be exclusively used by the MBS, thus no LBS can transmit in this band to protect MS of the highest layer to connect to the MBS.

3.3.1 Sequential Inter-Cell Interference-Coordination

Target of the ICIC algorithm based on game theory, which works in each small cell independently, is to minimize the interference for the macrocell users and to control the interference impact between the small cells. The overall spectrum is split up in subparts [69]. The macrocell user can be associated with an exclusive part to operate in a dedicated channel assignment mode. This guarantees a minimum performance in throughput for the cell edge macro users. The remaining resources are used in co-channel assignment mode. They can be used for transmissions inside the small cells whereas the macrocell BS can use all subbands for transmission. To minimize the own interference and thereby also the interference created in the other cells, the LBSs act as players in a game which results in a resource allocation of the least interfered resources.

First, within each LBS $i = 1, \ldots, N_{\mathrm{HBS}}$, the interference situation $I_{i,n}$ on each resource n is determined according to (3.6). In a **second step** the resources are ordered from low to high interference values. When an LBS has its turn, the process of resource selection starts. Then **third**, the D_i resources which provide least interference in the LBS i are selected for transmission. The reached state might be sub-optimal, nevertheless the interference level can be significantly reduced. The benefits of this technique which are easy implementation, no need for intensive communication and pre-configuration empower its application. During

the system-level simulations this algorithm is performed at the beginning of each scenario drop. The method is non-cooperative, but sequential and it's mandatory that just one cell actively changes the resource allocation at a time.

3.3.2 Probabilistic Inter-Cell Interference-Coordination

Adding a probabilistic element into the existing sequential deterministic algorithm from Section 3.3.1 which is based on parallel probabilistic decisions by the LBSs loosens first the constraint of adaptations one after another and second as shown below, the dependency on the number of small cells for convergence of the interference coordination algorithm. Again, the resources are divided into parts in the same manner as in Section 3.3.1.

A set of candidate resources which are least interfered has to be found. If there are candidates which show a better interference value, the LBS deviates from its previous decisions only with a certain probability. This helps that neighboring base stations with a similar interference situation do not update their resource allocation in parallel, which could result in a higher interference level.

The basic steps of the algorithm are as follows: **First**, the interference in all LBSs $i = 1,\ldots,N_{\mathrm{HBS}}$ has to be tracked. Again, the interference situation $I_{i,n}$ on each resource n is determined according to (3.6) which can be gained by measurement reports from the users connected to the local base station or by a downlink receiver. The LBSs continuously perform the process of reselection in parallel within each small cell until a minimum is achieved. Afterwards a restart is triggered from outside, after some pre-determined time interval or according to internal measurements.

In a **second step** D_i resources which experience the least interference in LBS i are compiled as the set of candidates. In the **third step**, the determined candidates are compared one by one with the previous assigned resources. In case the interference situation of the candidate resource is better than the original it is selected proportionally to a certain probability P_i. Otherwise the original remains in the set. In case the candidate is selected, it is removed from the candidate list.

In **step four**, the D_i determined resources are compiled and form the new set of selected resources for transmission $\mathfrak{s}_i$. The advantage of this algorithm compared to the sequential deterministic algorithm is the much faster adaptability for reasonable numbers of small cells and the simultaneous decisions of the players abandons the need for the LBSs to know whether they are the next in line to play. This method scales very well also in high density networks due to the simultaneous adaptation, without online communication. In this case the convergence is not guaranteed due to the probabilistic nature [69], nevertheless in real systems also manifested by intensive simulation throughout this work it results in desirable interference situations. On the whole, all LBSs decide at the same time on new resource assignments but change their resource allocation only according to a certain probability P_i.

In case two resources experience almost equal interference situations it is beneficial not to change the resource assignment. This can support the straighter convergence behavior but the allowed interference margin has to be defined carefully.

The interference margin I_m can be defined in terms of a deviation probability P_m from the interference level $I_{\text{previous selection}}$ of the previous selection

$$I_\mathrm{m} = P_\mathrm{m} I_{\text{previous selection}}, \tag{3.10}$$

or a predefined absolute value $I_{\mathrm{m,const}}$:

$$I_\mathrm{m} = I_{\mathrm{m,const}}. \tag{3.11}$$

The determined candidates are selected in case the interference on the new resource $I_{\text{candidate}}$ is lower than the previous together with the interference margin:

$$I_{\text{previous selection}} - I_{\text{candidate}} > I_\mathrm{m}. \tag{3.12}$$

3.4 Example of an Application Scenario

One application scenario could be a heterogeneous network with MBS and HBS. Thus, a small cell is in the following a femtocell, an LBS is an HBS and an LUE is an FUE (i.e. a user equipment connected to an FBS). The number of HBSs per MBS is ρ_HBS. This section gives an exemplary overview for a scenario with closed subscriber group (CSG) HBSs. With the CSG concept critical situations can occur, especially due to impossible handovers from MBS to FBS for the subgroup of MUEs which are not on the list of the CSG of the interfering HBS. Section 2.3.3 gives the details on the specialties of the HBSs which operate in CSG mode. A co-channel situation is considered which means that MBS and HBS use the same carrier.

When the resource usage for coordination is applied to the frequency dimension, the overall resources are given by the system bandwidth B_tot. Assuming resources of the same size, this leads to a bandwidth of $B_\mathrm{R} = \frac{B_\mathrm{tot}}{N_\mathrm{R}}$ per resource and the condition $N_\mathrm{s} = N_\mathrm{R}$. The overall available resources are divided in such a case, that the whole bandwidth in Figure 3.2 is divided into N_s, here $N_\mathrm{s} = N_\mathrm{R} = 5$ subbands which has shown to be a reasonable value by system-level simulations for the considered application.

A set of physical resource blocks (PRBs) or resources is exclusively used by the MBS to guarantee a minimum performance for cell-edge users in the macrocell marked red in Figure 3.2. Within this example the central subband, here subband three, is exclusively used by the MBS. This leads to a slightly reduced potential available bandwidth for the HBSs of $B_\mathrm{HBS} = B_\mathrm{tot} - \frac{B_\mathrm{tot}}{N_\mathrm{s}} = B_\mathrm{tot} - \frac{B_\mathrm{tot}}{5}$ denoted as the subbands 1, 2, 4, and 5 which is depicted in Figure 3.2.

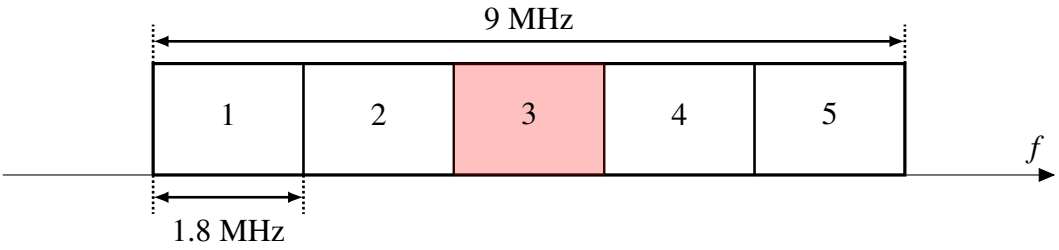

Figure 3.2: Example of a subband constellation with resource usage of $N_s = 5$ subbands, whereas one subband (marked with red) is reserved for users assigned to a macro base station

Using (partially) disjunct sets of PRBs for the HBSs minimizes the interference between HBSs. In order not to change the basic setup and reduce the bandwidth for the umbrella layer, the MBSs do not participate in the resource allocation game but contrary are eligible to use all available subbands. This guarantees that an MBS does not experience a reduction of the bandwidth and is protected if just a few or just one HBS is active in its service area. At least one subband is going to be exclusively used by the MBS, so no HBS can transmit in this band to protect MSs of the macrocell layer to connect to the BS. The HBS selects one resource n which can be composed of one subband or in an extension to the algorithm a set of subbands to minimize its own interference. This is done without communication between different BSs which results in a non-cooperative game.

Within the defined application scenario the number of resources is equal to the number of available subbands $N_R = N_s = 5$. The bandwidth per resource, which is in this example equivalent to a subband, is the fraction of total bandwidth and number of subbands: $B_s = B_R = \frac{B_{tot}}{N_R} = \frac{9\text{MHz}}{5} = 1.8\text{MHz}$. The overall available bandwidth in a femtocell is the difference from total and portion of the protection area of the MBSs and for one subband this is $B_{HBS} = B_{tot} - \frac{B_{tot}}{N_s} = 9\text{MHz} - \frac{9\text{MHz}}{5} = 7.2\text{MHz}$.

The set of resources in HBS i is a subset of the pool $\mathcal{R}_i = \{1,2,4,5\} \subseteq \mathcal{R}_{Pool} = \{1,2,3,4,5\}$ where the middle subband three is not included. The number of overall available resources is $N_{i,max} = 4$ here $N_{i,max} < N_s = 5$. The number of actually allowed subbands $D_i \in \{1,2,3,4\} \leq 4$, ranges between one and 4. The initial resource assignment set, also denoted as resource pattern, $\mathfrak{s}_i$ can be selected randomly, pre-configured from the macro base station or as the previous set before shut down.

Considering the given application scenario with five subbands in total, where one is exclusive for the MBSs Figure 3.3 draws all possible patterns. Subband three is exclusive for the MBSs and highlighted in red. The resources allowed within one pattern $\mathfrak{s}$ are highlighted in blue, whereas D_i is the sum thereof within one pattern. In Figure 3.3c $D_i = 3$ for example.

N_P denotes the number of overall resource combinations or subband combinations for one fixed D_i. For a configuration according to Figure 3.2 with the number of allowed subbands $D_i = 1,\ldots,4$ as depicted in Figure 3.3, N_P results in 4, 6, 4, and 1 correspondingly.

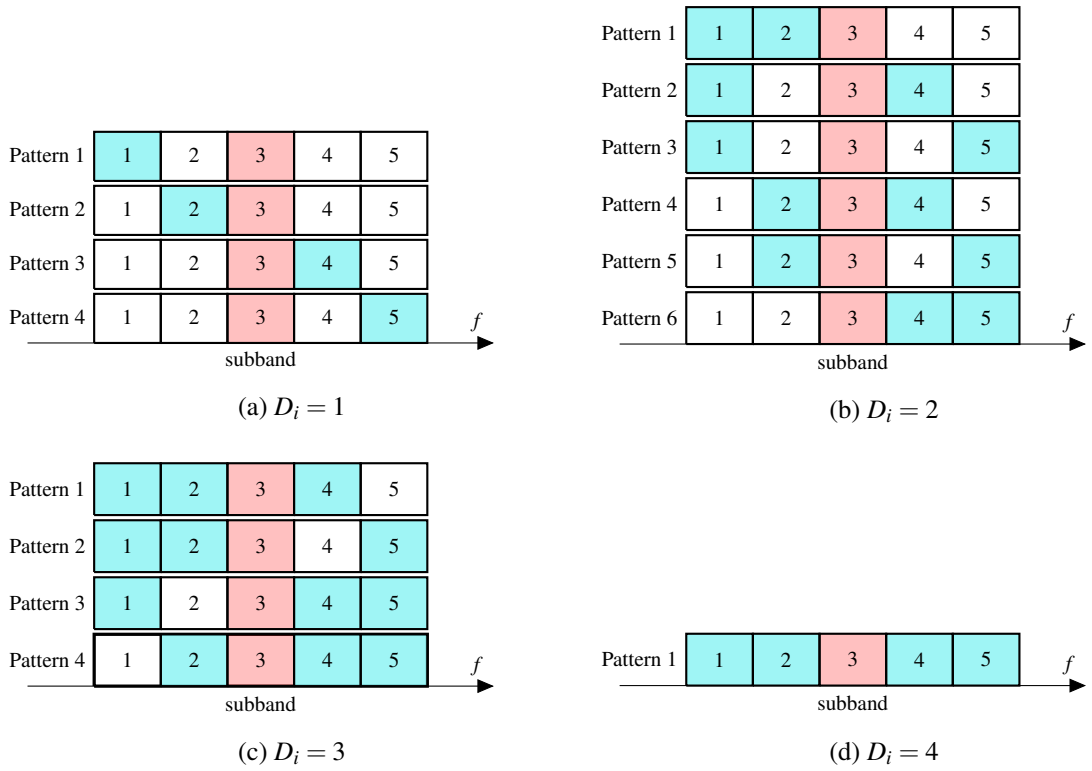

(a) $D_i = 1$ (b) $D_i = 2$

(c) $D_i = 3$ (d) $D_i = 4$

Figure 3.3: Available resource sets for $N_s = 5$ subbands and varying number of allowed resources D_i in cell i

The procedure of the algorithm can be either sequential, described in Section 3.3.1, where only one HBS is active and decides on the updated resource allocation per round, or simultaneous probabilistic where all HBSs decide in parallel according to a certain probability P_i whether to update their resource allocation. Both algorithms use multiple rounds, but the simultaneous probabilistic approach shows a faster convergence behavior for situations where a lot of HBSs are present. Section 3.6 shows this in detail.

An exemplary resource assignment is given in Figure 3.4 with $D_i = 2$. Within this application scenario seven UEs are located within the three sectors of one central cell. The total number of HBSs within this example is three, whereas here the number of HBSs per MBS ρ_{HBS} differs between the MBSs, but is on average $\bar{\rho}_{\text{HBS}} = 1$. The users of the MBS can use the whole bandwidth indicated with blue color for all subbands. In order to provide an advantageous interference situation, the scheduler in the MBS will assign MUE 1 resource blocks within subband one, three and five. The resources of subband two and four could be for example scheduled to MUE 2. This could be the result of the proportional fair scheduler. In order to provide the users of the tightly deployed femtocells 2 and 3 with a good situation, the proposed decentralized interference coordination technique will result for this setting in a configuration with orthogonal subbands by evaluation of the local interference information. The FUE 2 gets subband 2 and 5, whereas FUE 3 can use subband 1 and 4 for transmission.

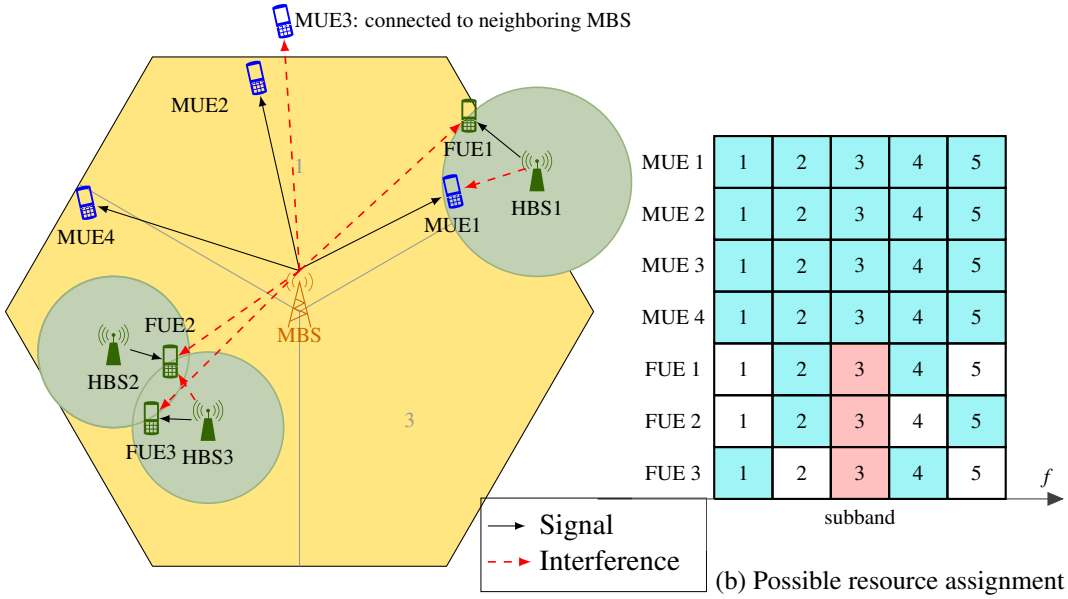

(a) Overview on critical interference situations

(b) Possible resource assignment

Figure 3.4: Exemplary resource assignment for a resource sets of $N_s = 5$ subbands and number of allowed resources $D_i = 2$

3.5 Global Optimizer as a Reference

In order to evaluate the efficiency of the advanced interference coordination method a classical optimization method is used. This can be utilized to provide a benchmark from gobal perspective which could be reached in case global information would be available. The interference coordination task can be written as an integer linear problem (ILP) similar to [69]. The sum of all interferences measured at each HBS of the network weighted with the resource pattern is to be minimized according to:

$$\min \sum_{i=1}^{N_{\mathrm{HBS}}} \sum_{n=1}^{N_{\mathrm{R}}} \sum_{j=1, j\neq i}^{N_{\mathrm{HBS}}} |h_{i,j,n}|^2 b_{i,n} b_{j,n} \tag{3.13}$$

$$\text{subject to} \quad \sum_{n=1}^{N_{\mathrm{R}}} b_{i,n} = D_i \,\forall i \tag{3.14}$$

where $D_i \leq N_{i,\max} \leq N_{\mathrm{R}}$ has to be fulfilled for the HBSs. The optimization variables are $b_{i,n}, b_{j,n} \in \mathbb{B}$ on resource n. $\mathbb{B} = \{0,1\}$ gives the set of binary digits. The channel gain $|h_{i,j,n}|^2 \in \mathbb{R}$ between HBS i and HBS j on resource n is constant during the optimization. The solution of (3.13) results from an exhaustive search with high complexity when applied to large-sized femto and macrocell layouts. The search space computes to $N_{\mathrm{ssp}} = {N_{\mathrm{P}}}^{N_{\mathrm{HBS}}}$, where N_{P} is the number of different resource patterns per HBS for one combination of D_i and $N_{i,\max}$. A pattern with fixed $D_i = D = 1$ or $D = 3$ and $N_{i,\max} = 4$ results in $N_{\mathrm{P}} = 4$. Even for small numbers of HBSs this results in an enormous search space and is intractable for computer simulations for approximately $N_{\mathrm{HBS}} > 18$. Beyond, different techniques which

perform optimization on clusters, whereas each cluster contains only a lower number of HBSs could be thought of. Even though the result from (3.13) leads to the optimum from a global perspective it might not provide a fair solution.

3.6 Convergence Behavior

When a new HBS is introduced in the network due to relocation or restart after some time it causes new interference to the system. The interference is measured within each HBS or by the FUEs which feed back this information to their serving HBS. This newly introduced interference has to be addressed instantly in order to protect all other femtocells in the surroundings and to lower the impact of interference per resource. Thus, in order to be deployable in real communication systems, the coordination techniques require a fast convergence behavior. Convergence in reasonable time depended on the actual situation is essential. The performance of the sequential deterministic method depends on the number of femtocells. According to current observations the required convergence time increases linearly with the overall amount of HBSs in the network. This seems realistic, as within the sequential deterministic method all HBSs adapt to the interference situation one after another. More beneficial, the simultaneous probabilistic technique provides as well a very good interference situation, but only a minor increase in the required time results if the size of the network is increased.

Within this section the convergence behavior of the advanced ICIC algorithms is investigated for three up to 1008 HBSs in the network. ICIC "SeqDet" stands for the sequential deterministic approach where one HBS decides after another, and ICIC "SimProb" denotes the simultaneous probabilistic approach where all HBSs decide at the same time but change their resource allocation only with a certain probability P_i. The global optimizer is denoted by "Global Opt" which can be used in small scenarios as a benchmark from global perspective.

Throughout the analysis of the convergence behavior subband-sizes D_i of one, two, three, and four are used. Further, the subband-size will be equal for all femtocells, thus $D_i = D \; \forall \; i$. The number of evaluated sectors is three or 21 and the wrap around technique, described in Section 4.1.1, is always applied to get rid of border effects. The initial selection of the resource patterns in every femtocell is selected randomly and not according to a worst case scenario where every cell starts with the same setting.

The representation of the results is illustrated as follows: The average interference per allocated resource caused by HBSs measured at each HBS $\bar{I}_{\mathrm{HBS}}$ is drawn through a solid line and described in the caption of the legend by "HBS int". The interference caused by the sum of all kinds of BSs $\bar{I}_{\mathrm{t}}$, as the sum of HBS and MBS interference, with a dashed line and described by "MBS+HBS int" in the figures. The details are given within (3.15)–(3.17). The sequential deterministic approach is plotted in green, and the simultaneous probabilistic in red color. For low density deployments and one central cell scenarios the global optimizer is included and plotted in blue.

Already for a small number of HBSs, the global optimizer has to conduct an enormous number of iterations and for currently used hardware it is only solvable for a network which comprises up to 12 HBSs. For a higher number of HBSs, the computation time takes from

several months to years. Even though the global optimizer might be computed as a reference for small network sizes, when considering a real communication cellular network already the low density scenario seems intractable. Nevertheless, its introduction renders the possibility to assess the proposed dynamic interference coordination techniques.

The individual figures plot the average interference of all HBSs per allocated resource in dBm over the number of iterations, whereas $I|_{\mathrm{dBm}} = 10\log\left(I/1\,\mathrm{mW}\right)$. The average interference at the HBSs caused by all MBSs computes as the average over all HBSs and utilized resources in the individual HBSs, whereas N_{MBS} and N_{HBS} give the number of MBSs and HBSs, respectively:

$$\bar{I}_{\mathrm{MBS}} = \frac{1}{N_{\mathrm{HBS}}} \sum_{i=1}^{N_{\mathrm{HBS}}} \frac{1}{D_i} \sum_{n=1}^{N_{\mathrm{R}}} \sum_{j=1}^{N_{\mathrm{MBS}}} P_{\mathrm{rx},i,j,n} b_{i,n}. \tag{3.15}$$

The received power from MBS j at HBS i on resource pattern n is $P_{rx,i,j,n}$ and N_{R} gives the total number of resources. $b_{i,n}$ defines if HBS i uses resource n. If $b_{i,n} = 1$, resource n is used by HBS i and $b_{i,n} = 0$ if resource n is not used. $D_i \leq N_{i,\max} \leq N_{\mathrm{R}}$ defines the number of available resources for HBS i, which is also reflected in $b_{i,n}$ as $D_i = \sum_{n=1}^{N_{\mathrm{R}}} b_{i,n}$. Similar to (3.15), the average interference caused by the HBSs is

$$\bar{I}_{\mathrm{HBS}} = \frac{1}{N_{\mathrm{HBS}}} \sum_{i=1}^{N_{\mathrm{HBS}}} \frac{1}{D_i} \sum_{n=1}^{N_{\mathrm{R}}} \sum_{j=1, j\neq i}^{N_{\mathrm{HBS}}} P_{\mathrm{rx},i,j,n} b_{j,n} b_{i,n}. \tag{3.16}$$

Therein in addition to (3.15) $b_{j,n}$ is introduced which defines if resource n is used by HBS j. The total interference caused by MBSs and HBSs in the femtocells $\bar{I}_{\mathrm{t}}$ is the sum of (3.15) and (3.16):

$$\bar{I}_{\mathrm{t}} = \bar{I}_{\mathrm{MBS}} + \bar{I}_{\mathrm{HBS}}. \tag{3.17}$$

One iteration step is equal to one snapshot of one TTI which in here corresponds to a time span of 1ms. For the sequential deterministic method, the resource assignment (i.e. the selection of a new resource pattern) of only one HBS can be changed during one iteration step. Different, the resource assignment of the simultaneous probabilistic method can be changed in all HBSs in parallel dependent on the switching probability P_i. Thus, during the initialization of the interference coordination technique on the interval of 1ms the resource assignment could be changed in order to reach stepwise to a desired configuration. Within each sector a deployment ratio of $\frac{1}{240}$ up to 20%, which defines the number of apartments deployed with an active femtocell within one MBS sector, is considered. The HBS deployment density levels of $P_{\mathrm{d}} = 0.42\%, 1.7\%, 5\%,$ and 20% will be referred to as minimum, low, medium, and high density, respectively.

3.6.1 Dynamic Interference Coordination Techniques for Increasing Femtocell Densities and Comparison to the Global Optimizer

Within this subsection increasing femtocell densities with 3 and 21 sectors are evaluated. The deployment factor P_d determines the number of HBSs per MBS. A low deployment factor results in a low HBS density and a high factor in a high HBS density. In here, values for $P_\mathrm{d} = \frac{1}{240}, \ldots, 0.2$ are analyzed. The details on the deployment factor are given in Section 4.1, whereas (4.1) gives the relation of deployment factor P_d and number of femtocells per MBS ρ_HBS. In combination with the number of sectors an overall number of femtocells in the network of 3, 12, 21, 144, 252, and 1008 are depicted. Within this section, the switching probability is fixed at a reasonable value $P_i = 0.1$. Please keep in mind, that the minimum achievable interference level depends on the number of small cells in one sector. Thus, even larger number of overall HBSs in the network can show a better reachable interference level, which is reasonable.

In order to show the potential to find an advantageous resource pattern setting, a small cellular system with only one macrocell, containing 3 sectors, is simulated for different very low deployment densities. For small configurations with deployment factors as $P_\mathrm{d} = \frac{1}{240}$ and $P_\mathrm{d} = \frac{1}{60}$, which give in total 3 and 12 HBSs, respectively, the performance of the sequential deterministic and simultaneous probabilistic approach can be compared to the global optimizer as a benchmark which gives the theoretical minimum interference situation.

A fraction of $\frac{1}{240}$ active femtocells results in a total of 1 HBS per sector and for one center cell overall 3 HBSs in the network. The evaluation of this very small deployment setting is shown in Figure 3.5.

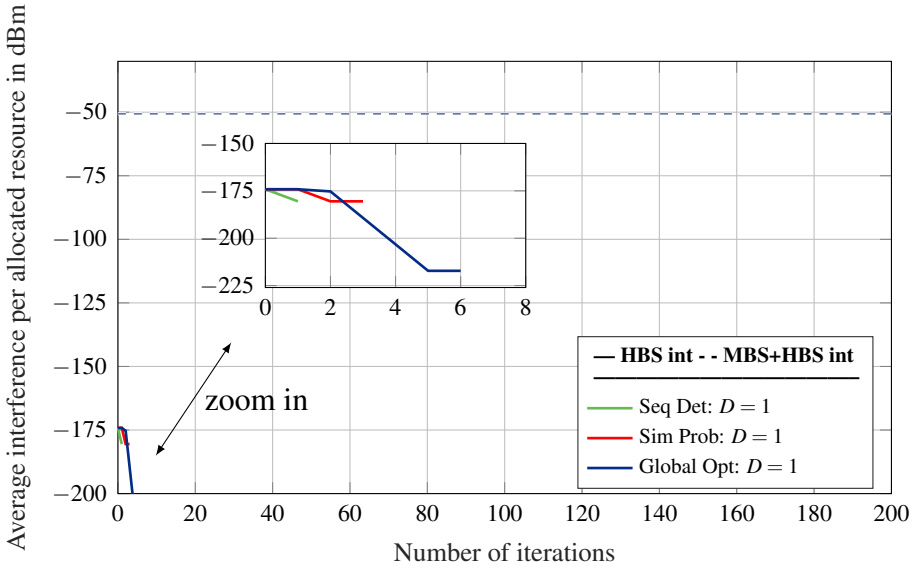

Figure 3.5: Convergence behavior of the two dynamic ICIC methods and the global optimizer for a minimum HBS density, with 3 MBSs and 3 HBSs, one scenario

Hereby the outcome of the interference coordination algorithm should result in a configuration where each femtocell is assigned an orthogonal subband, for the exemplary number of selectable subbands four (as in Section 3.4) and the number of allowed resources per femtocell $D = 1$. As can be seen in the figure, the interference from the small cells can be completely removed, starting from around two to seven iterations. Thus, the algorithm is eligible to find the beneficial orthogonal resource assignment only according to local information without communication and coordination between the cells.

To extent the investigation on the convergence behavior of the suggested techniques in more detail and show their absolute performance, again a small setting, now with slightly increased deployment factor P_d of $\frac{1}{60}$ active HBSs which gives 4 HBSs per sector and in total 12 HBSs in the network is considered. Figure 3.6 depicts the convergence behavior of one home base station deployment drop for this configuration. In here, the interference value for each search step of the global optimizer is plotted with a blue straight line. The minimum achievable interference value after its finalization achieved after around 1.092.444 steps is depicted with a blue dotted line.

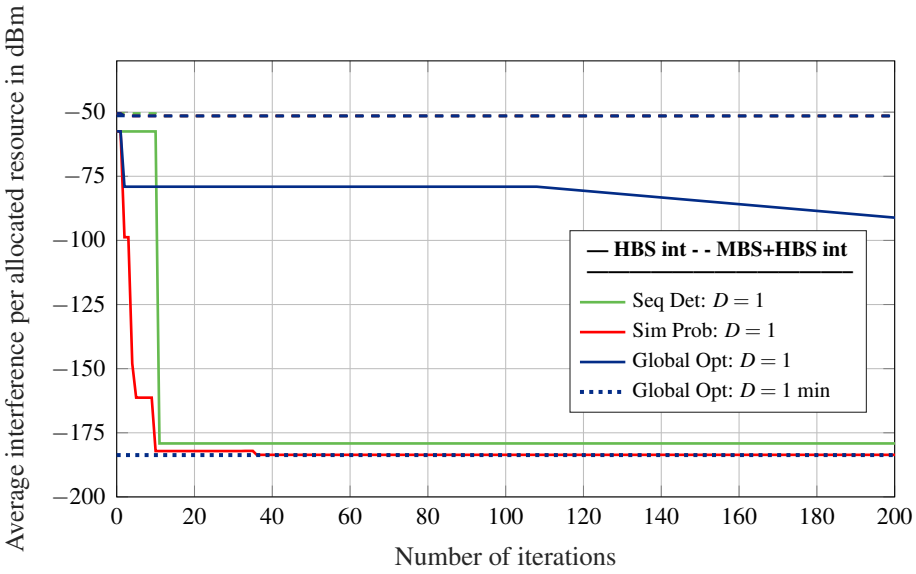

Figure 3.6: Convergence behavior for one network deployment drop of the two advanced ICIC methods for a low HBS density, with 3 MBSs and 12 HBSs and the global optimizer as a reference

The convergence behavior is comparable for both algorithms and both reach a close to optimal interference level. Figure 3.7 shows the mean convergence behavior over a multiple (here 28) of home base station deployments, again for a center cell with 4 HBSs per sector and 12 HBSs in total. As can be seen the overall interference level increases and a gap between global optimizer and the two advanced interference coordination techniques is present. The increased interference level results from averaging of critical drops with femtocells next to the MBSs. But even in these scenarios the interference for the macrocell is at a reasonable level due to the protected macrocell only subband. The gap to the global optimizer is due to

some scenarios where the techniques lower the interference in the network significantly but do not reach the optimum and might deviate from the lowest interference value. Nevertheless both techniques show a remarkable performance and are suitable solutions so reduce the interference level.

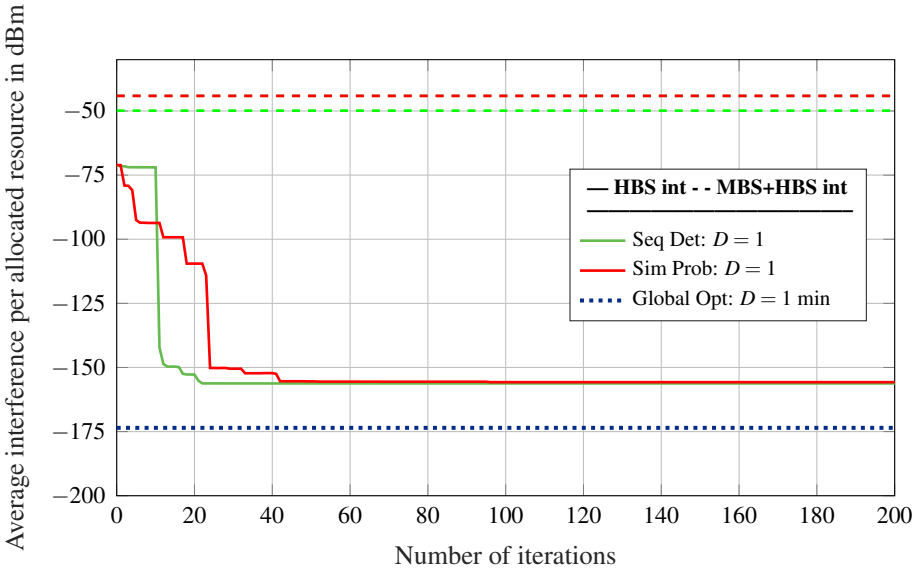

Figure 3.7: Convergence behavior of the two dynamic ICIC methods for a low HBS density, with 3 MBSs and 12 HBSs and the global optimizer as reference, mean over 28 BS deployment scenarios

Moving to a network deployment with a central cell and one ring, Figure 3.8 compares the convergence behavior of the sequential deterministic and the simultaneous probabilistic approach for a low network deployment density with one HBS per sector.

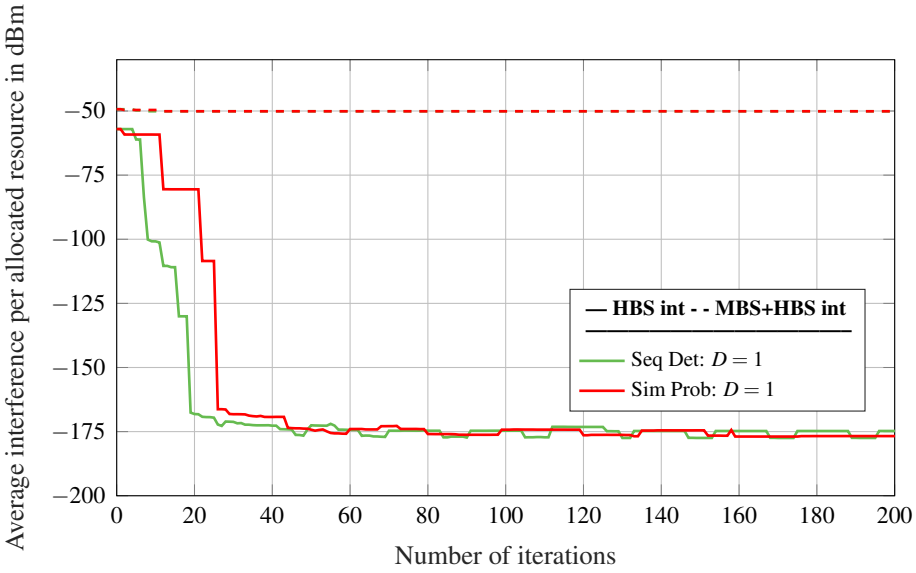

Figure 3.8: Convergence behavior of the two dynamic ICIC methods for a low HBS density, with 21 MBSs and 21 HBSs, mean over all simulated scenarios

The total of 21 sectors results in overall 21 HBSs. The number of selectable subbands per HBS is still $D = 1$. On average, the sequential deterministic is a bit faster, dependent on the scenario drop, but also opposite situations can occur. The scenario still contains only a low number of base stations and corresponds to a very low density of HBSs in each cell. This could represent a rural scenario with big macrocell sizes and only a few houses widely spread. These will most probably not cause a lot of issues even when the system is used without interference coordination. With the introduction of the interference factor threshold I_{th}, according to Section 3.2, even the whole set of resources can be reused in each of the cells within these situations. The speed of convergence for the two approaches is similar and depends on the present interference situation. On average the two approaches perform similar with a slight advantage for the sequential algorithm.

When the number of femtocells increases, the potential of the simultaneous probabilistic approach and the limitations of the sequential deterministic approach crystallize, as can be seen in Figure 3.9 for one scenario and in Figure 3.10 for an average over several simulation drops. Both depict the convergence behavior for a center cell with 48 HBSs per sector. It results in a total of 144 HBSs.

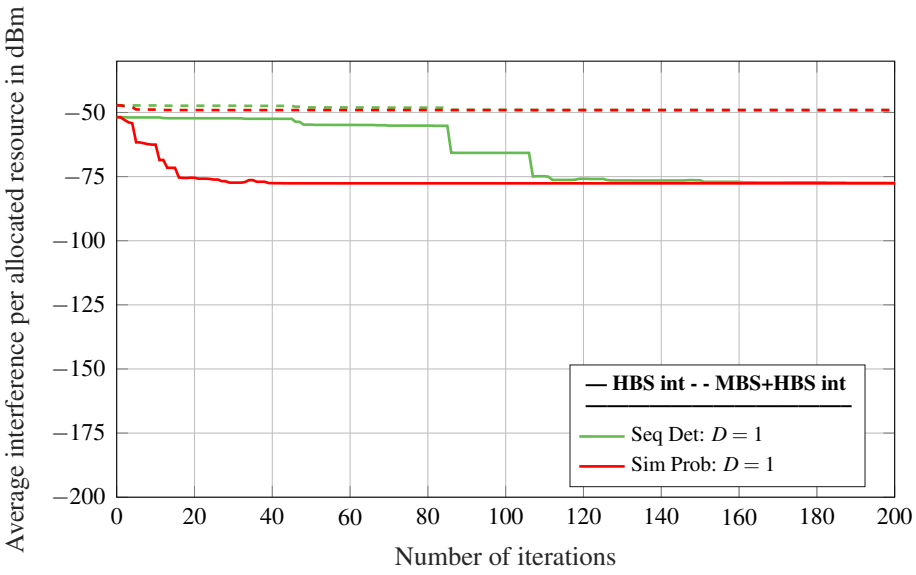

Figure 3.9: Convergence behavior of the two dynamic ICIC methods for a high HBS density, with 3 MBSs and 144 HBSs, one scenario

As can be seen, the convergence behavior of the simultaneous probabilistic technique is almost the same as in the smaller setting. Contrary, the time to converge for the sequential deterministic approach is substantially enlarged. In numbers by a factor of six. Thus, the gap between the two proposed techniques is escalated. The sequential approach takes about 100 iterations more to provide a beneficial interference situation than the simultaneous method. These more dense scenarios with larger numbers of femtocells might represent scenarios of a real system within suburban to urban deployment situations. In there, the advantage of the simultaneous approach over the sequential technique shows up. Further, also the

offloading effect for the MBS will be even more advantageous, in there. Thus, for real networks especially the simultaneous probabilistic approach is a promising candidate.

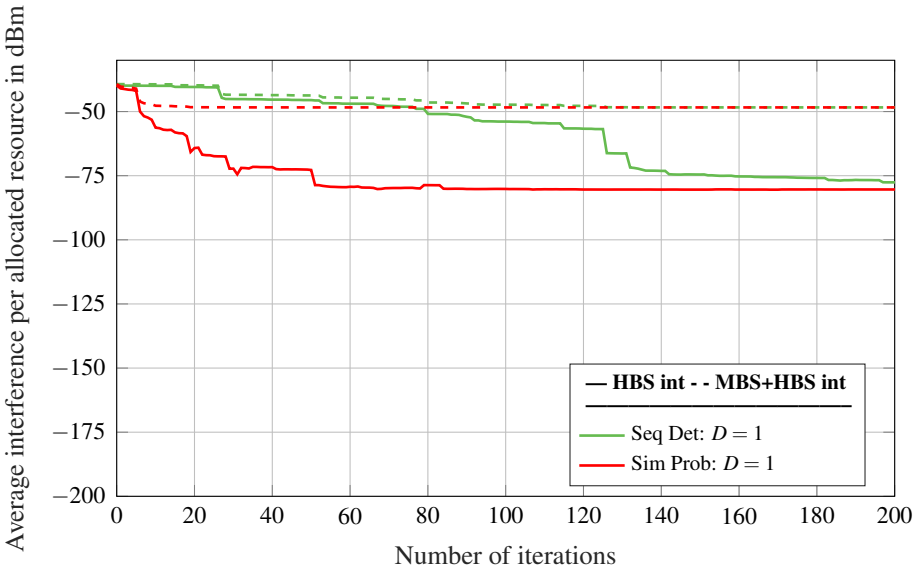

Figure 3.10: Convergence behavior of the two dynamic ICIC methods for a high HBS density, with 3 MBSs and 144 HBSs, several BS deployment scenarios

Figure 3.11 shows the convergence behavior of the sequential deterministic and the simultaneous probabilistic approach for a medium network deployment density with 12 HBSs per sector and a total of 7 cells resulting in 21 sectors. This results in a total of 252 HBSs.

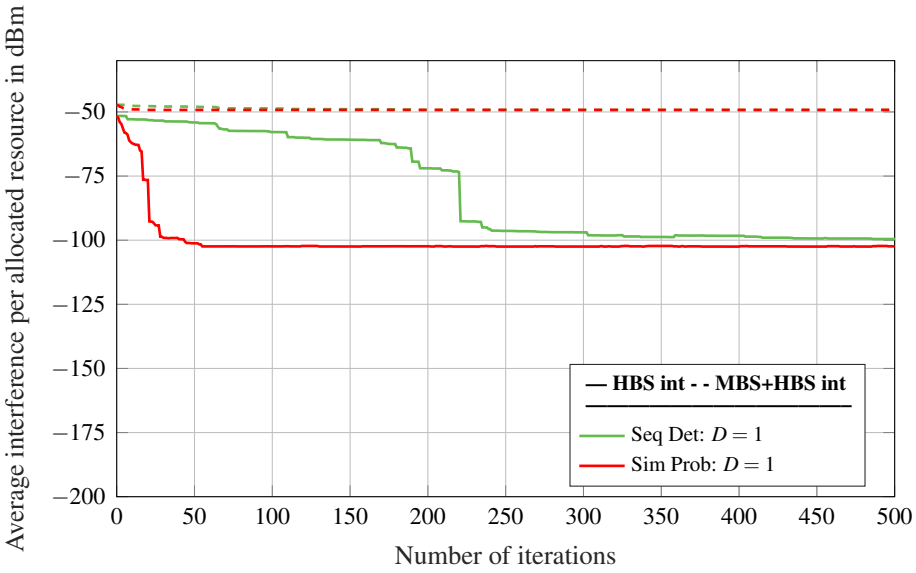

Figure 3.11: Convergence behavior of the two dynamic ICIC methods for medium HBS density, with 21 MBSs and 252 HBSs, mean over several BS deployment scenarios

Again, the number of selectable subbands per HBS is $D = 1$. The figure shows the average

over roughly 10 scenarios. The sequential deterministic and the simultaneous probabilistic approach have been simulated now for 500 iterations and more. Please note, the scale on the abscissa is changed, precisely the number of depicted iteration steps is increased from previous 200 to now 500.

The sequential deterministic approach converges around 160-220 iterations later, and even slower dependent on the considered interference value, this means it takes around 200ms longer to reach its minimum. Already here the advantage, which has been shown for marginal deployments, of the stepwise computation against the simultaneous approach due to the probabilistic element P_i which protects not two HBS adapt simultaneously is balanced and even put to the opposite. Within this setting, the sequential deterministic approach takes about 10 times longer than the simultaneous probabilistic approach.

Moving to a higher network density, now with 48 HBSs per cell, the results are shown in Figure 3.12. The setting of 48 HBSs per sector together with 21 sectors leads to a total of 1008 HBSs. Apart from the density of the HBSs all other parameters remain unchanged compared to the previous settings considered before. The simultaneous probabilistic approach has been simulated up to 240 iterations. Its extrapolated resumption is drawn in dash-dotted lines. Again, the scale on the abscissa is changed, precisely the number of depicted iteration steps is increased from previous 500 to now 2000.

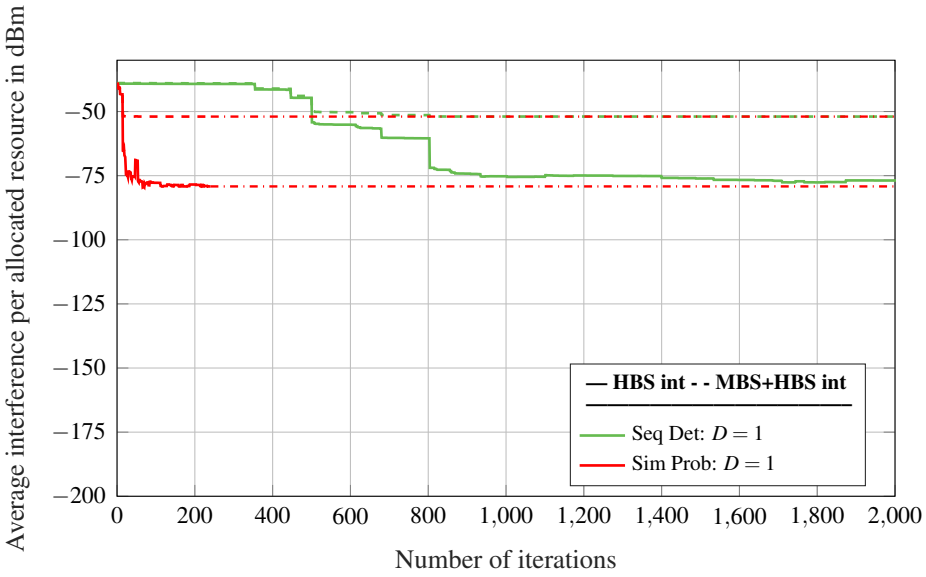

Figure 3.12: Convergence behavior of the two dynamic ICIC methods for a high HBS density, with 21 MBSs and 1008 HBSs

The simultaneous probabilistic method reaches around 800 and 1800 iterations earlier its minimum as can be seen in Figure 3.12 and Figure 3.13, respectively, whereas each represents one drop. Within Figure 3.13 the simultaneous probabilistic approach has been simulated up to 1008 iterations and its extrapolated resumption is drawn again in dash-dotted lines. While the simultaneous probabilistic method still maintains a similar or only slightly

increased convergence speed, the time to reach the minimum interference situation for the sequential deterministic technique increases tremendously and shows its intractability for real communication systems. The benefits of the simultaneous probabilistic approach can be seen. To summarize, the slower adaptation due to the sequential nature crystallizes and enforces the demand for an adaptation of it. The probabilistic interference coordination method adapts much faster than the sequential approach, especially when the femtocell density increases.

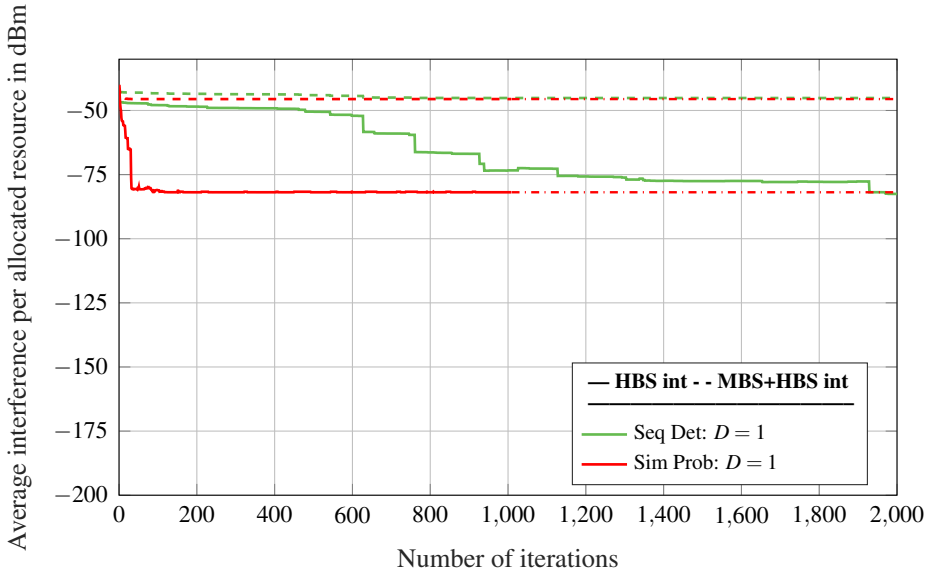

Figure 3.13: Convergence behavior of the two dynamic ICIC methods for a high HBS density, with 21 MBSs and 1008 HBSs

3.6.2 Dependency of the Time to Converge on the Femtocell Density

The necessary time to obtain a beneficial overall interference situation is essential for real applications. At the start, high interference situations might arise which have to be revealed. With the findings of Section 3.6 a relationship between the number of small cells in the network and the necessary number of iterations can be obtained.

In order to demonstrate the dependency of the iteration speed on the number of femtocells N_{HBS} in the network Figure 3.14 shows the number of iterations needed to reach a minimum interference threshold within a cell on the ordinate and the number of HBS on the abscissa for the sequential deterministic as well as for the simultaneous probabilistic approach for a switching probability of $P_i = 0.1$.

The required number of iterations for the sequential deterministic technique increase approximately linear with a slope of around 1.75. Differently the simultaneous probabilistic method shows for larger femtocell deployments a much smaller slope of around 0.04. As can be seen, from about 20 femtocells in the network, the simultaneous probabilistic approach provides a much lower number of iterations.

Considering the advantageous dynamic simultaneous probabilistic interference coordination method additional investigations can be made. The findings for the fixed switching probability of $P_i = 0.1$ are an important indication for network operators in order to tune the network properly. The appropriate stopping criteria N_{stop} of the interference coordination algorithm can be read from the figure. Higher network densities require more iterations than lower ones. The lower bound in order to provide on average every femtocell the possibly for adaption is $N_{\text{stop}} = \frac{1}{P_i}$. In order to provide an interference reduction close to the minimum achievable value, a more conservative number of iterations is advisable. The results for a switching probability of 10% suggest an offset value of around 50 iterations, to leave a margin for protection. Fast adaptation as well an appropriate stopping criteria would be even more relevant, when a non-fully loaded system is considered where in addition the interference situation is gained on the transmitted information datastream, and not according to some control channels. This is important for such scenarios, as the measured interference situation changes in there quickly.

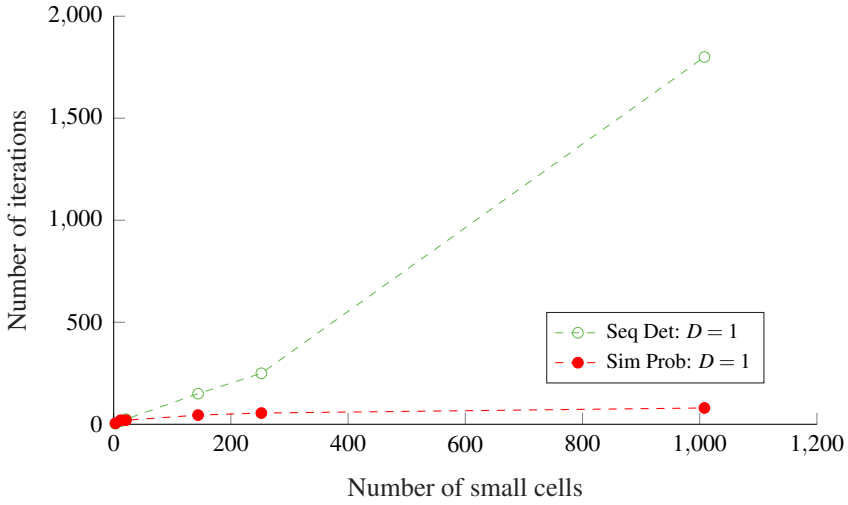

Figure 3.14: Convergence behavior of the sequential deterministic and the simultaneous probabilistic ICIC method in dependency of the number of small cells in the network

3.6.3 Simultaneous Probabilistic Method with Different Loads of Resources

The potential interference reduction depends on the load of allowed resources D_i in the network. The reachable minimum interference level decreases when the number of subbands is increased. Figure 3.15 shows the convergence behavior for one simulation drop with 12 HBSs per cell and 21 cells in total, thus 252 HBSs in the network. As can be seen in Figure 3.15 the minimum interference level increases together with increased subband sizes, nevertheless an improvement can be obtained as long as a certain degree of freedom is left.

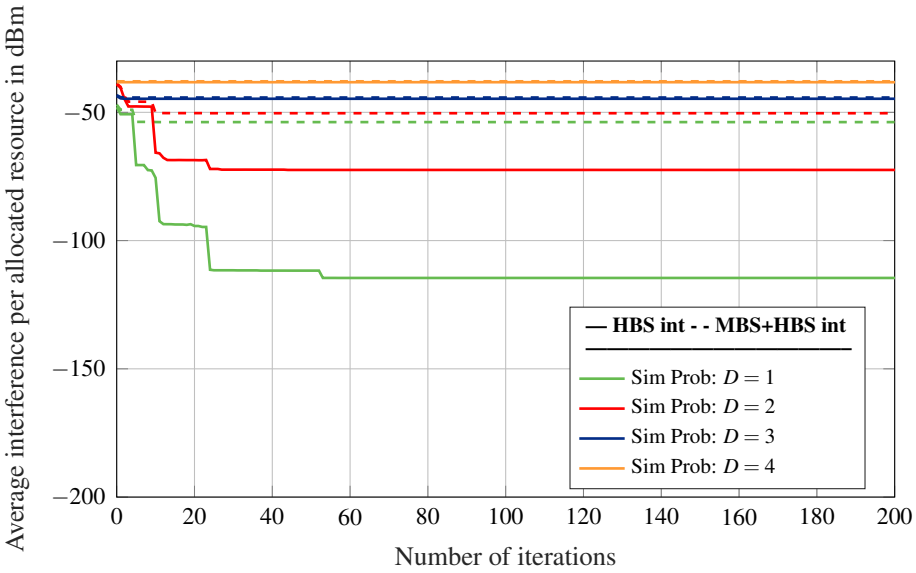

Figure 3.15: Convergence behavior of the simultaneous probabilistic ICIC method with $D = 1,\ldots,4$ for a medium HBS density, with 21 MBSs and 252 HBSs

3.6.4 Simultaneous Probabilistic Method for Different Resource Adaptation Probabilities

In order to prevent the occurrence of two home base stations to decide on a new resource allocation simultaneously, which might result in a worse interference situation and therefore could toggle between states, a probabilistic element is introduced. As described in Section 3.3.2 the switching probability P_i defines the probability whether to switch to a beneficial resource situation or not. Simulations are given with switching probability P_i ranging from 0.0% to 100.0%. Throughout this section a deployment factor of $P_\mathrm{d} = 0.05$ is used. The switching probability has to be set carefully in order to get a balance between convergence speed and stability. The evaluation for border probabilities close to 0.0% and for high probability values is given in Figure 3.16. The setting is a center cell with one ring, thus 21 MBSs and 252 HBSs with different P_i for one selected simulation drop.

The evaluation of these non-optimized settings with extreme values shows, that especially very low and very high values have to be avoided. As can be seen in Figure 3.16 with the yellow curve for a switching ratio of $P_i = 1.0$, when the resources are always and everywhere updated on every iteration step the interference coordination method will never converge and stay at the highest interference value or even increases. Values around 50% converge faster but show a flip-flop performance after the start of the procedure. In case the femtocells decide only with a very low switching value as $P_i = 0.01$ where each BS changes only on average every 100st iteration it is clear that the time to converge is getting along with it. This is depicted with the green curve where the time to reach a very low interference level increases tremendously compared to the values around 50%. Even after 200 iteration steps

only about half of the overall interference reduction can be obtained. This is plausible, as after 200 iterations still some of the base stations might not had the possibility to change their resource assignment.

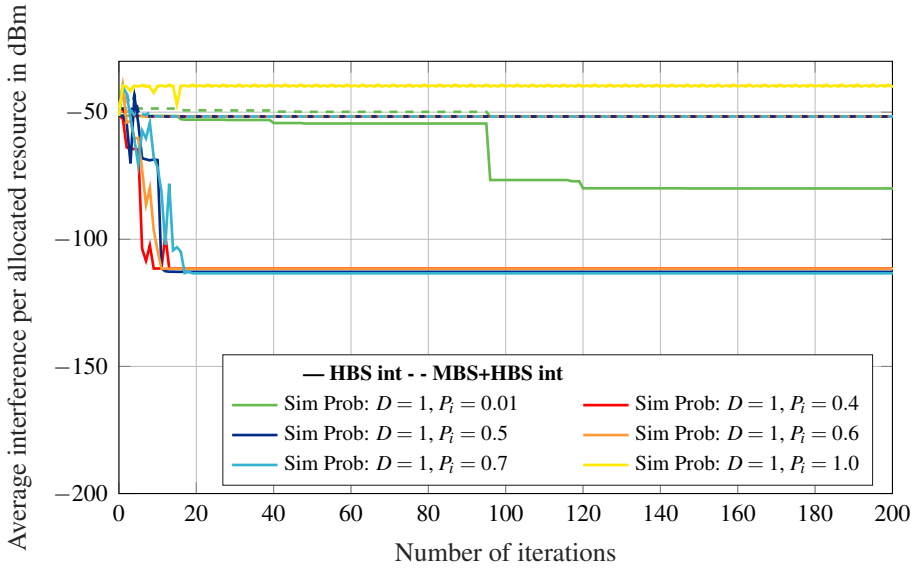

Figure 3.16: Convergence behavior of the simultaneous probabilistic ICIC method for a medium HBS density, with 21 MBSs and 252 HBSs, one scenario

In order to further determine an optimum value, reasonable values around $P_i = 30\%$ are further analyzed. The time to converge is increasing with decreased probability P_i, as can be seen in Figure 3.17 for values of P_i from 5% to 30% in a setting with 21 MBS and 252 HBSs for one simulation drop.

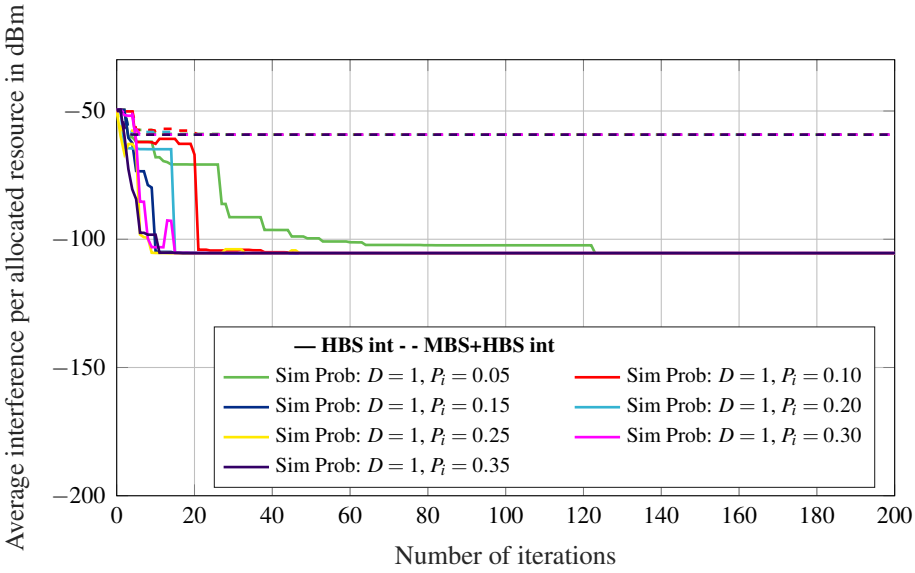

Figure 3.17: Convergence behavior of the simultaneous probabilistic ICIC method for a medium HBS density, with 21 MBSs and 252 HBSs

A value of $P_i = 5\%$ takes still a lot of iterations and is therefor not preferable. Values around $P_i = 10\%$ to 30% provide a reasonable time to converge. Figure 3.18 gives the results for worst case deployment situations with 3 MBSs and in total 36 HBSs. In here also critical situations, with tightly located small cells, are included. This might lead to slight flip-flopping. Anyhow, the interference situation can be lowered significantly in any case. The smallest switching probability in this scenario of $P_i = 0.05$ shows extended adaptation time compared to the higher values. This can be explained by the less frequent occurrence of the switching event trigger, in numbers only in five percent of the cases where an improvement of the interference situation is foreseen the adaption is enforced.

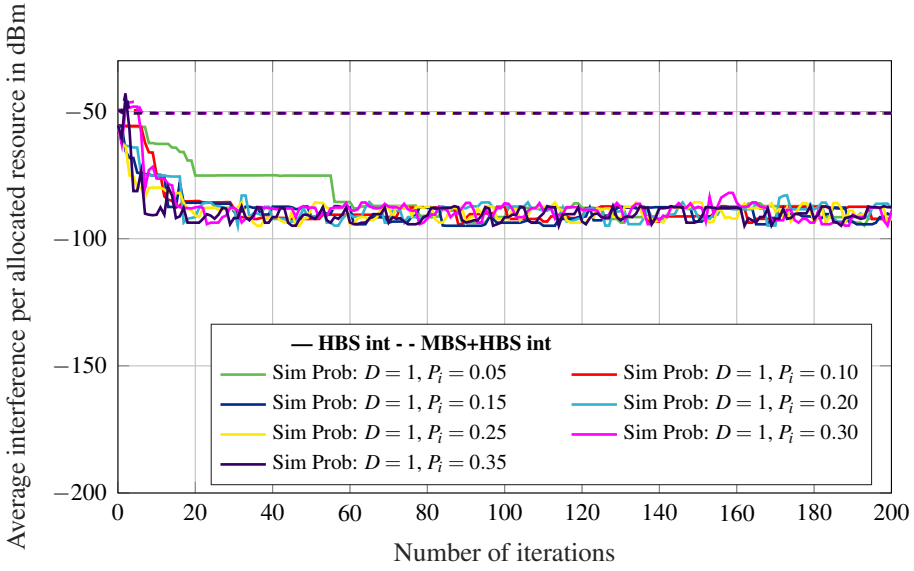

Figure 3.18: Convergence behavior of the simultaneous probabilistic ICIC method for a medium HBS density, with 3 MBSs and 36 HBSs, several scenarios

Figure 3.19 draws an overview on the number of necessary iterations dependent on the resource switching probability P_i for the previously described number of HBSs from 3 up to 1008. The distribution for each fixed number of HBSs shows a bathtub curve. The number of iterations increases below values of $P_i = 0.1$ and values beyond $P_i = 0.7$. Thus, the recommendation is to use a value within this range. The result given within this figure are the summary of the previously shown simulations and also furthers. The result are derived as an average over all available simulation drops, for smaller densities 100 simulations. The deployment density is increased from a deployment factor of $P_\mathrm{d} = \frac{1}{240}$ up to $P_\mathrm{d} = 0.2$ and the overall number of femtocells are $N_\mathrm{HBS} = 3$ up to $N_\mathrm{HBS} = 1008$. Each point in the graph, depicted by a circle marker, is derived from one simulation. Where a sufficient number of simulation points is present, a dashed line indicates the approximated intermediate probability values. To summarize, the convergence behavior depends on the switching probability as well as the number of femtocells in the network. A switching probability of $P_i = 0.1$ gives a good balance between speed of convergence and stability. The number of necessary iteration steps increases with the number of femtocells N_HBS in the network and for very large and very low values.

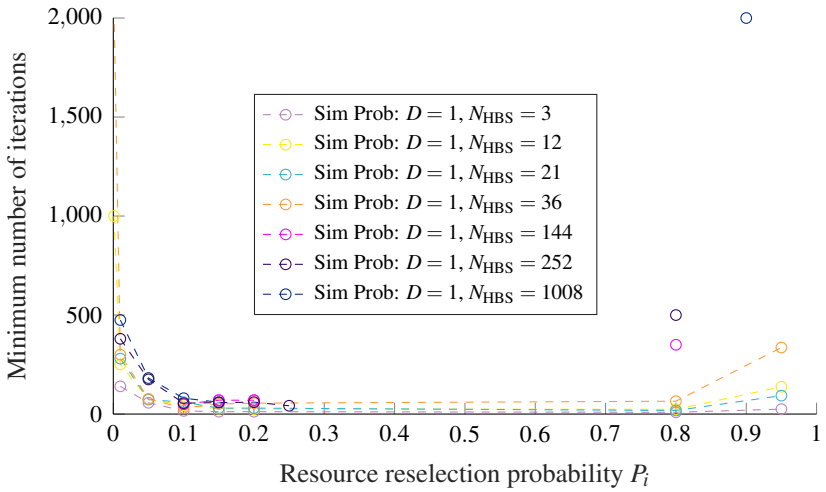

Figure 3.19: Convergence behavior of the simultaneous probabilistic ICIC method in dependency of the switching probability P_i

3.6.5 Simultaneous Probabilistic Method for Different Candidate Switching Margins

When the selection of a new resource candidate offers only a marginal interference improvement, it can be preferential not to change the resource pattern. In order to address this, the interference margin, defined in Section 3.3.2 is investigated within this chapter. The interference margin I_{m} is given as a function of the deviation ratio P_{m}, in here. Figure 3.20 draws the convergence behavior for different switching margin ratios for one deployment drop.

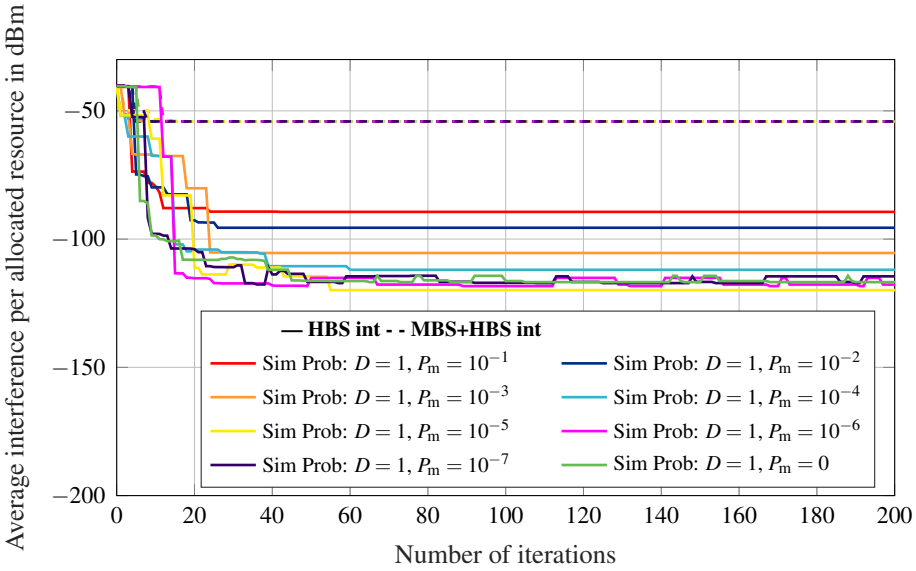

Figure 3.20: Convergence behavior of the simultaneous probabilistic ICIC method for a medium HBS density, with 21 MBSs and 252 HBSs, investigation of the switching margin P_{m}, one scenario

Switching margin ratios of $P_{\mathrm{m}} = 0, 10^{-1}, 10^{-2}, \ldots, 10^{-7}$ are shown. When the interference margin is increased, the minimum reachable interference situation increases as the algorithm might not deviate from a resource selection due to the defined margin. Thus, the resource switching margin has to be set carefully. $P_{\mathrm{m}} = 10^{-4}$ offers good results concerning the stability together with a fair deviation to the minimum.

3.7 Conclusion

As a conclusion, considering realistic scenarios with moderate to high density of HBSs, the simultaneous probabilistic ICIC method adapts much faster than the sequential deterministic based approach. As can be seen in the figures it converges around ten times faster for $D = 1$ used subband and 12 HBS per sector with a total of 21 sectors. The faster convergence behavior is an important aspect especially if the number of HBSs increases. The sequential deterministic approach scales with the number of HBSs in contrast to the simultaneous probabilistic method. The dependency of the convergence speed on the number of femtocells is supported by Figure 3.14 for a selectable subband size of one. It shows for the sequential deterministic approach an approximately linear dependency on the number of small cells. Differently, the simultaneous probabilistic method is only marginally increased and starting from about 50 femtocells it increases only marginally when the amount of femtocells is increased.

Further, a comparison to a global optimum is shown. In order to classify the overall performance of the two proposed methods and to compare the overall convergence behavior, a global optimizer is introduced in Section 3.5. It determines the global optimum of the overall deployment from a global perspective. As shown in Figure 3.8 on average over several simulation drops, which contain also critical interference situations, the developed techniques reveal very good results, whereas the methods can get close to the optimum performance shown in Figure 3.7.

Chapter 4

Simulation Results of Throughput and Outage

The introduced dynamic decentralized coordination technique is a powerful method to overcome the critical interference situations in heterogeneous networks and in addition to this can be even used for more general types of resource assignments. Its basic idea is to protect the MBSs while being kept unchanged. The HBSs tune their resource allocation individually to achieve an overall optimized performance. It applies moderate restrictions together with adaptive resource allocation. Due to the complexity of the overall system, analytical closed-form solutions are practically unfeasible. Thus, the results are obtained via simulations. Monte Carlo Simulation, as a stochastic scenario analysis, relies on iterative sampling with the help of the law of large numbers. It serves to numerically evaluate different network deployments. The simulator models a heterogeneous network deployment according to 3GPP, with consecutive deployment of random scenarios, during each of them fast-fading can be simulated. The outdoor mobile stations are randomly set over the macrocell area, whereas the indoor mobile stations are placed inside a femtocell block. The users of a femtocell are randomly set inside an active apartment [73]. For one scenario, the pathloss between the transmitter and receiver is fixed, as the positions of the MUEs and FUEs remain constant during one drop.

Chapter 4 depicts the findings of intensive system-level simulations. First, the network deployment is introduced in Section 4.1 including different femtocell deployment models, an overview on the simulation settings, the wrap around concept, and a detailed explanation on the representation of the results. Further, a small cell scenario without interference coordination is given as a reference in Section 4.1.3. Afterwards, the dynamic interference coordination techniques are introduced and discussed in detail regarding density of the femtocell network and the parameters of the simultaneous probabilistic interference coordination technique in Sections 4.2–4.5. The investigation of the cumulative distribution function (CDF) curves in Section 4.6 is followed by a brief summary in Section 4.7.

4.1 Network Deployment

Figure 4.1 shows the network deployment based on a hexagonal grid for a center cell with one ring which results in a macrocell layout with 7 sites and 21 MBSs. The center cell comprises sectors one up to three, which are served by MBSs one to three, and is marked with yellow background. The three MBSs of the center cell are located in the origin and marked with an orange dot. The remaining 18 sectors surrounding the center cell are highlighted in cyan. The position of the serving MBSs from a group of macrocells, called site, is located on a circle with distance d_{ISD} around the site of the center cell base station and is again the position of the transmitter for the three sectorized cells. d_{ISD} denotes the distance between neighboring sites. Throughout the remainder of this work MBS cell and sector are used interchangeably. To eliminate imbalance of the interference situation at the borders, the wrap around technique is used. Thus, also users located at the edge of the hexagonal cell layout experience statistically the same interference as the mobile stations in the inner zone. For more details, please refer to Section 4.1.1. The inter-site distance d_{ISD} is fixed. Unless otherwise indicated each macrocell serves on average 10 MUEs and each femtocell one FUE. All BSs have always data to transmit, so full buffer is assumed as a worst case scenario [7]. The position of the HBSs and outdoor UEs is randomly set over each macrocell and stays constant during one simulated scenario. A certain ratio of indoor to outdoor MUEs can be set.

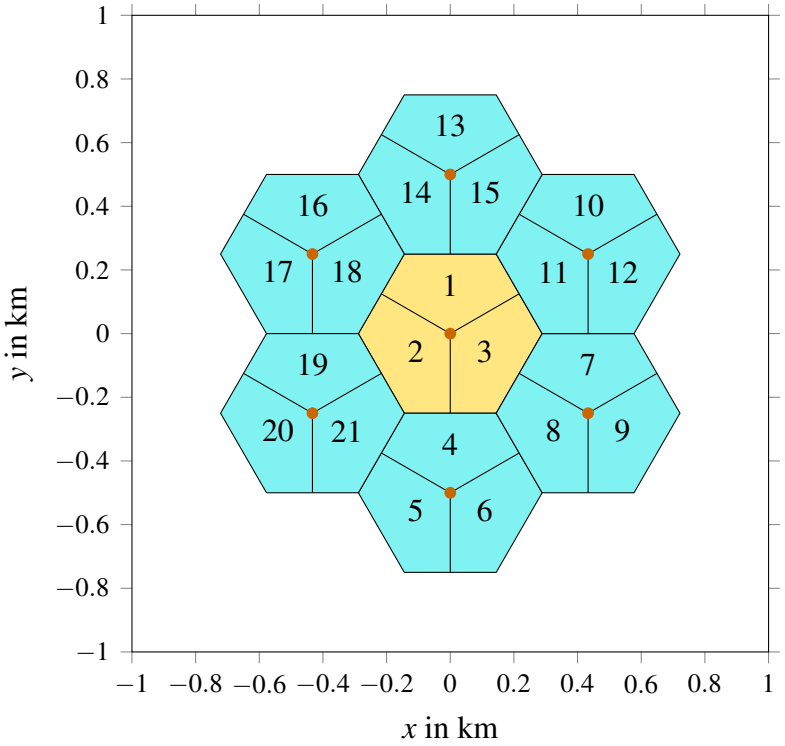

Figure 4.1: Depiction of the network deployment layout of the macrocell layer with three sectors in the center cell and 18 surrounding sectors resulting in a total of 21 sectors with 21 macro base stations

The fraction of the indoor MUEs is dropped arbitrary within the femtocell block buildings corresponding to the overlayed macrocell. The HBSs are installed inside the buildings at a random position inside an urban house or an apartment as is later on explained with Figures 4.2–4.4.

Models to investigate different femtocell deployment scenarios are (i) the femtocell block dual stripe model shown in Figure 4.4, (ii) the detached house model for suburban considerations in Figure 4.2, and (iii) a dense urban 5×5 model [74] [75] [76] depicted in Figure 4.3. The femtocell block model can reflect the situation in dense-urban areas.

The detached house model assumes individual houses installed with a single femto basestation for residential house areas, with one floor as depicted in Figure 4.2. The location of the HBS is randomly set over the inside area of the residential building and the UE connected to the HBS is dropped randomly over the entire house, or it might be outside with a certain preconfigurable probability in the surrounding outdoor area colored in red shade for the detached house model.

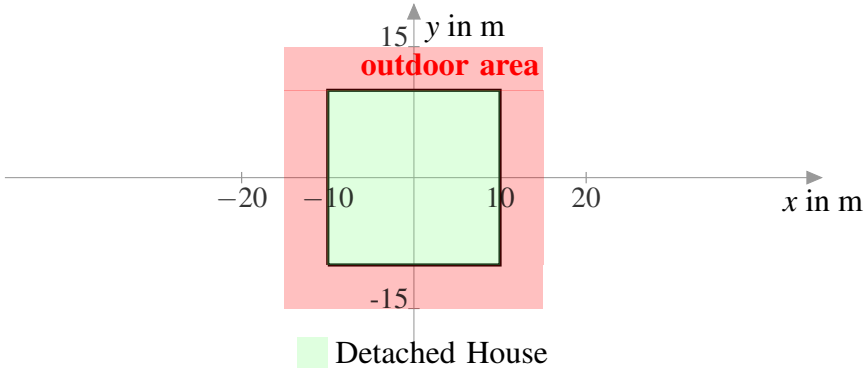

Figure 4.2: Model of detached house beneficial for evaluation of residential areas

Figure 4.3 shows the 5×5 femtocell model for dense urban investigations.

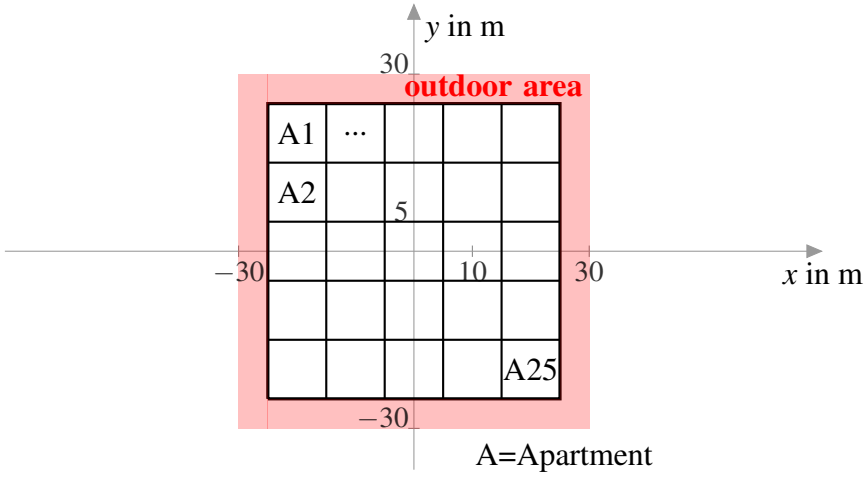

Figure 4.3: Model of dense urban femtocell deployment

Five apartments are stringed together in x- and y-direction to form the grid of apartments where each thereout might contain a femtocell according to a certain probability. This results in a total of 25 apartments per floor. Within the equipped apartments, the position of the base station and mobile station is defined random uniformly over the spanned area.

Figure 4.4 shows the widely used dual stripe model suitable to make miscellaneous investigations. The femtocell block model uses two stripes of apartments divided by a street corridor over a selectable number of floors. Each apartment can be deployed with a femtocell. When using one block with low deployment ratio a sparse interference situation is created and with a high deployment ratio and more blocks per cell a high interference situation is depicted. The femtocell dual stripe model, describing an environment where critical interference situations arise, is used throughout this thesis. It comprises of two symmetrical apartment or business towers separated by a street of 10m.

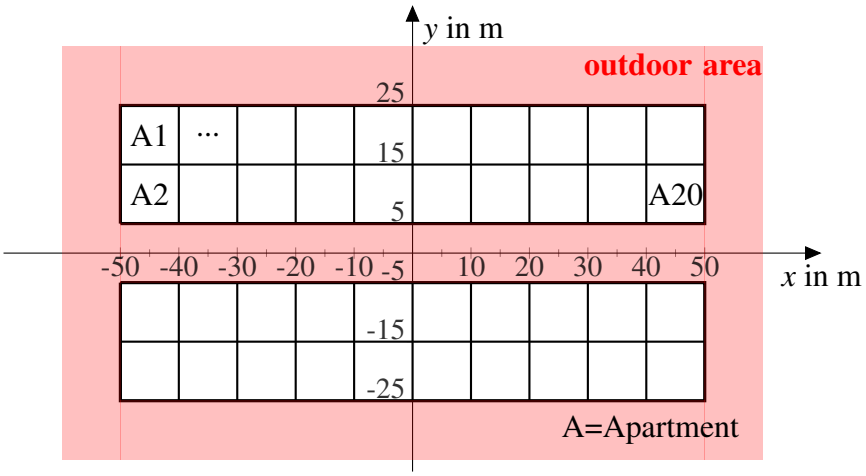

Figure 4.4: Modeling of femtocell deployment with dense urban dual stripe model exemplary for one floor

Each block has several floors which can be set for simulations, here six floors are used. Within this work, each stripe of building contains $2 \cdot N_a = 2 \cdot 10$ apartments, thus each tower has length 100m and width 10m and contains 20 apartments per floor. Thereof each apartment is of size 10m $\times$ 10m. A certain percentage, which can be set, of the apartments are equipped with an HBS and there-out a certain percentage is active. Given a certain fraction for the deployment P_d, the density ρ_{HBS} as the number of femtocells per MBS site computes as:

$$\rho_{HBS} = \rho_{FCB} N_t \cdot 2 \cdot N_a \cdot N_{floor} \cdot P_d, \tag{4.1}$$

with the number of towers $N_t = 2$, the number of floors N_{floor}, and the number of femtocell blocks per MBS ρ_{FCB}. The assumption of equal number of floors per femtocell block could easily be extended to the general case. The location of the HBS can be at any position inside the apartment. To involve structural conditions non-overlapping buildings are presumed. Each femtocell is assumed to be active which does not restrict the generalization as the additional deployment ratio factor is present.

Exemplary for the femtocell block model, which represents the most flexible and most critical arrangement, Figure 4.5 depicts a cellular network with one site as a subspace of the the macrocell layout from Figure 4.1. It comprises three sectors, where each sector is deployed with one femtocell block (FCB). This results in a total of three femtocell blocks per MBS. The presumption of a deployment ratio of $P_{\mathrm{d}} = \frac{1}{60}$, which implies that one out of 60 apartments are equipped with an HBS, results with (4.1) in

$$\rho_{\mathrm{HBS}} = 1 \cdot 2 \cdot 2 \cdot 10 \cdot 6 \cdot \frac{1}{60} = 4 \tag{4.2}$$

four femtocells per MBS sector and a total of 12 for the underlined overall network scenario under the assumption of six floors per building. The position and orientation of the femtocell buildings is defined by translation and rotation of the standard building from Figures 4.2–4.4. The elucidation on the rotation vector and the transation is given in Section A.1.1.

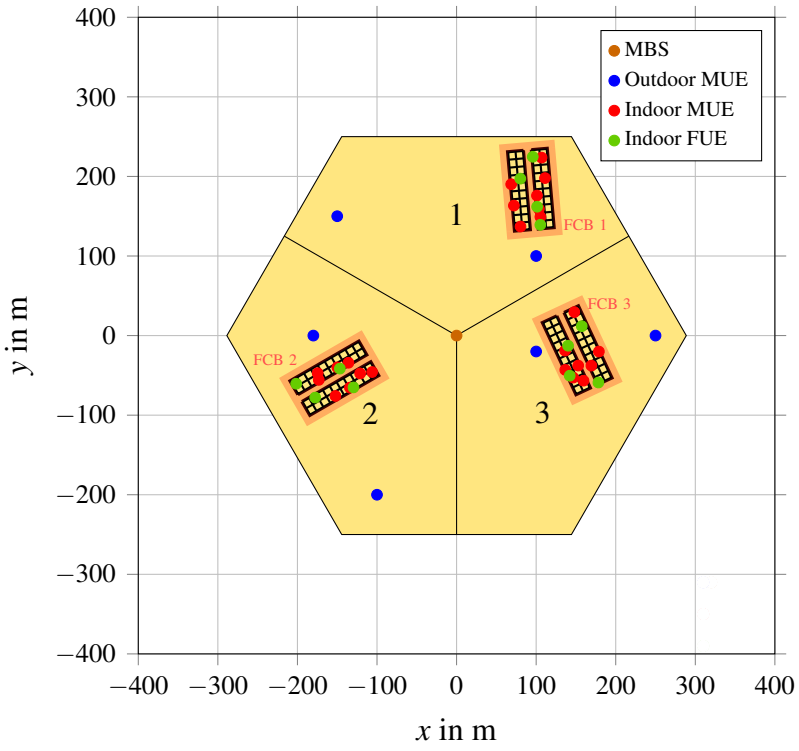

Figure 4.5: Depiction of network deployment layout of macro- and femtocell layer for 3 macro base stations (MBSs) and four home base stations (HBSs) per macro base station (MBS)

The femtocell blocks according to Figure 4.4 in Figure 4.5 are deployed and rotated randomly on the MBS sectors with the restrictions that no two femtocell blocks overlap. The positions of the BSs and MSs are highlighted with a colored circlet. The blue bullet • depicts the position of the outdoor MUEs and the red circle • shows the positions of the indoor

MUEs. Further the position of the indoor FUEs is displayed with green color ●. The position of the MBS ● is located at the origin in orange. The positions of the HBSs are not shown in order to maintain clearness owing to their close position within the same appartment to the FUE bullets ●. Each femtocell block contains four femtocells, arising from the deployment ratio of $P_{\mathrm{d}} = \frac{1}{60}$, where each supplies one UE. An increased deployment probability of $P_{\mathrm{d}} = 0.2$ results in a more dense environment with 48 HBS per sector.

In order to evaluate the performance of the advanced interference coordination algorithms, the following basic settings are used throughout all simulations, if not stated differently. A co-channel situation is examined where HBS and MBS use the same radio frequency (RF) carrier. The downlink of a cellular system with 10MHz and an FDD frame structure is applied. A dense-urban setting with femtocell blocks resulting in high interference scenarios is considered. The simulations are conducted with a bandwidth of 10MHz, nevertheless the performance of the dynamic technique scales with the number of antennas and available bandwidth. Hence it can smoothly be integrated in wider bandwidth deployments also with increased number of antennas. As for the femtocell, CSGs are assumed, thus some users might not be granted access to, and no direct data exchange between two HBS might be available. The HBSs are equipped with a DL receiver to sense the current interference. This fact does not limit the considerations at hand, as the information can also be gained by measurement reports. As a worst case benchmark, the handover to an MBS or other HBSs is not allowed. Service for the corresponding UEs is provided when the throughput of the MUE (i.e. an MS@MBS) is above 100kbit/s and for an FUE (i.e. an MS@HBS) which experiences a MS throughput of more than one Mbit/s. Consequential a UE which has a throughput lower than the given limits is determined to be in outage. The number of users in outage divided by the total number of users within each group determines the outage rate, which will be described in the following with the term outage probability.

The simulations use a system-level simulator where the macro-cellular network can be overlayed with low power cells with different density and positions. Table 4.1 shows the basic set of parameters used for the system-level simulations.

Table 4.1: Overview on simulation settings

Parameter	Value
Cell Parameters	
Cellular layout	Hexagonal grid (3 sectors per macrocell)
Number of MBSs	3 (single site) and 21 (one ring)
Number of MUEs per MBS	On average 10
Inter-side distance d_{ISD}	500m
f_c	2GHz
System bandwidth	10MHz
$N_{\mathrm{sc,RB}}$	12
Cyclic prefix	Normal (4.7µs)
DL access scheme	OFDMA
Δf	15kHz
Fading channel profile	UL: Typical Urban, 3 km/h DL: HBS urban
Scheduling algorithm	Proportional fair and round robin
Mobile receiver	MRC (single stream transmission) MMSE (dual stream transmission)
Traffic model	Full queue
MBS total transmit power	46dBm
MBS antenna gain	14dBi
Angle spread for 3dB attenuation	70°
Antenna front-to-back ratio	20dB
Small Cell Parameters	
Femtocell deployment	Femtocell block and suburban homes
Number of femtocell blocks per MBS	1
Number of floors of a femtocell blocks	6
Ratio of apartments with an HBS P_{d}	$\frac{1}{240} \ldots 0.5$
Active femtocells	100 %
HBS total transmit power	$\leq$ 20dBm
HBS antenna gain	0dBi
Parameters for SINR Computations	
Penetration loss of outer wall L_{ow}	20dB
Penetration loss of inside wall L_{iw}	5dB
Shadow correlation	Between sites: 0.5 Intra site: 1.0
Thermal noise density	−174dBm/Hz
ICIC Parameters	
Number of iterations for seq det ICIC	$20 \cdot N_{\mathrm{HBS}}$
Number of iterations for sim pro ICIC	≥ 240
Minimum distance between MS and MBS	35m
Minimum distance between MS and HBS	20cm
Switching probability of resources in HBS i P_i	0.1

4.1.1 Wrap Around Concept

In order to model the inter cell interference accurately, the wrap around technique is introduced. Hereby, the actual evaluated area is mirrored and thereby effects at the edge of the evaluation environment are encountered. Figure 4.6 shows the evaluation area with one center cell and a surrounding ring of 6 cells. This area is copied one to one circularly around at each side resulting in a total of 6 copies. The copied area is just used to consider the interference on the evaluation area and not evaluated on its own. Beside their location all copies are identical.

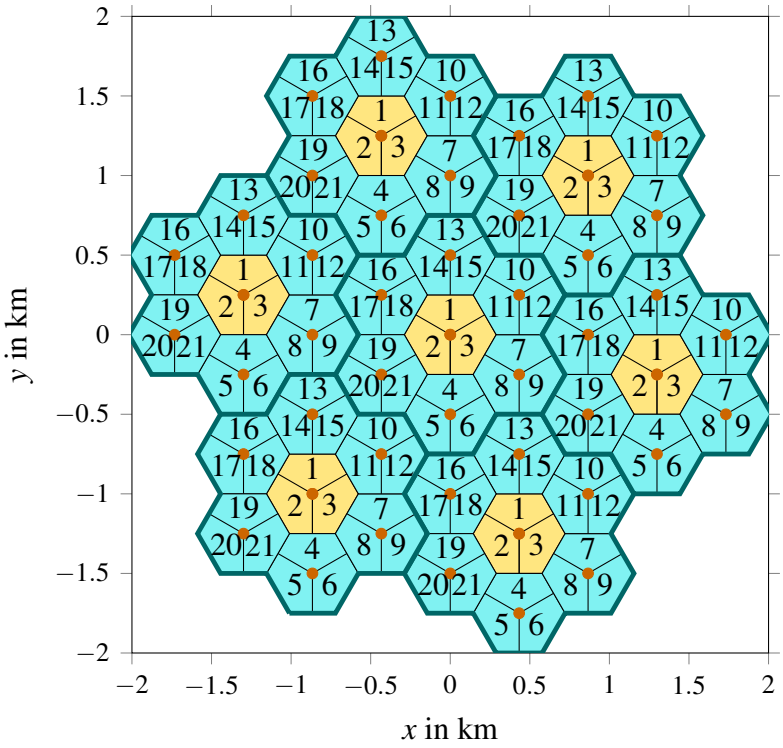

Figure 4.6: Wrap around for a hexagonal cellular network with a center cell and one ring

4.1.2 Representation of Results

In order to get a detailed analysis, the results for all user groups together and also separately for indoor and outdoor users of the macrocell as well as femtocell are examined. For the sake of base station sector investigations, data of each user class connected to the BS are gathered. The evaluation of the simulation results uses cdf-plots as well as bar diagrams. Within this chapter, the results of various simulations are shown for HBS deployment density levels of $P_{\mathrm{d}} = 0.42\%, 1.7\%, 5\%,$ and 20% which will be referred to as minimum, low, medium, and high density, respectively.

Figure 4.7 and Figure 4.8 show the structure of the bar plots. A key performance indicator is the achievable throughput, explained in Figure 4.7, which is evaluated in detail as follows.

The first two groups on the abscissa of the bar plots represent the throughput of the HBSs and MBSs in Mbit/s and 100kbit/s, respectively. The values are read from the left ordinate. If not stated differently, all users of a femtocell reside indoor, as a result no plot for outdoor FUEs is shown. The light colored part stands for the average and the dark colored for the cell edge throughput standing for the fifth percentile.

The left part of each of the two groups depicts the outdoor users, whereas the right part gives the performance of the indoor users. The performance of the indoor FUEs is colored in light and dark green and for outdoor FUEs in light and dark yellow, for mean and cell edge performance, respectively. For the critical group of the macrocell users, the throughput for outdoor UEs is drawn in blue and indoor UEs in red variants.

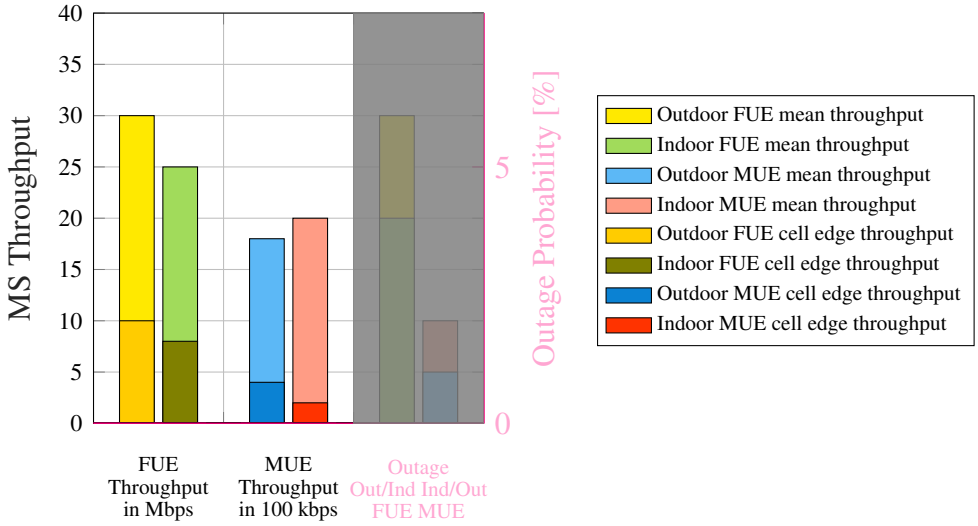

Figure 4.7: Representation of simulation results: Mobile station (MS) throughput for user equipment connected to an FBS (FUE) and user equipment connected to an MBS (MUE)

In a heterogeneous network with non-symmetric power levels and interference situations, next to the achievable throughput, an important parameter is the outage of the macrocell UEs depicted in Figure 4.8. Users within a femtocell could be handed over to the superimposed macrocell, thereby their critical interference situation can be solved. In contrast to this, the users within the coverage area of a femtocell, which are not a member of the CSG are not granted access, and experience thereby a sever interference situation which has to be taken care of. The outage probability of the users of the macrocell is the most critical thus has to be addressed.

The representation of the outage probability values can be read from the right ordinate. The bar in blue shows the outdoor MUE outage and the light red one the indoor MUE outage. Similar for FUEs, yellow for outdoor and light green for indoor users.

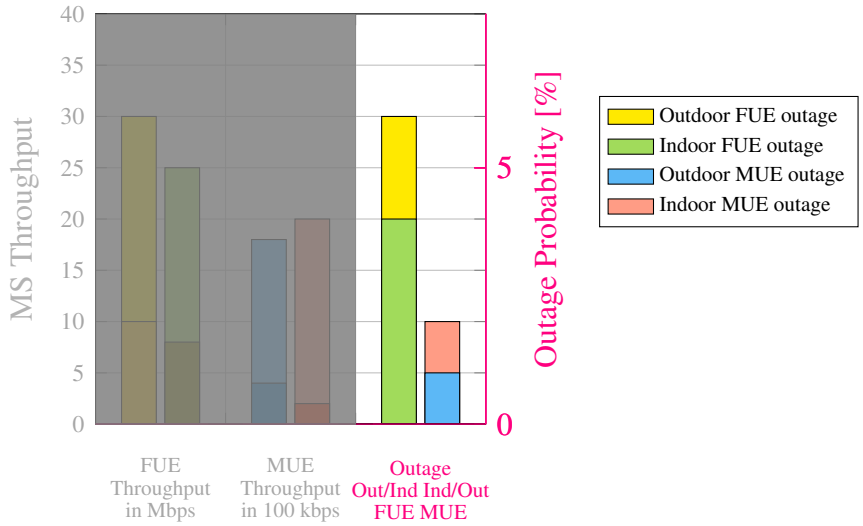

Figure 4.8: Representation of the simulation results: Outage Probability

4.1.3 Reference

In order to evaluate the performance of the developed dynamic interference coordination techniques, baseline simulations with (i) macrocell only, (ii) femtocell only as well as (iii) simulations with both layers for different HBS transmit powers are shown. Within the investigations of (i) and (ii) only base stations from one layer transmit, in the first case no femtocells are present and in the second case no macro base station transmits data. The performance of the baseline scenarios for a minimum density of femtocells, with one out of 240 apartments equipped with an HBS is given within Figure 4.9.

Figure 4.9a gives the throughput and outage of the outdoor and indoor MUEs for the baseline scenario according to (i). The average throughput is 1.29Mbit/s for outdoor and 1.26Mbit/s for indoor UEs connected to the MBS, whereas the throughput for the users at the cell edge is at around 250kbit/s for all users. Here a marginal number of users are in outage, in terms of numbers 0.06% of the users experience a throughput of less than 100kbit/s.

In order to increase the overall throughput in the network, the introduction of femtocells, discussed throughout the remainder of this chapter serves as an additional source. As can be seen in the subplot Figure 4.9b, femtocells as an additional layer can be introduced as a source of additional system throughput. Here only femtocells without data transmission on the umbrella MBS layer are present. The FUEs achieve a throughput of 39.24Mbit/s, close to the maximum achievable which calculates as

$$\begin{aligned} \Upsilon_{\text{total}} &= N_{RB} \cdot B_{\text{RB}} \cdot \Upsilon'_{\text{max}} \\ &= 50(12 \cdot 15\text{kHz})4.4\text{bit/s/Hz} = 39.6\text{Mbit/s}. \end{aligned} \tag{4.3}$$

The values for the calculation underlie the system-level simulation setting according to Table 4.1. They are in numbers 10MHz bandwidth and thus correspondingly 50RBs. Further,

the number of subcarriers per RB are $N_{\text{sc,RB}} = 12$ and the bandwidth per resource block is $B_{\text{RB}} = N_{\text{sc,RB}}\Delta f$. The maximum throughput per Hertz is $\Upsilon'_{\text{max}} = 4.4\frac{\text{bit/s}}{\text{Hz}}$, as given in Section A.3. Practically, no outage is present with value close to zero. The minimum deviation results from the occurrence of a very unlikely tight adjacent location close to co-location of two femtocells.

When the macrocell layer and the femtocell layer are both deployed and use the same spectrum, depicted in Figure 4.9c, high outage probability results for the users of the HBS which transmit only with 0dBm and outage for the MUEs is introduced due to the inauguration of the second layer. Signal attenuation due to path loss and penetration loss especially of the outer walls of buildings, together with the short distance to a HBS inside the building, causes 10.8% of the macrocell users experience throughput values below the defined threshold of 100kbit/s and these are therefore denoted as users in outage. The throughput for the femtocells is reduced to 18.49Mbit/s due to the reduced transmit power and introduced interference of the macrocell compared to case (ii). The performance of the MUEs of 1.056Mbit/s for outdoor and 1.018Mbit/s for indoor users is reduced around 15% but is still at a reasonable level due to the fact that only very few femtocells are introduced. Different, the values for the least five percent are reduced to only about 62kbit/s, indicated by the dark red and blue bars in the plot, which corresponds to a reduction of 75%. Compared to (ii) also outage for the femtocells is present with about 8.2%.

If the transmit power for the femtocell UEs is increased to 20dBm, as in Figure 4.9d, the throughput of the HBSs is increased to 35.21Mbit/s on average and 12.96Mbit/s for the fifth-percentile, but the outage probability for MUEs within a building is further increased.

Consequently, measures to encounter the introduced interference from the second layer are required, in order to provide all users reliable data transmission. A promising method to encounter this is the dynamic ICIC technique proposed in this thesis. The results are presented within the next sections.

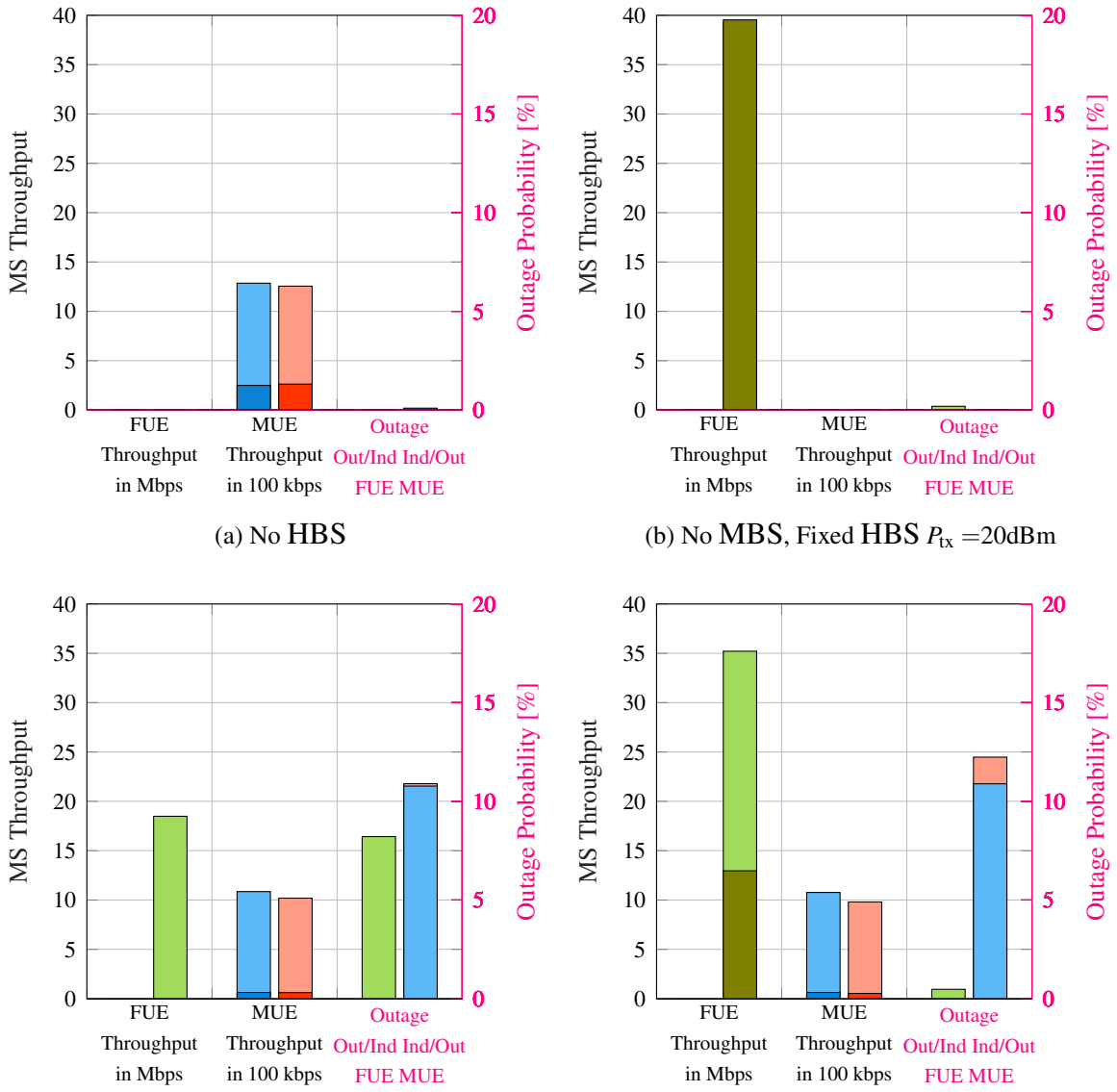

(a) No HBS

(b) No MBS, Fixed HBS P_{tx} =20dBm

(c) Fixed HBS P_{tx} =0dBm

(d) Fixed HBS P_{tx} =20dBm

Figure 4.9: Simulation results: Reference simulations without inter-cell interference coordination for a minimum density of home base stations (HBSs) i.e. one HBS per macro base station (MBS) and 21 MBS in total, $P_{\text{d}} = 0.42\%$

When the density of the HBSs in the network is increased, additional interference is introduced in the system. Exemplary for a deployment ratio of $P_{\text{d}} = 0.05$, which results in 12 HBSs per MBS, Figure 4.10 presents based on Figure 4.9 the baseline for higher femtocell density. Compared to the scenario with fewer femtocells, now, especially the throughput for the least five percent is tremendously decreased to due to the introduced interference. Before, all femtocells where sufficiently separated and did not affect each other beside an insignificant case. Thus,depicted in Figure 4.10b, the average throughput is reduced from 39.24Mbit/s to 34.43Mbit/s and the fifth-percentile is reduced to 5.63Mbit/s, compared to the less deployed setting. Now, 1.79% of the femtocell users are below the previously given threshold. For the setup with MBSs and HBSs with 0dBm and 20dBm the throughput is

reduced for all users and the outage probability for indoor MUEs increased to 16.7% for a transmit power of 0dBm and even 33.13% for 20dBm. Especially indoor users of a macrocell experience higher interference which gives a reduced throughput of only 900.3kbit/s and 684.9kbit/s, respectively on average and marginal throughput for the cell edge users. As can be seen, the denser the network, the more demand on techniques to address this interference.

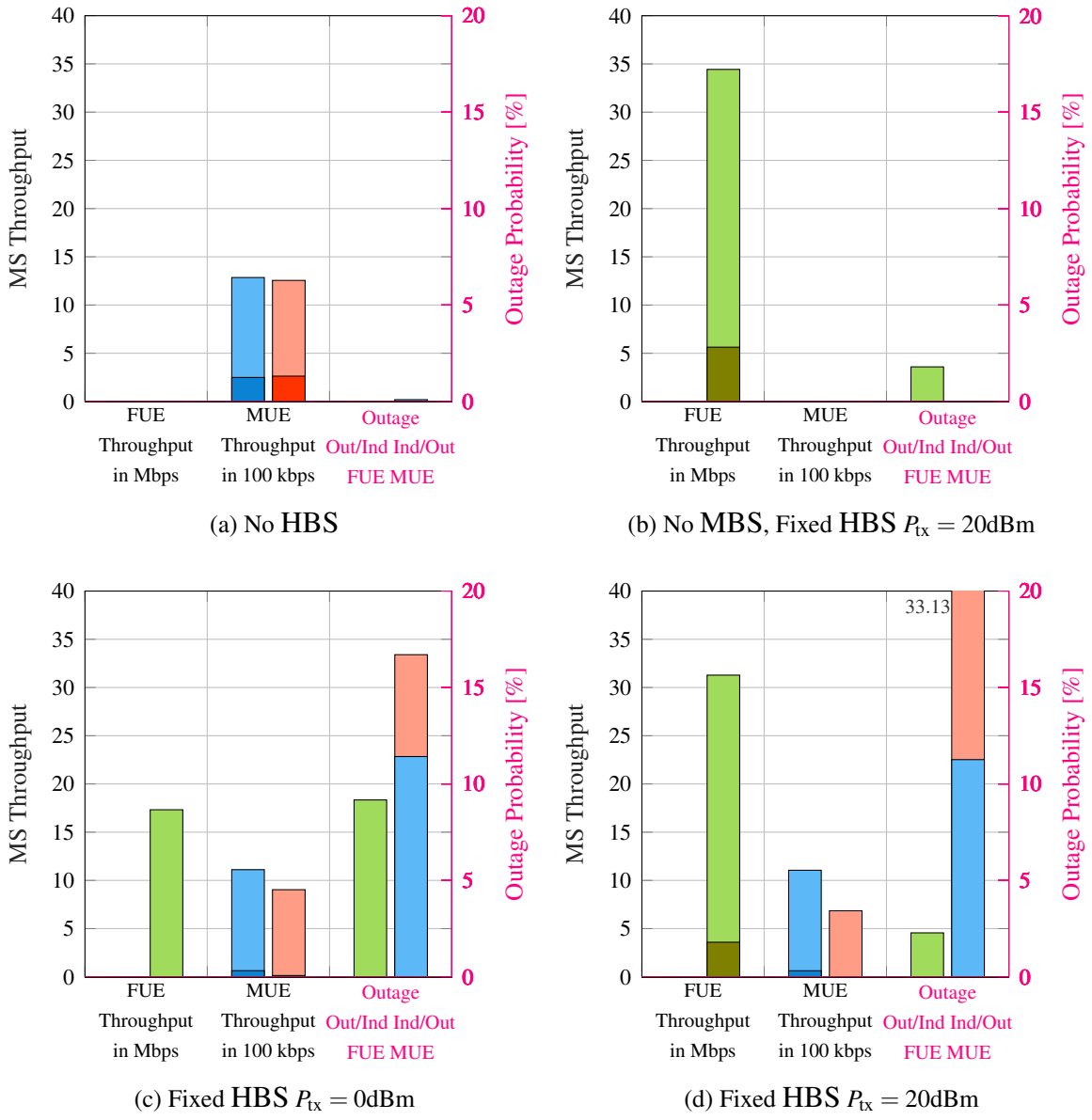

(a) No HBS

(b) No MBS, Fixed HBS $P_{\text{tx}} = 20\text{dBm}$

(c) Fixed HBS $P_{\text{tx}} = 0\text{dBm}$

(d) Fixed HBS $P_{\text{tx}} = 20\text{dBm}$

Figure 4.10: Simulation results: Reference simulations without inter-cell interference coordination for a medium density of home base stations, $P_{\text{d}} = 5\%$

The results for an even more dense deployment with $P_{\text{d}} = 20\%$ are presented in Figure 4.11. Here each macrocell contains 48 HBSs. With 21 MBS sectors, this results in a total of 1008 HBSs. The achievable throughput decreases on average over all users, as well as for the cell edge user and the outage especially for the macrocell users further increases. If the transmit power for the femtocell UEs is increased from 0dBm to 20dBm, the throughput of

the HBSs is increased, but the outage probability for MUEs within a building is tremendously increased. Further, the improvement for the FUEs is lower compared to the medium density deployment. The higher the density of the femtocells gets in a network, the more clear becomes the demand for techniques to encounter the critical interference situations.

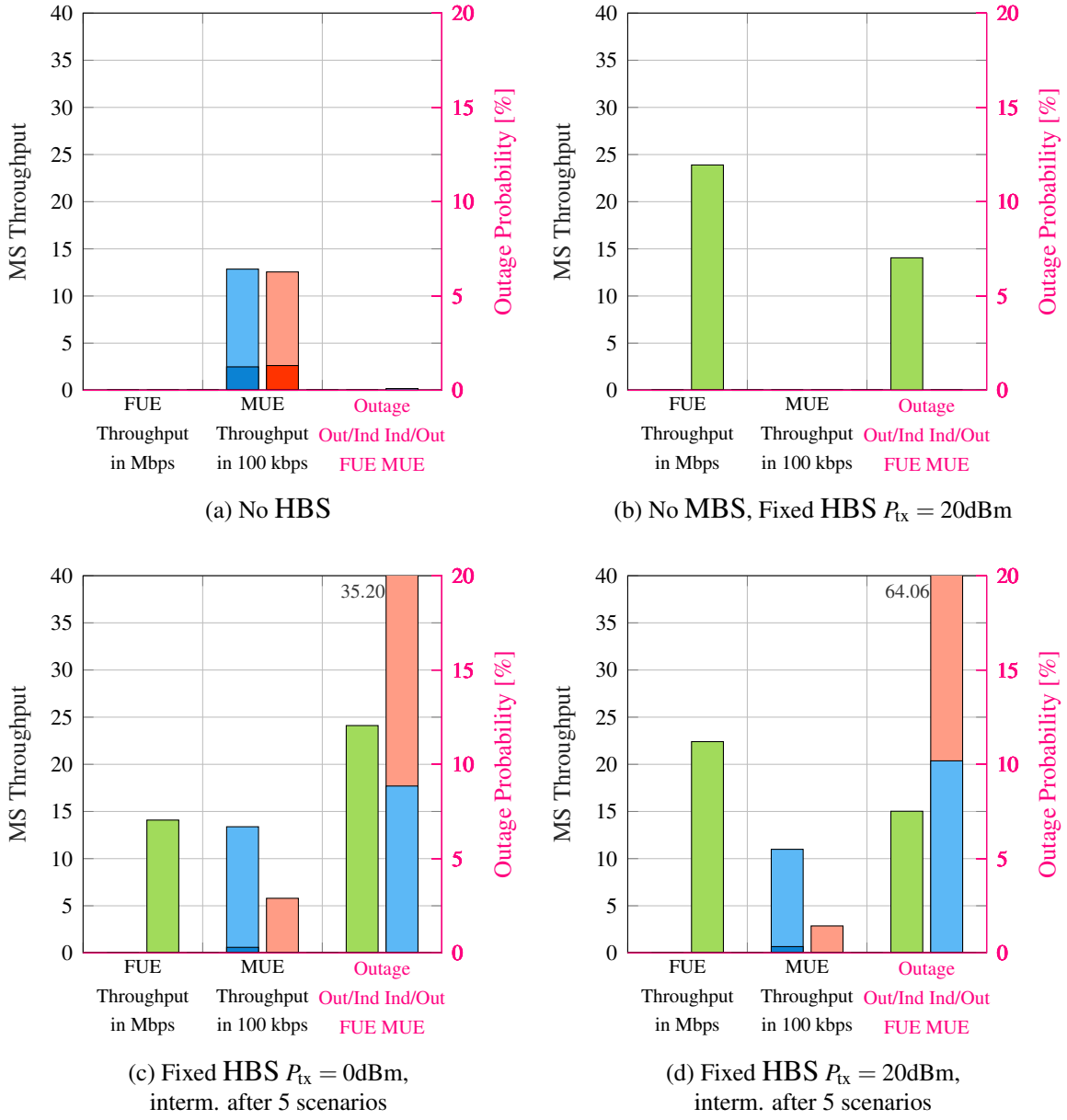

(a) No HBS

(b) No MBS, Fixed HBS $P_{\text{tx}} = 20\text{dBm}$

(c) Fixed HBS $P_{\text{tx}} = 0\text{dBm}$, interm. after 5 scenarios

(d) Fixed HBS $P_{\text{tx}} = 20\text{dBm}$, interm. after 5 scenarios

Figure 4.11: Simulation results: Reference simulations without inter-cell interference coordination for a high density of home base stations, $P_{\text{d}} = 20\%$

To summarize, the outage of indoor FUEs is minimized for the maximum allowed HBS transmit power of 20dBm. However, this reduces the throughput of the macrocell significantly. High outage of the MUEs occurs, where especially the portion of the indoor macrocell edge users show unacceptable outage probability. Overall, this makes the introduction of methods to coordinate the interference situation necessary.

4.2 Application of Sequential Deterministic Interference Coordination

When femtocells are inserted into a homogeneous cellular system, additional interference is introduced as has been discussed within Section 2.4 and shown within the previous section supported by simulation results. In order to guarantee a good co-existence of the different cells, interference coordination is essential. Within this section, the sequential deterministic method is discussed. As a first comparison, the sequential deterministic method is shown next to the reference simulation without interference coordination from the previous chapter, for a low deployment setting with four HBSs per MBS which results in a total of 12 HBSs as one central cell is considered in Figure 4.12.

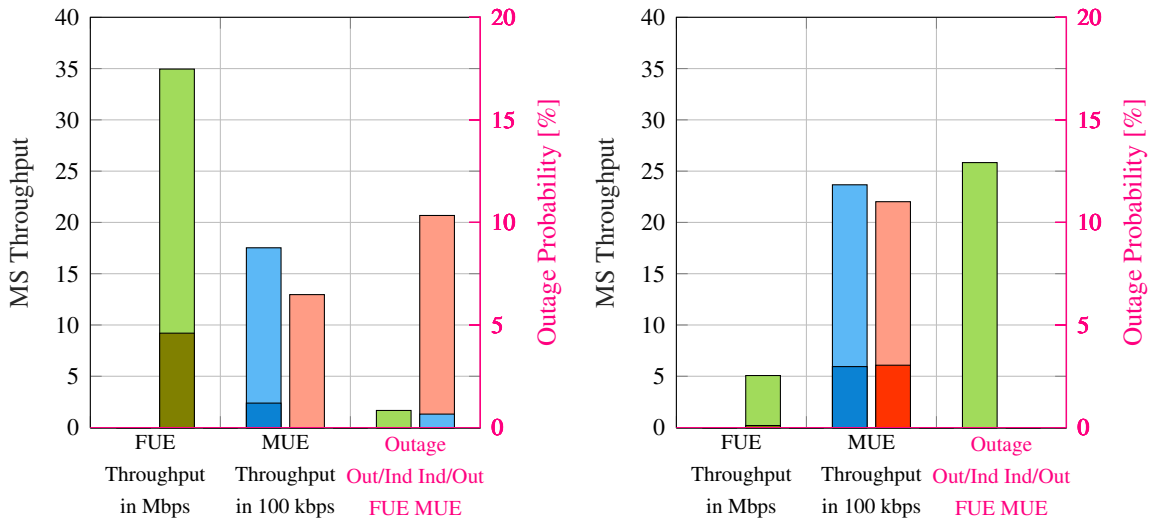

(a) No ICIC

(b) Sequential deterministic

Figure 4.12: Comparison of sequential deterministic and no inter-cell interference coordination for a low deployment density with four home base station per macro base station (MBS) and three MBS overall, $P_{\mathrm{d}} = 1.7\%$

In here the number of used resource blocks per HBS is low as the number of allowed subbands $D_i = 1$ is set at the minimum. What can be seen is that the FUE throughput is reduced to about 5Mbit/s which comes along with an increased outage probability for users of the femtocells but what is really most important, the outage probability for the MUEs is completely removed. In general, the average and cell edge throughput for all users of the macrocell improves significantly. Thus, the interference coordination technique is a solution to protect the highest layer. When loosening the constraint of only one subband at a time per HBS the performance of the local low power base stations can again be improved which is shown within Section 4.4 and further.

Figure 4.13 again compares the sequential deterministic with the setting without coordination for a denser network with $P_{\mathrm{d}} = 0.2$ which results in 48 HBSs per MBS.

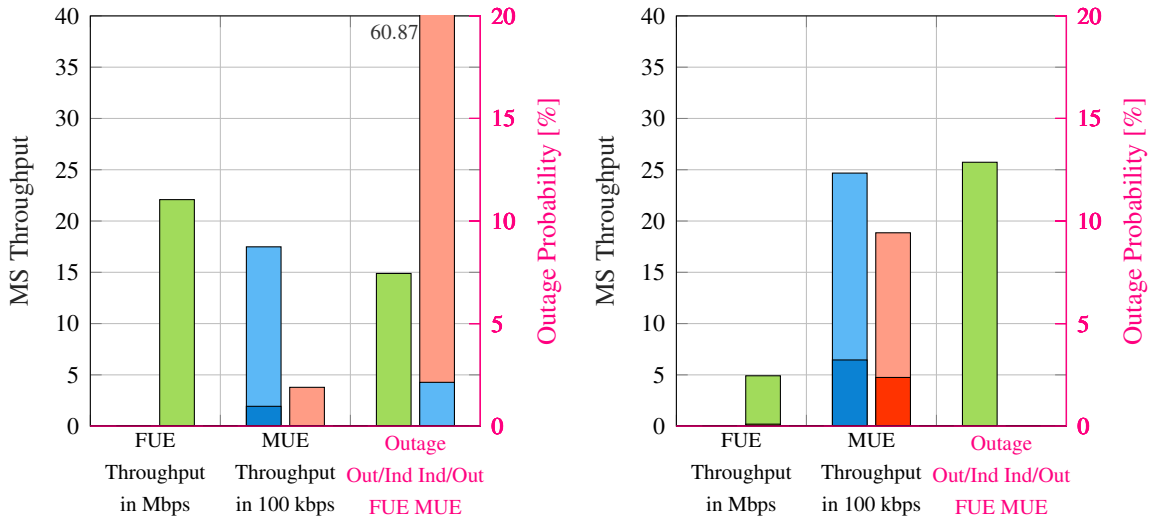

(a) No ICIC

(b) Sequential deterministic

Figure 4.13: Comparison of sequential deterministic and no inter-cell interference coordination for a high deployment density with 48 home base station per macro base station (MBS) and three MBS overall, $P_{\mathrm{d}} = 20\%$

When the number of HBSs per MBS increases from 4 to 48 as can be seen from Figure 4.12a to Figure 4.13a, respectively, the performance for the heterogeneous setting without coordination of the interference tremendously decreases, whereas the cell edge users and in particular the indoor MUEs experience the strongest impact with unacceptable outage probability. The throughput of the users of the femtocell is again higher than for ICIC but already decreases by around 37% compared to the low deployment density situation. On the other side, with interference coordination the throughput rate for the FUEs decreases only marginally if more femtocells are introduced and the average and cell edge user throughput for the MUEs is still hardly affected when the density is increased as presented from Figure 4.12b to Figure 4.13b. In sum, the throughput for the FUEs is still much lower with ICIC but can be improved with a higher number of allowed resources D_i shown in Section 4.4. The performance for the MUEs is considerably improved if ICIC is used.

4.3 Comparison of the Advanced Interference Coordination Techniques

Within this section, the advanced simultaneous probabilistic method is introduced and discussed in relation to the global optimum and the sequential deterministic technique. The simultaneous probabilistic method shows a very good performance, close to the results from the global optimizer which has been shown for the tractable deployment scenarios and similar to the sequential deterministic approach in Section 3.6. This section compares the different coordination algorithms to handle interference and shows the results of various simula-

tions with low and medium HBS deployment density levels. While the global optimizer can only be compared for minimum and low deployment scenarios due to the intensive required simulation time, the other proposed techniques can be simulated also for very dense situations and it is conceivable that the dynamic simultaneous probabilistic method is able to be integrated in real mobile cellular communication systems.

First, the sequential deterministic, the simultaneous probabilistic techniques, and the global optimizer are compared for a low deployment setting with four HBSs per MBS which results in a total of 12 HBSs as one central cell is studied in Figure 4.14. In here the number of used resource blocks per HBS is low whereas the number of allowed subbands $D_i = 1$ is set at the minimum value.

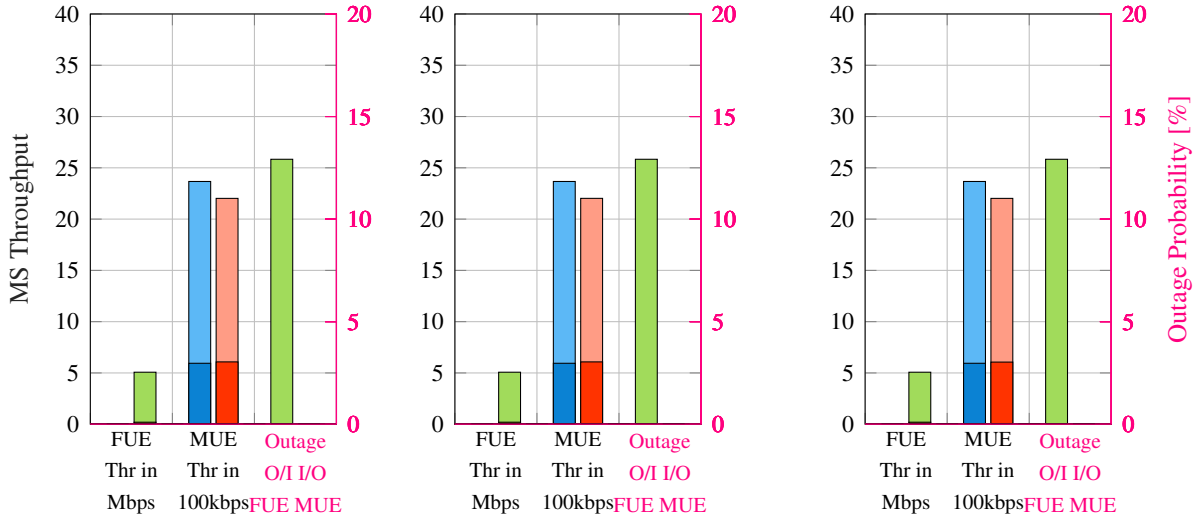

(a) Sequential deterministic (b) Simultaneous probabilistic (c) Global optimizer

Figure 4.14: Comparison of sequential deterministic, simultaneous probabilistic inter cell interference coordination algorithm, and global optimizer for a low deployment density with four home base station per macro base station (MBS) and three MBS overall, $P_{\mathrm{d}} = 1.7\%$

As can be seen from Figure 4.14, the performance in terms of throughput and outage probability is similar for both interference coordination techniques and the global optimizer. Their main difference is the time to converge, discussed in detail within Section 3.6 and a slight difference also due to the optimization criteria where the global optimizer cares for the overall minimization of the interference and the sequential deterministic and the simultaneous probabilistic care for the interference situation present within each femtocell. As a result, the simultaneous probabilistic method is preferable due to the previously mentioned scalability for real deployment densities and its independence to communicated successive processing.

The same relation holds, when the deployment density is increased as shown in Figure 4.15. This figure compares the two interference coordination methods for a home base station deployment with a center cell and one ring with 12 HBSs per sector, thus in total 252 HBSs. As can be seen, again within this medium dense situation, the methods perform similar in

terms of throughput and outage probability as in the less dense and smaller setting. Further simulations with a high density of HBSs show the same relation therein witness the findings.

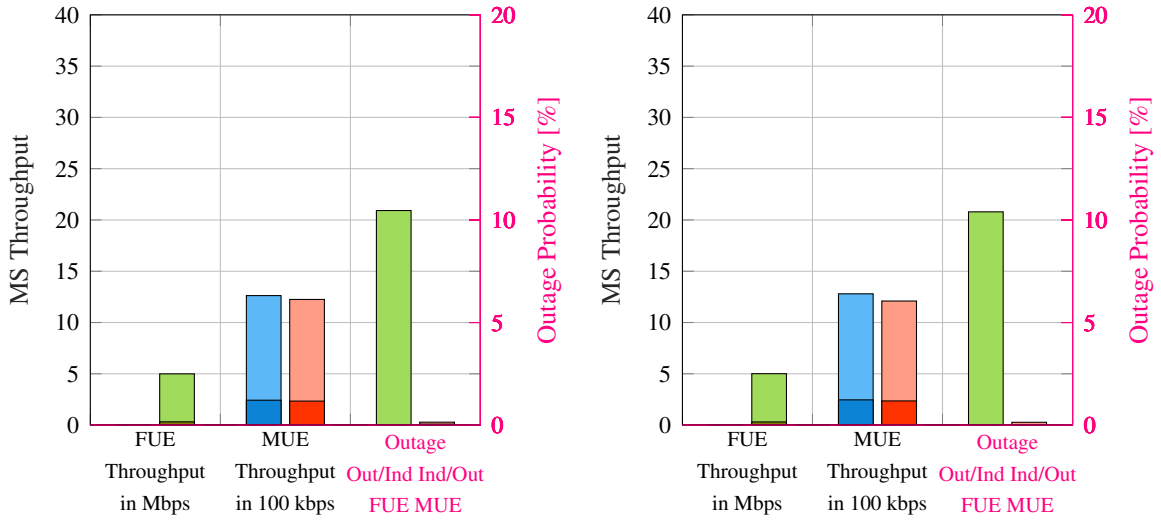

(a) Sequential deterministic, 50 scenarios

(b) Simultaneous probabilistic, 100 scenarios

Figure 4.15: Comparison of sequential deterministic and simultaneous probabilistic inter cell interference coordination algorithm for a medium deployment density with 12 home base station per macro base station (MBS) and 21 MBS overall, $P_{\mathrm{d}} = 5\%$

On the whole, the sequential deterministic and the simultaneous probabilistic algorithm perform similar in terms of throughput and outage and their main difference is the convergence behavior and adaptability to real world scenarios.

4.4 Simultaneous Probabilistic Method with Different Loads of Resources

Within Section 4.2 the interference coordination technique has been introduced and the potential to significantly reduce the impact on the femtocell and macrocell layer highlighted. On the other hand, the achievable throughput in the femtocell is reduced by limiting the amount of available resources to the minimum. To lower this impact, the number of available subbands in the femtocells is discussed as introduced in Section 3.4. Further, this section shows the results of various simulations with HBS density levels from minimum, medium to high, in Figure 4.16, Figure 4.17 , and Figure 4.18, respectively, as well as for the number of available resources in HBS cell i of $D_i = 1,\ldots,4$ used subbands in each HBS. Figure 4.16 shows the results for 21 MBSs and 21 HBSs in total for subband sizes rising from one in Figure 4.16a up to four in Figure 4.16d.

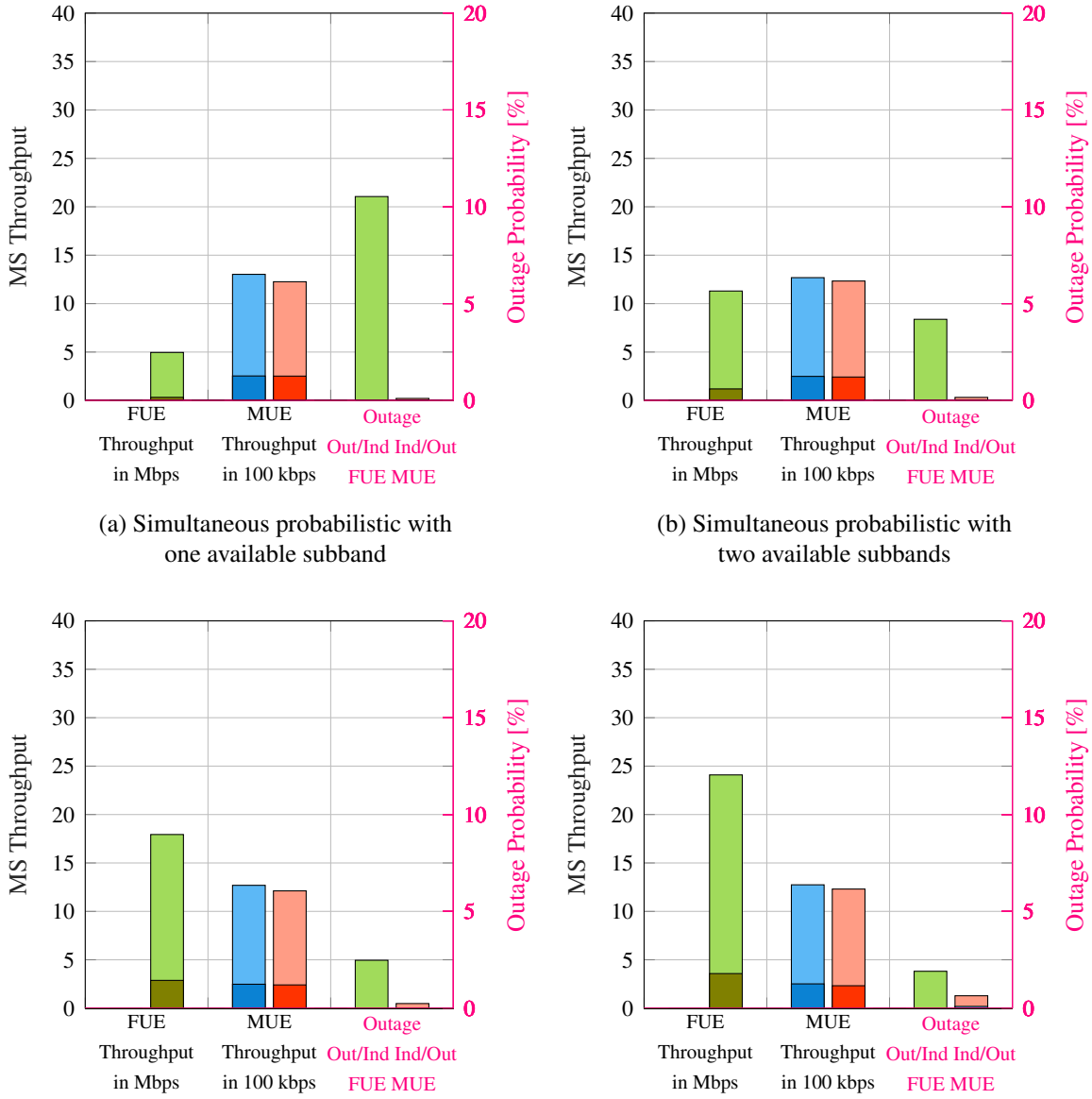

(a) Simultaneous probabilistic with one available subband

(b) Simultaneous probabilistic with two available subbands

(c) Simultaneous probabilistic with three available subbands

(d) Simultaneous probabilistic with four available subbands

Figure 4.16: Simulation Results: Simulation with ICIC simultaneous probabilistic for a minimum HBS density, 1 HBS per MBS, 21 MBS in total and number of available subbands D ranging from 1 up to 4 subbands

This scenario represents a minimum density deployment, where interference between femtocells is hardly present and also the macrocell users do not experience sever interference. Thus the performance is not interference limited but mainly influenced by the regulations of the resource patterns. The throughput of the macrocell users remains nearly the same when the number of subbands used in the femtocells is increased and the outage probability for the macro users increases minimally. Opposite for the femtocell users, where the number of subbands increases approximately linear with the number of allowed subbands. This is reasonable, as in non-interference limited deployments the increase in throughput is propor-

tional to the increase in the available bandwidth. Reverse, the outage probability decreases when the subband size is increased, as highly interfered users of the femtocell which can only transmit with low modulation and coding schemes increase their rate to a reasonable value.

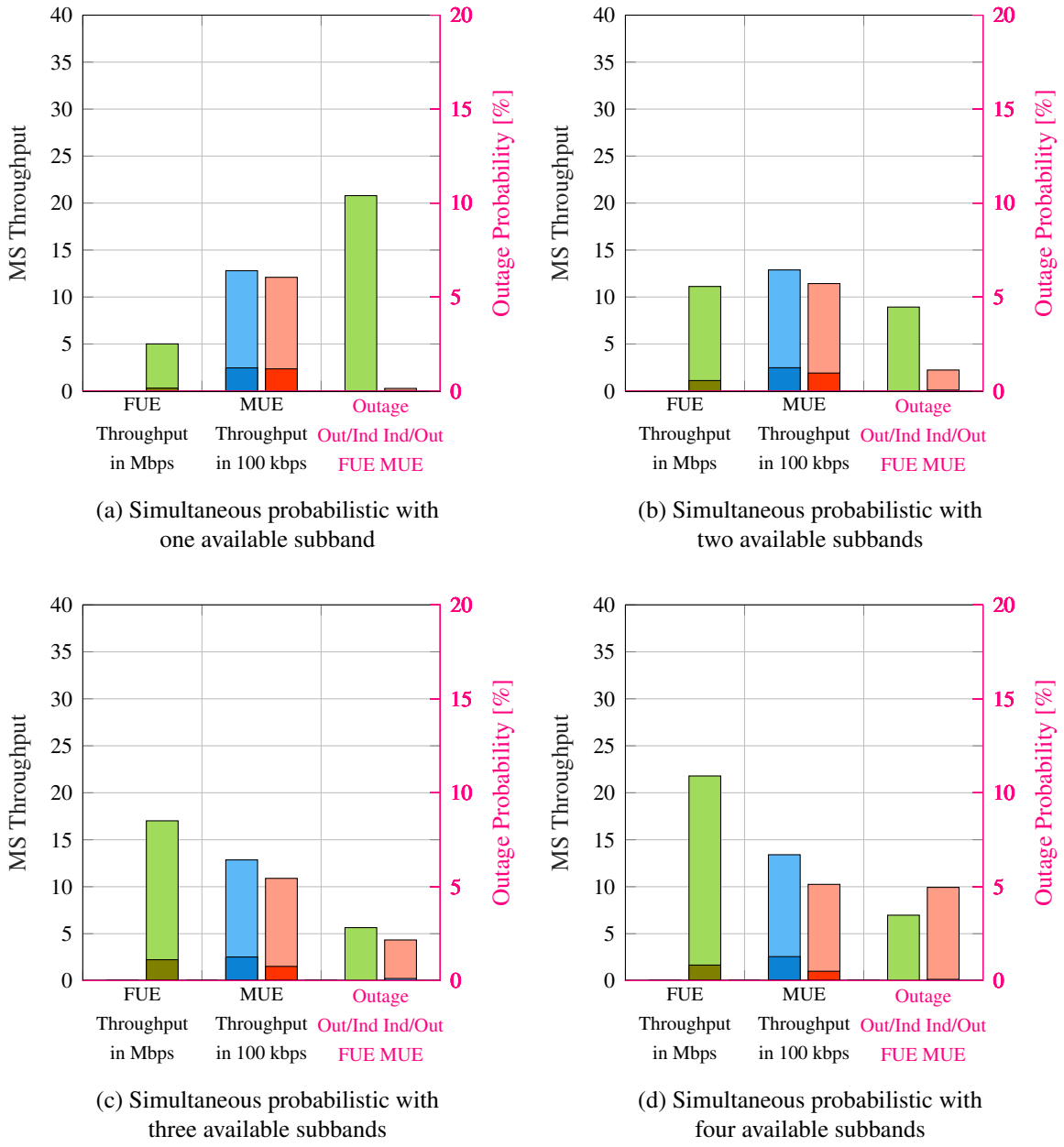

(a) Simultaneous probabilistic with one available subband

(b) Simultaneous probabilistic with two available subbands

(c) Simultaneous probabilistic with three available subbands

(d) Simultaneous probabilistic with four available subbands

Figure 4.17: Simulation Results: Simulation with ICIC simultaneous probabilistic for a medium HBS density i.e. 12 HBS per MBS, 21 MBS in total and number of available subbands D ranging from 1 up to 4 subbands

When the number of femtocells is increased to a medium density, the throughput for the macrocell users is decreased slightly and especially the average and cell edge throughput for indoor users decreases when the number of subbands in the HBSs increases. The detailed depiction of the results for the simultaneous probabilistic method is shown in Figure 4.17.

While for few used subbands the outage is very small, it increases up to five percent for the indoor MUEs. The throughput for the FUEs still increases with the number of available subbands but less than before as interference between femtocells forces the HBSs to use lower modulation and coding schemes in order to maintain reliable transmission. As a result the throughput for the users of a femtocell does not increase linearly with the number of subbands anymore.

The details of the simultaneous probabilistic algorithm with 1008 HBSs are depicted in Figure 4.18

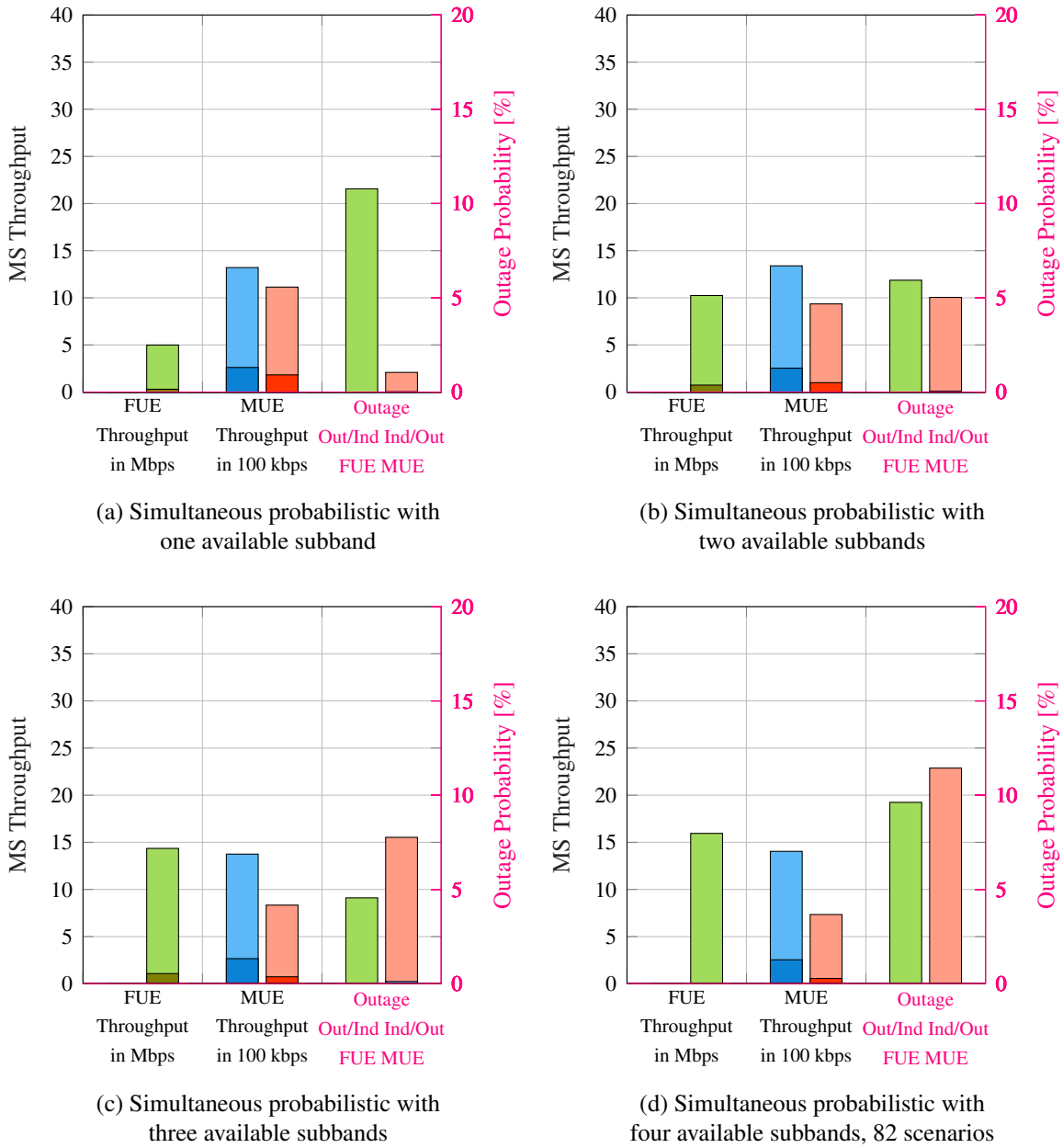

(a) Simultaneous probabilistic with one available subband

(b) Simultaneous probabilistic with two available subbands

(c) Simultaneous probabilistic with three available subbands

(d) Simultaneous probabilistic with four available subbands, 82 scenarios

Figure 4.18: Simulation Results: Simulation with ICIC simultaneous probabilistic for a high HBS density i.e. 48 HBS per MBS, 21 MBS in total and number of available subbands D ranging from 1 up to 4 subbands

In case the density of the femtocells is increased even further to high density, the throughput for the macrocell users is further decreased and especially the average and cell edge throughput for the indoor users decreases when the number of subbands in the HBSs increases. The details for the simultaneous probabilistic algorithm are depicted in Figure 4.18. While for few used subbands the outage is small, it increases up to about 13.5% for the indoor MUEs. The throughput for the FUEs still increases with the number of available subbands but less than before as the interference between femtocells forces the HBSs to use lower modulation and coding schemes in order to maintain reliable transmission. The throughput for the users of a femtocell does not increase linearly with the number of subbands as in the low deployment scenario.

The optimum number of subbands for transmission changes with the deployment density of the network. As a consequence, an interference threshold to adapt the number of allowed subbands in the femtocells will further optimize the overall performance.

4.5 Simultaneous Probabilistic Method for Different Resource Adaptation Probabilities

When the resource adaptation probability P_i, which ranges from 0 to 100%, is changed the throughput for reasonable values is similar as depicted in Figure 4.19 but the convergence behavior is increasing with decreased probability P_i as discussed in detail within Subsection 3.6.4. Figure 4.19 presents the average, cell edge throughput, and outage probability exemplary for values in the range from 0.05 up to 0.3 in four bar plots. In here, the evaluation starts after 240 iterations.

The evaluation of the inter-cell interference coordination algorithm starts after the predefined number of iterations. As long as the method converges before it is applied, there is only a marginal difference between the different variants of the simultaneous probabilistic methods with different resource adaptation probabilities. This is also reflected in Figures 4.19a–4.19d.

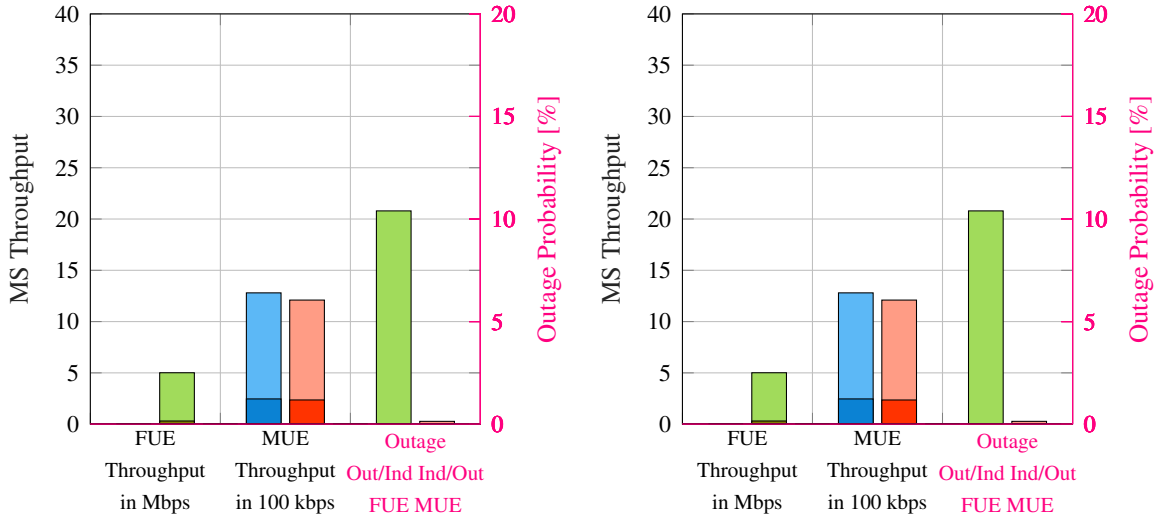

(a) Simultaneous probabilistic with $P_i = 0.05$

(b) Simultaneous probabilistic with $P_i = 0.10$

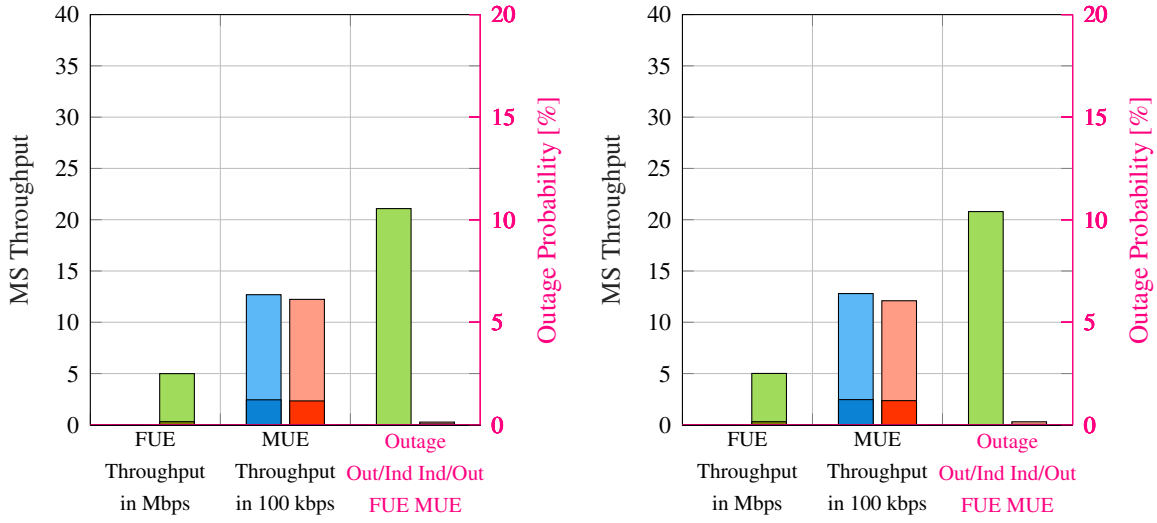

(c) Simultaneous probabilistic with $P_i = 0.15$

(d) Simultaneous probabilistic with $P_i = 0.30$

Figure 4.19: Simulation Results: Simulation with ICIC simultaneous probabilistic for a medium HBS density i.e. 12 HBS per MBS, 3 MBS in total and number of available subbands D=1, changing P_i from 0.05 to 0.3

Different from Figure 4.19 with resource adaptation probabilities from 5 to 30%, Figure 4.20 depicts the average, cell edge throughput, and outage probability for low values of 0.1 and 1% as well as for high values as 80 and 95% in four bar plots. Again, the evaluation starts after 240 iterations. Now, other than in Figure 4.19 changing the adaptation probability especially to very low as 0.1% or very high as 95% shows a difference in performance. Values within this range decrease the user throughput and increase the outage probability compared to the selected values in Figure 4.19. The necessity to select an appropriate value for P_i has already been discussed during the evaluation of the time to reach a beneficial interference

level within Subsection 3.6.4. As a conclusion, the resource adaptation probability has to be chosen reasonably, as the system-level simulations suggest, preferentially larger than 1% and below 80%.

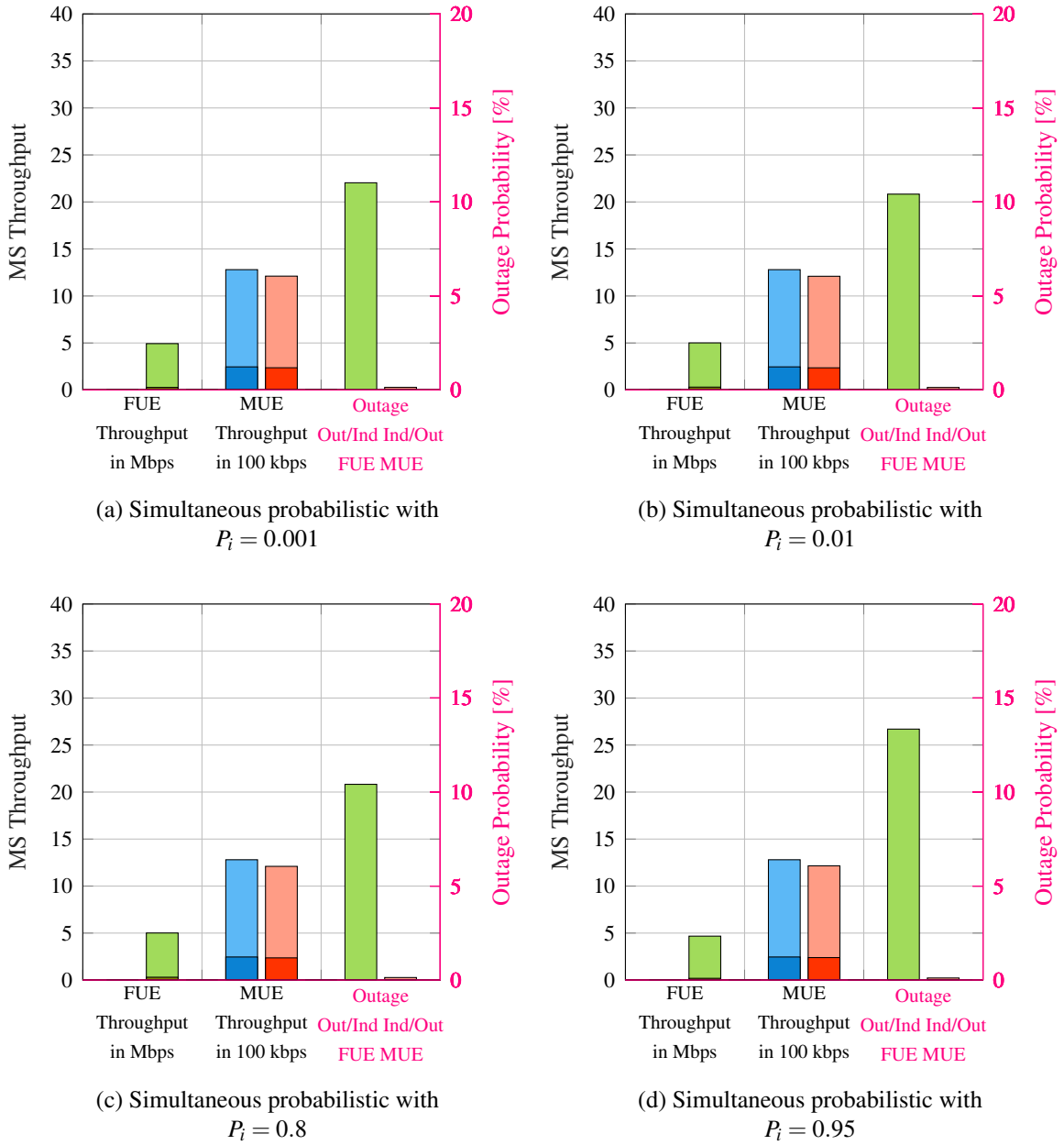

(a) Simultaneous probabilistic with $P_i = 0.001$

(b) Simultaneous probabilistic with $P_i = 0.01$

(c) Simultaneous probabilistic with $P_i = 0.8$

(d) Simultaneous probabilistic with $P_i = 0.95$

Figure 4.20: Simulation Results: Simulation with ICIC simultaneous probabilistic for a medium HBS density i.e. 12 HBS per MBS, 21 MBS in total and number of available subbands D=1, changing P_i from very low to very high probabilities

Thus, the resource pattern adaptation probability P_i has to be selected according to the present deployment scenario as a trade-off between convergence speed and behavior. The system-level simulations endorse $P_i = 0.1$ as a suitable value for the present heterogeneous network.

4.6 Detailed Investigation by Means of the Cumulative Distribution Function of Throughput and Signal-to-interference and Noise Ratio

Within this section, the details of the system-level simulation results are shown by means of the CDF. The investigations underly the assumptions of Table 4.1. SISO transmission within a bandwidth of 10MHz is used. For increasing bandwidths, accumulating increasing number of CCs, and application of MIMO techniques, the rates scale with the bandwidth, the number of available CCs, and the number of spatial multiplexing streams, respectively.

The different techniques are abbreviated as follows: The sequential deterministic by "SeqDet", the simultaneous probabilistic as "SimProb", and the global optimizer as "GlobalOpt". In Figures 4.21 and 4.22 overall 12 HBSs are present on top of the MBS area. Figure 4.21 shows the CDF of the throughput of all mobile stations in the network. The cdf(x_0) is the probability that the throughput is below or equal to x_0. The curves for the SeqDet, SimProb, and Global Opt do overlap.

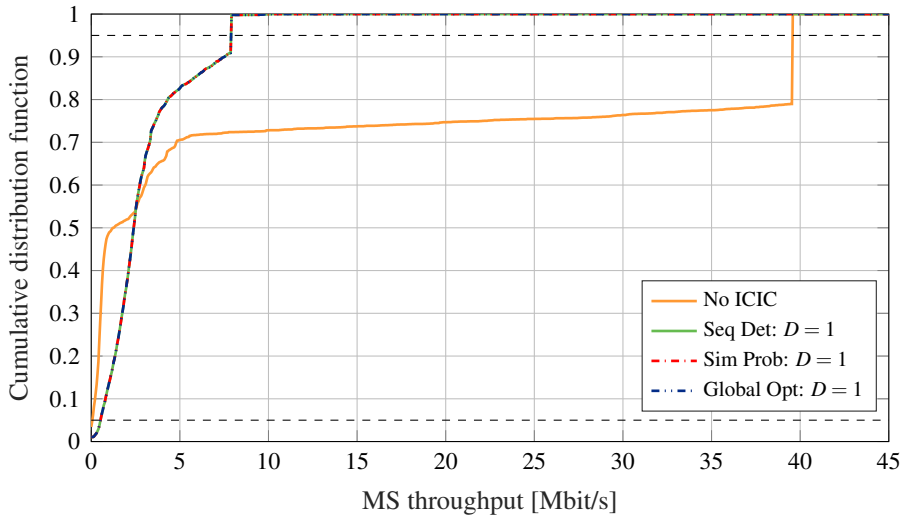

Figure 4.21: ICIC sequential deterministic, simultaneous probabilistic, global optimizer, and no ICIC for a low HBS density, with 3 MBS and 12 HBS: CDF of the throughput of all mobile stations in the network

In Figure 4.21 45% of the users gain a higher data rate with interference coordination, but the rest of the users experiences only minimal throughput rates down to even zero. The kink in the throughput curve, for no interference coordination at around 39.55Mbit/s and for the sequential deterministic, the simultaneous probabilistic, as well as the global optimizer at about 7.9Mbit/s, results from the limits due to the maximum implemented MCS. The derivation of the maximum achievable throughput value is given in (4.3) within Section 4.1.3. As a result, even within this low deployment setting a lot of users are interfered by the femtocells. Figure 4.22 investigates the throughput of the users connected to the MBS which are located

outdoor, indicated with the dashed colored curves. In addition, it gives the throughput of the users connected to the MBS which are located inside the same building as the femtocell, drawn with a solid line. Again, as in Figure 4.21 the lines of the curves for the SeqDet, SimProb, and Global Opt match.

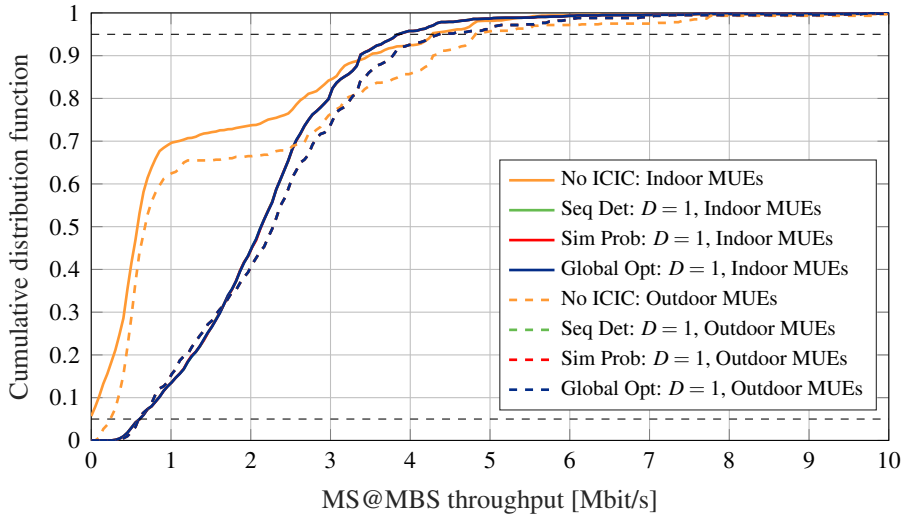

Figure 4.22: ICIC sequential deterministic, simultaneous probabilistic, global optimizer, and no ICIC for a low HBS density, with 3 MBS and 12 HBS: CDF of the throughput of outdoor and indoor mobile stations connected to the MBS

The throughput of the outdoor MUEs draws 20% of the users which gain up to about 1Mbit/s higher data rates without interference coordination, but the rest of the users has only minimal data rates decreasing even to zero. The observation made for the outdoor users is even more sever for the MSs located indoors which can directly be shown with the throughput curve. Now, even more severe: 12% of the users gain up tp about 750kbit/s higher data rates with no interference coordination but the remainder of the users receives only minimal rates below 1Mbit/s for 70% of the users and up to 5% of the users have zero rate. In sum, ICIC presents much higher cell edge and average throughput. Even in this minimum density deployment the indoor MUEs experience unacceptable interference levels.

The following considerations are made for a high density deployment with 1008 HBSs in the network. Again, the interference coordination techniques are compared to the situation without coordination. Figure 4.23 gives the UE throughput of all mobile stations in the network. For the overall throughput holds, as much more HBSs are introduced in the network which results also in a higher number of FUEs (1008) and the number of MUEs, in numbers 210, is much lower, that the crossing point moves. Now 78% of the users gain higher data rates without interference coordination but the rest has only minimal rates down to nothing at all. 12% of the users get even no throughput without interference coordination. When ICIC is applied only 2.5% remain with zero throughput within this very dense scenario. Thus, the weak performance for the cell edge users, which leads to a lot of users in outage, when no interference coordination is used, is unacceptable. Figure 4.24 depicts the throughput of the

users connected to the MBS. The users are split in two groups: First, the users connected to the MBS which are located indoors in the same building with the femtocell. And second, those users who are located outdoor. As before, the curves for the SeqDet and SimProb method, if not depicted differently, lie on top of one another.

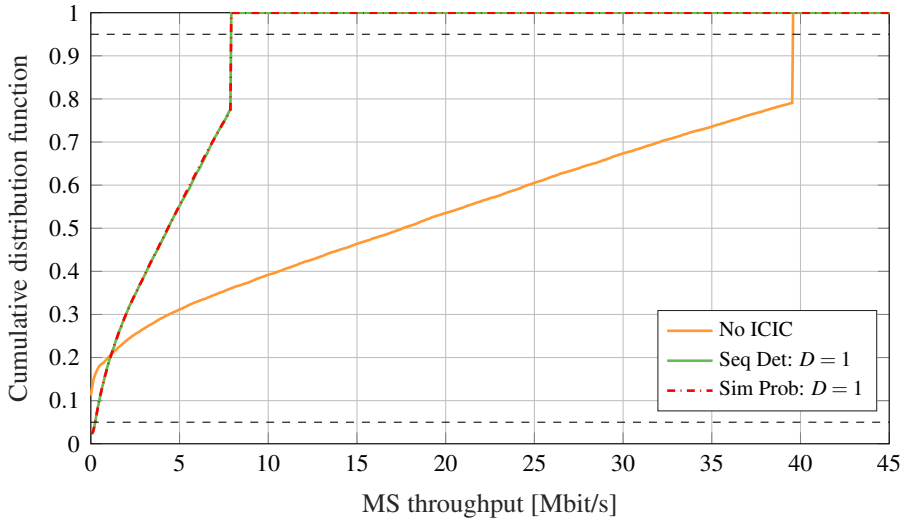

Figure 4.23: ICIC sequential deterministic, simultaneous probabilistic, and no ICIC for a high HBS density, with 21 MBS and 1008 HBS: CDF of the throughput of all mobile stations in the network

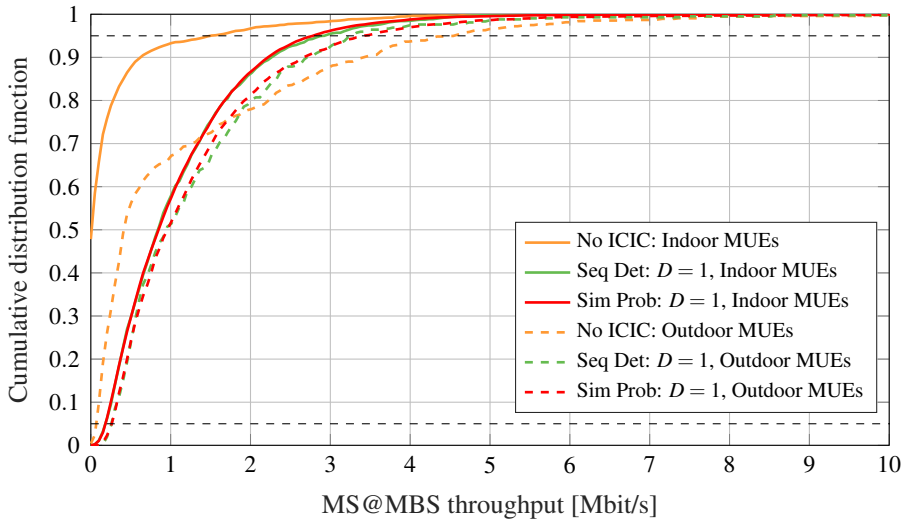

Figure 4.24: ICIC sequential deterministic, simultaneous probabilistic, and no ICIC for a high HBS density, with 21 MBS and 1008 HBS: CDF of the throughput of outdoor and indoor mobile stations connected to the MBS

When interference coordination is used, 75% of the outdoor users now experience a better situation. In here, the demand for interference coordination gets even more clear: All indoor users experience a better situation as without coordination. With ICIC no users have zero

data rate. Without coordination approximately 50% of the indoor MUEs are not able to receive any data. With this it gets even more clear, that interference handling measures have to be taken. Figure 4.25 shows the SINR within this dense deployment. In case of no coordination, the SINR of the cell edge users gets below -10dBm, which is very bad. Differently, when ICIC is applied it is still below 0dB but can be increased by about 7dB. The average SINR with the interference coordination technique is still 2.5dB better than when no countermeasures are taken.

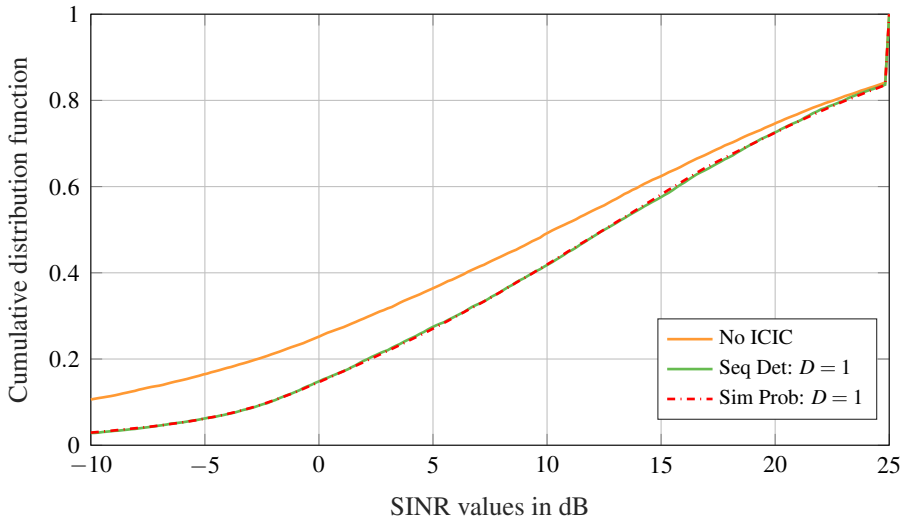

Figure 4.25: ICIC sequential deterministic, simultaneous probabilistic, and no ICIC for a high HBS density, with 21 MBS and 1008 HBS: CDF of signal-to-interference-plus-noise ratio

Figures 4.26–4.28 draw the CDF of the MS throughput for minimum HBS density with one HBS per MBS, 21 MBS in total which results in overall 21 HBS. Each figure draws a different number of subbands $D_i = D = 1,\ldots,4$.

Figure 4.26 shows the overall MS throughput for all users including MUEs and FUEs. With 10 MUE on average per MBS and 21 MBS overall, there are in total about 210 users connected to the macrocells. This is much higher than the number of users connected to the femtocells, as only 21 are present in total. In sum, there are much more macrocell users than femtocell users. This user distribution is also reflected in the overall mobile station throughput curves. The femtocells with the potential for high throughput rates mainly contribute to the best 10% of the users. The values below follow in this case the macrocell users.

The total achievable throughput increases with the number of available subbands. The kink in the curves around the 95-th percentile results from users with very good SINR which can transmit with the maximum modulation and coding scheme which limits the maximum achievable rate in this case.

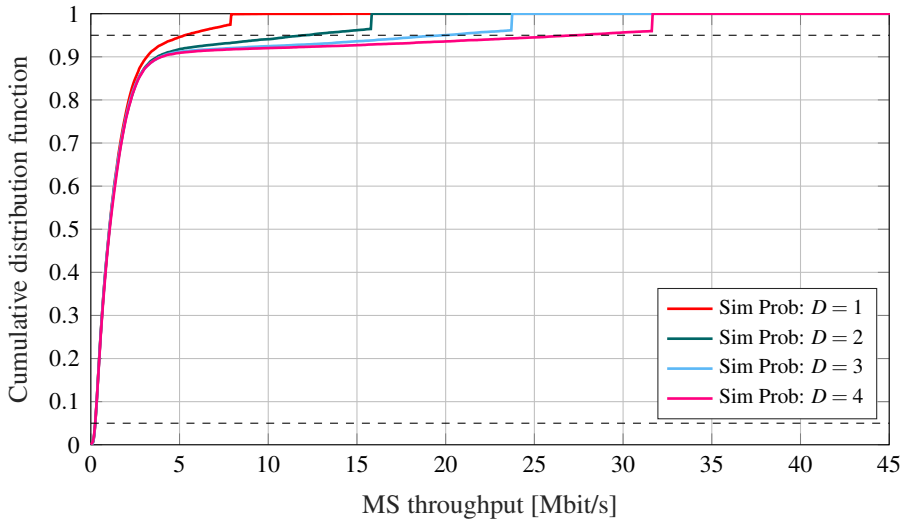

Figure 4.26: ICIC simultaneous probabilistic for a minimum HBS density, with 21 MBS and 21 HBS and increasing number of subbands D from one to four: CDF of the throughput of all mobile stations in the network

Figure 4.27 shows the MS throughput for the users connected to the femtocell. The total achievable throughput for the FUEs increases with the number of available subbands.The kink in the curves again results from users with very good SINR which can transmit with the maximum modulation and coding scheme which limits the maximum achievable rate in this case.

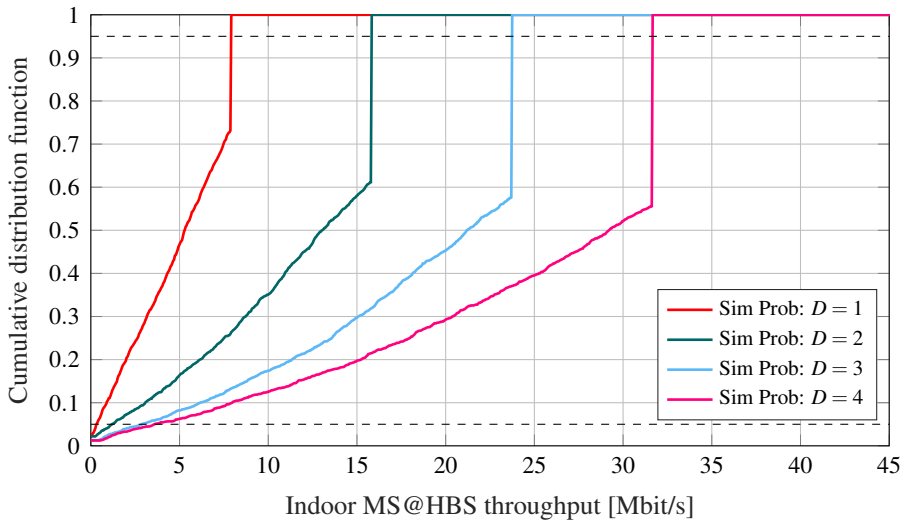

Figure 4.27: ICIC simultaneous probabilistic for a minimum HBS density, with 21 MBS and 21 HBS and increasing number of subbands D from one to four: CDF of the throughput of all mobile stations connected to a femtocell

Figure 4.28 depicts the MS throughput for indoor as well as for outdoor users connected to the macrocell. For such a low femtocell density, the total achievable throughput for the

MUEs is hardly effected. Further, it does not decrease significantly when the number of available subbands in the femtocell increases.

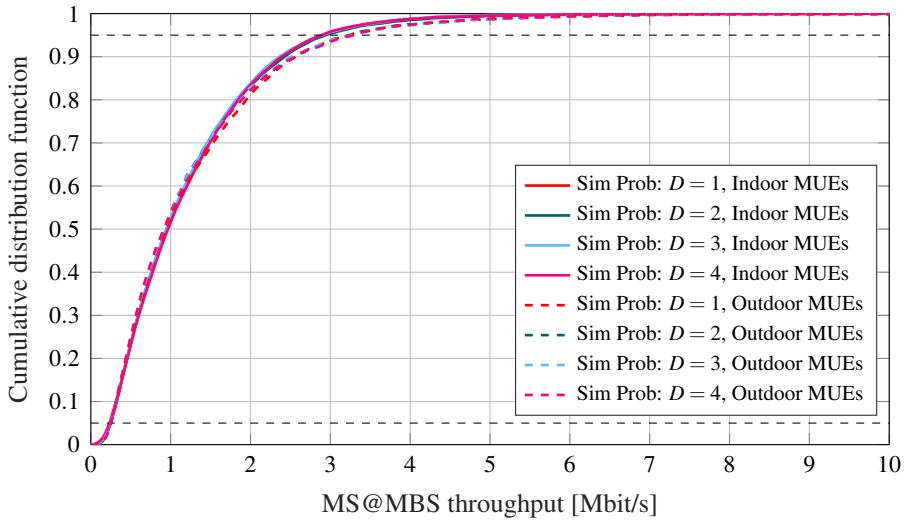

Figure 4.28: ICIC simultaneous probabilistic for a minimum HBS density, with 21 MBS and 21 HBS and increasing number of subbands D from one to four: CDF of the throughput of outdoor and indoor mobile stations connected to the MBS

Previous investigations for increasing subband sizes considered only a minimum density of femtocells. The following Figures 4.29–4.31 show a much denser deployment. In here, $D = 1,\ldots,4$ for a deployment factor of $P_{\mathrm{d}} = 0.2$ which drops in total 1008 HBS in the network are considered. As before, if not depicted differently, the lines of the curves for the sequential deterministic approach with $D = 1$ and the simultaneous probabilistic method with $D = 1$ match.

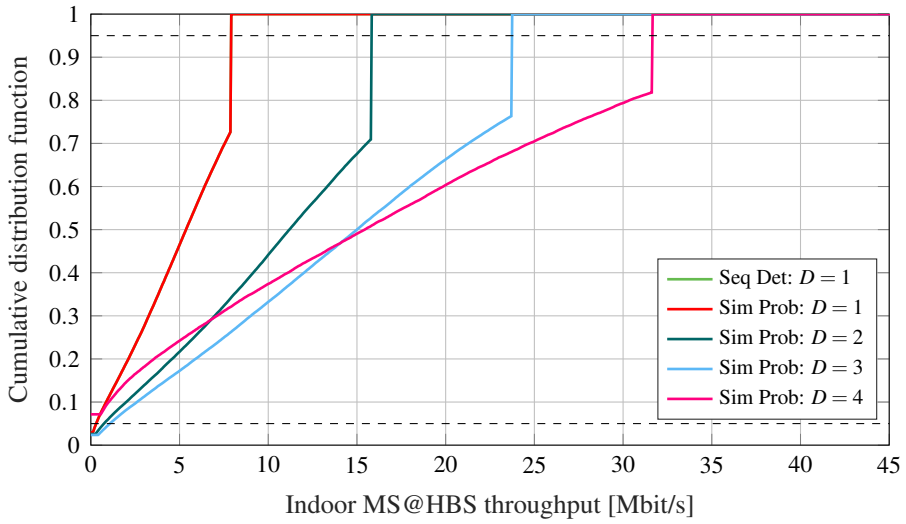

Figure 4.29: ICIC simultaneous probabilistic for a high HBS density, with 21 MBS and 1008 HBS and increasing number of subbands D from one to four: CDF of the throughput of all mobile stations connected to a femtocell

The achievable throughput of the users connnected to the femtocell increases with increasing subband sizes up to a subband size of $D = 3$. With 4 subbands used in total, the maximum achievable rate is still increased but critical interference situations cannot be solved adequately. In here, no degree of freedom to find more beneficial resources is left. Now, even 45% of the users could achieve a better rate with a subband size of three. Thus, in order to provide an overall preferential situation, the network providers should select the number of allowed subbands in the femtocells properly according to the interference situation.

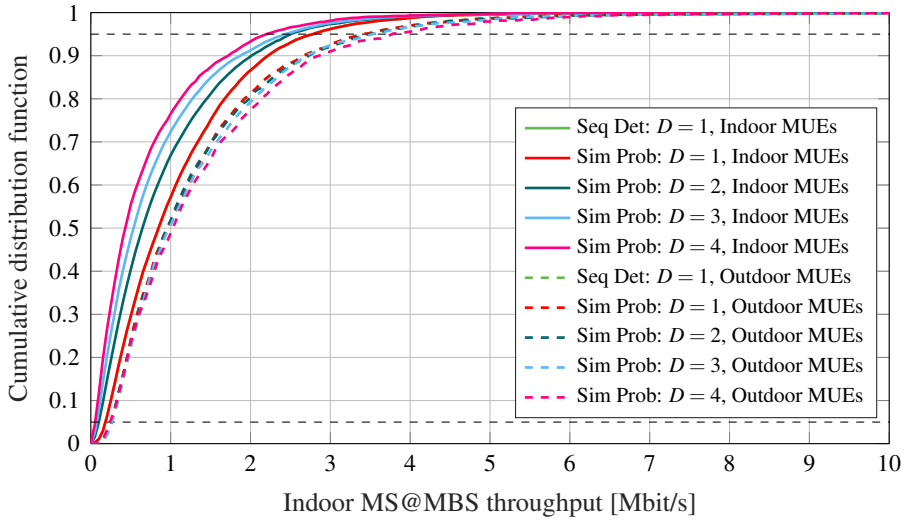

Figure 4.30: ICIC simultaneous probabilistic for a high HBS density, with 21 MBS and 1008 HBS and increasing number of subbands D from one to four: CDF of the throughput of outdoor and indoor mobile stations connected to the MBS

The throughput of the outdoor MBSs is similar for different numbers of selected subbands. Differently, when the number of subands increases, the throughput for the indoor MUEs decreases notably but still communication seems possible as all users receive a minimum throughput rate.

Figure 4.31 shows the CDF of the SINR for all scheduled user in the network.

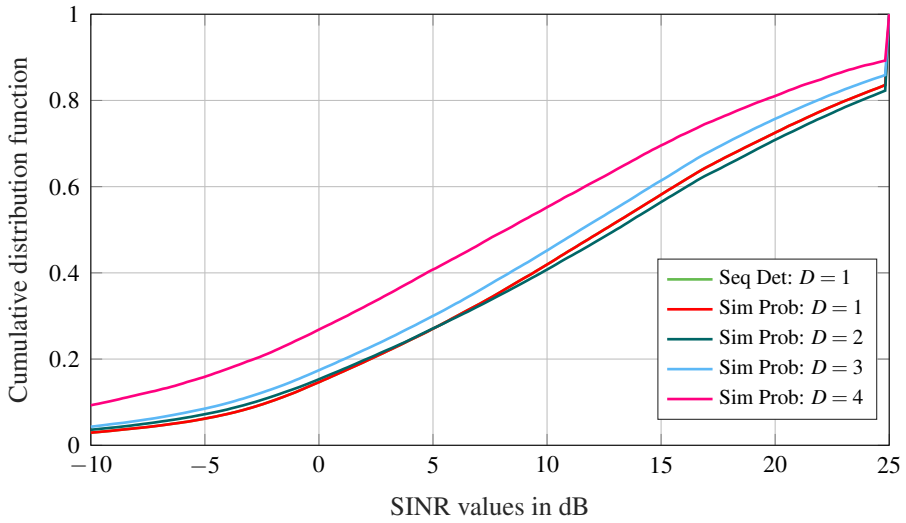

Figure 4.31: ICIC simultaneous probabilistic for a high HBS density, with 21 MBS and 1008 HBS and increasing number of subbands D from one to four: CDF of signal-to-interference-plus-noise ratio

The SINR decreases when the number of selected subbands increases. Whereas, for subbandsizes $D = 1,\ldots,3$ the SINR is within a similar range, increasing to a number of 4 subbands where no coordination of the resources between the femtocells is possible anymore but only protection of the MBSs due to the dedicated middle subband is possible. In sum, on average the reduction in SINR is increasing with the number of allowed subbands D.

4.7 Conclusion

System-level simulations show that interference coordination is mandatory for macro-femto cell coexistence. The interference situation especially for the indoor macrocell users leads to a situation with poor throughput. As these users can not be handed over to the femtocell, phone calls might be dropped and data transmission is jammed. This work develops and further enhances an interference coordination approach based on sequential deterministic and simultaneous probabilistic coordination of the available resources. The proposed ICIC algorithms are suitable for macro-femto cell deployment scenarios. When applied in the baseline form with only very limited resources, the interference impact on the macro UEs is significantly reduced which is very good, but the achievable HBS throughput is reduced by a factor of five which is bad. By allowing more than one subband per HBS the throughput for the femto UEs can be increased again to a reasonable level which provides in sum a preferential result. Overall, this makes in-home communication services attractive. The number of used subbands has to be adapted based on the interference value in order to get the trade-off between acceptable amount of interference and reuse of frequency resources.

Chapter 5

Conclusion

Small cells offer a high potential for mobile communication systems, but inter-cell interference coordination (ICIC) is essential in order to protect the macro base station (MBS) users. With the proposed ICIC method, multi-layer networks become possible and attractive. The proposed algorithm handles the interference in heterogeneous networks with macrocells and small cells. The proposed dynamic ICIC technique is applicable to different kinds of resource patterns composed of subbands, component carriers or spatial multiplexing streams among others. Within this work, the performance of the advanced ICIC method is investigated in terms of subband assignment, which results from the divisibility of an orthogonal frequency division multiple access (OFDMA) symbol in frequency domain. Therewith, in here the term resource pattern is equivalent to a group of subbands. Hence, it can easily be integrated in current and future commercial 4^{th} generation of mobile cellular networks (4G) and 5^{th} generation of mobile cellular networks (5G). Within Chapter 2, an overview on cellular communication systems is given, with the potential of small cells for remarkable improvement of the overall data rates but also their limits due to additional asymmetric and changing interference situations, which eventually disturb data transmission on the macrocell and small cell layer. Theses aspects are treated in Section 2.4 and addressed in Chapter 3 with the introduction of the advanced interference coordination techniques based on sequential deterministic and simultaneous probabilistic resource assignment within the small cells.

Different subgroups of small cells are applied each on their specific use case. Picocells can be installed in hotspots as stadiums or shopping malls, relays to supply areas without a wired backhaul and femtocells can be installed in office buildings or residential houses. All require distinct considerations of the ICIC methods with some adaptations within the implementation. In this work, the most critical aspect of closed subscriber group (CSG) femtocells is treated as a worst case scenario for quasi stationary users close to a home base station (HBS) and potentially fast users shortly moving by. These femtocells can be deployed by the end user who can connect its home base station to the backbone via the Digital Subscriber Line (DSL). They are less advanced than provider deployed huge MBSs and dedicated for the usage in buildings with limited backhaul connection and restrictions on signaling between network nodes. Dedicated spectrum, opposed to co-channel assignment,

designated to each group of cells removes interference but reduces the achievable data rates significantly, thus is not preferable as spectrum is precious. As a result, interference cannot only be addressed in the network planning phase due to dynamic and unpredictable interference situations as a consequence of ever changing deployments. The proposed algorithm is applicable to open access, where the interference situation is not that critical. Further, it can be used for the critical CSG situations, where especially the non access-granted user equipments connected to an MBS (MUEs) have to be protected. With self-configuration and self-optimization the interference scenario can be evaluated in each small cell individually and adapt to changing environments online. The small cells sense the environment on the air interface and tune the parameters accordingly. With slight modifications, the proposed algorithm can also be applied in picocell scenarios.

In Chapter 3 the dynamic ICIC technique is introduced and explained in detail. The convergence behavior of the methods is compared. The sequential deterministic method scales with the number of home base stations (HBSs) in the network, consequently the time to converge enlarges dramatically when the network increases. On the other hand the simultaneous probabilistic method converges little later for tiny scenarios but for realistic scenarios it remains nearly constant and shows a favorable behavior. It converges for medium deployment scenarios in around 20 iterations which in here corresponds to 20ms. These observations have been further illustrated in Figure 3.14 which gives the number of necessary iterations to converge as a function of the number of small cells in the network. This information is very useful in order to select the number of required iterations properly. In order to classify the performance of the proposed techniques, a global optimizer is introduced. As presented in Chapter 3 and Section 4.3 the proposed techniques provide very good results with only a small spacing on average to the benchmark and provide similar results in terms of cell edge and mean throughput as well as outage probability.

In order to clarify the necessity for countermeasures on the critical interference situations, Chapter 4 presents the system-level simulation results for the baseline setting without coordination. These demonstrate the poor performance especially of the users connected to the macrocell which are located inside a building together with a femtocell. In this baseline setting, users are even in outage and have an unacceptable throughput, which increases with the number of femtocells in the network. In order to present all users acceptable and even very good data transmission rates, new techniques have to be evolved. The techniques developed and enhanced within this thesis are promising candidates for this. The femtocells autonomously select beneficial resources due to their strategic interdependence leading to a good situation which balances the protection of the victim MUEs with the overall achievable throughput.

The proposed method is a promising candidate for cellular communication systems as it is (i) easily implementable due to its low computational complexity, (ii) requires no signaling between base stations after configuration, and (iii) can easily be extended to other heterogeneous network scenarios for example based on several component carriers as a degree of freedom. System-level simulations for reference macro and femtocell co-channel de-

ployments without interference coordination discussed in Chapter 4 show that interference coordination is mandatory for their coexistence. Further detailed simulations confirm that the proposed interference coordination algorithms are suitable for macro-femto cell deployment scenarios. The interference impact on the UEs is significantly reduced with reasonable throughput level of FUEs, which makes in-home communication services attractive.

Future work: With the introduced network interference factor one can dynamically increase or decrease the amount of utilizable subbands within each HBS depending on the currently present interference situation. Within further investigations, an optimized suitable factor for a flexible deployment can be determined. Cells experiencing low interference and therefore reciprocally also sparsely introducing interference to the surrounding can harness more subbands for transmission compared to cells with high interference levels. Further, the introduction of an exclusive subband can be renounced in the following cases. (i) If a mechanism is used which scans the surrounding of the cell and no victim UE is detected, or (ii) if a hybrid access mode is used which grants access to UEs not on the closed subscriber group list. Simulation of open access, in which case simulations without protected area are possible, can be pursued. In the situation of open access scenarios the interference is not as critical as in situations where some users are completely excluded from using a certain small cell. Additionally, the speed of the MSs could be taken into account for the handover process from MBS to HBS, HBS to HBS, and HBS to MBS. Future systems may self-organize the interference coordination based on a previously trained neural network (using computer generated data) and reinforce learning on the fly to tune the presented parameters.

Appendix A

System Level Simulator

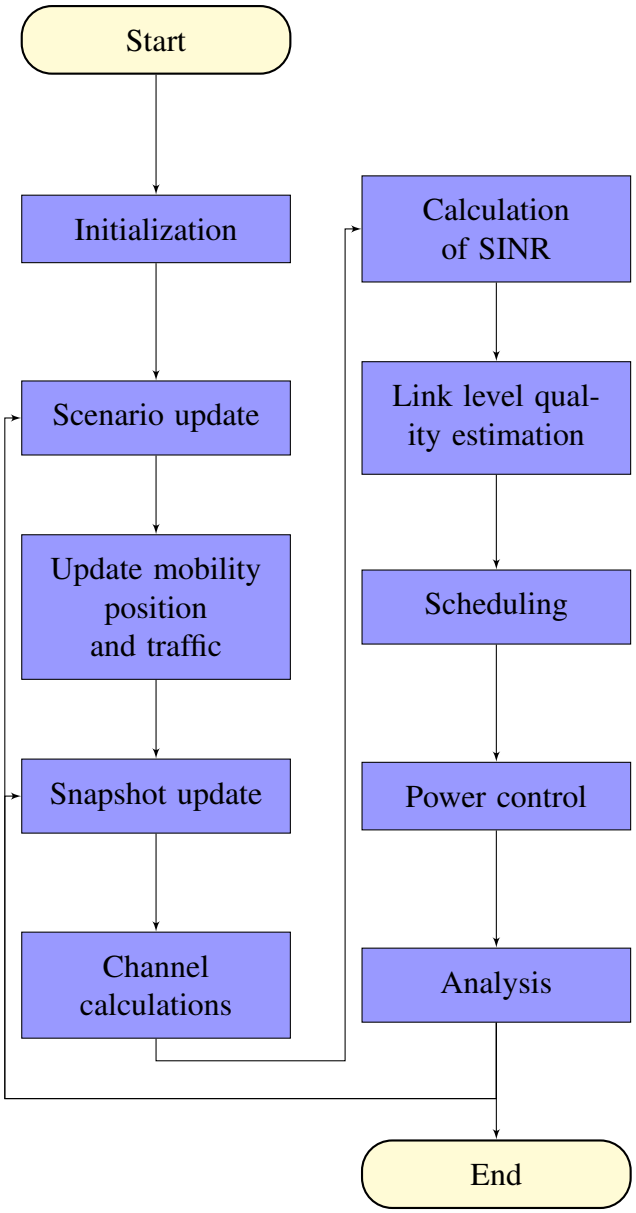

Figure A.1: Schematic flow diagram on individual steps within the system-level simulator

A.1 Placement of Local Base Stations and Mobile Stations

A.1.1 Femtocell

Figure A.2 shows the extract of one floor for the femtocell block model in detail according to [74]. The apartments are separated by indoor walls introducing a propagation loss factor of L_{iw} of 5dB, whereas for indoor/outdoor communication the signal penetrating the outdoor wall (indicated with thicker black line) experiences more attenuation L_{ow} of 20dB.

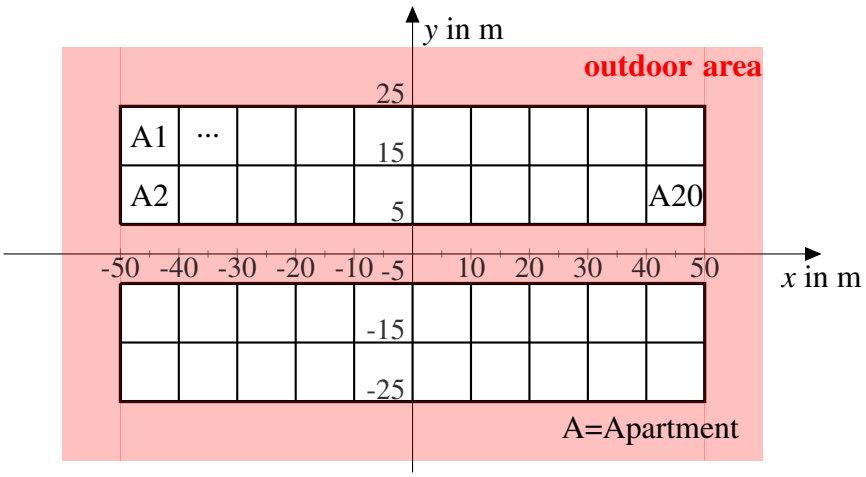

Figure A.2: Modeling of femtocell deployment exemplary for one floor

Figure A.3 shows an exemplary side view of the femtocell block for six floors and 10 apartments per row. Overall the horizontal, vertical, and elevation of each device and base station is taken into consideration.

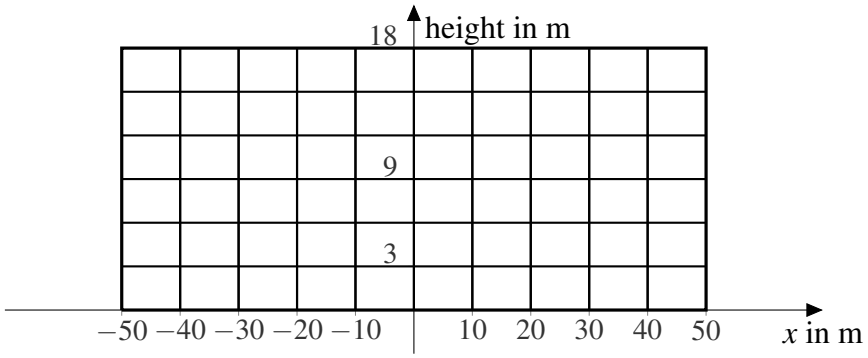

Figure A.3: Lateral view of femtocell block

$\mathbf{p}_{\text{fb}}$ denotes the points in x- and y-direction to define the dimensions of the femtocell block and each femtocell location in it. The ratio of apartments deployed with an active femtocell per macrocell can be set. The position and orientation of the femtocell block is randomly set over the macrocell area. The position is determined by the reference point parallel translated

to the random absolute position and the orientation is given by the rotation of the building by angle α which transform the dimensions of the building using the rotation matrix. Is the transformation from $\mathbb{R}^2$ to $\mathbb{R}^2$ the rotation of a plane by angle α [77], the following holds: $\mathbf{A}$ is a rotation matrix is equivalent to $\mathbf{A}$ is of Cartesian basis and its determinant $\det(\mathbf{A}) = 1$ and equivalent to

$$\mathbf{A} = \begin{pmatrix} \cos(\alpha) & -\sin(\alpha) \\ \sin(\alpha) & \cos(\alpha) \end{pmatrix}. \tag{A.1}$$

As a result, the femtocell block building positions $\mathbf{p}$ compute to a combination of translation and rotation [78]:

$$\mathbf{p} = \mathbf{A}\mathbf{p}_{\text{fb}} + \mathbf{t} \tag{A.2}$$

With translation vector $\mathbf{t} = \begin{pmatrix} t_x & t_y \end{pmatrix}^T$. The femtocell block buildings are set randomly in each macrocell and are completely located within the service area which is built by the sum of all macrocells.

A.1.2 Mobile Station

The mobile stations located outdoor connected to a MBS are randomly placed over its service area but not indoor, whereas the indoor mobile stations are randomly dropped inside the corresponding femtocell block over all apartments and floors. Contary the indoor user of a HBS are bound to the apartment of their serving femtocell. An optional downlink receiver is located at the same position as the HBS. Independent from these locations, the user of a femtocell determines its position randomly inside the respective apartment.

A.2 Path Loss Models for Home Base Station Scenarios

The path loss (PL) L_{p} describes the loss in power from a transmit node to a receive node, between two network nodes. The PL function depends on the distance of transmit and receive node d and on the number and consistency of penetrated walls. In the following, distances are used in meters. Depending on the position of the transmit and receive node, it can be modeled for urban deployments according to the 3GPP standard [79] as follows [80], [81]:

MBS to UE

UE outside and BS outdoors:

$$L_{\text{p}}\Big|_{\text{dB}} = 15.3 + 37.6\log\left(\frac{d}{\text{m}}\right)\text{[dB]} \tag{A.3}$$

UE inside an apartment and BS outdoors:

$$L_{\text{p}}\Big|_{\text{dB}} = 15.3 + 37.6\log\left(\frac{d}{\text{m}}\right) + L_{\text{ow}}\,\text{[dB]} \tag{A.4}$$

HBS to UE

UE inside the same building with considered HBS:

$$L_{\mathrm{p}}\Big|_{\mathrm{dB}} = 38.46 + 20\log\left(\frac{d}{\mathrm{m}}\right) + 0.7\left(\frac{d_{\mathrm{i}}}{\mathrm{m}}\right) + 18.3 n_{\mathrm{f}}^{\left(\frac{n_{\mathrm{f}}+2}{n_{\mathrm{f}}+1} - 0.46\right)} + qL_{\mathrm{iw}}\,[\mathrm{dB}] \quad \text{(A.5)}$$

UE outside the building:

$$L_{\mathrm{p}}\Big|_{\mathrm{dB}} = \max\left[\left(15.3 + 37.6\log\left(\frac{d}{\mathrm{m}}\right)\right), \left(38.46 + 20\log\left(\frac{d}{\mathrm{m}}\right)\right)\right] + 0.7\left(\frac{d_{\mathrm{i}}}{\mathrm{m}}\right) + 18.3 n_{\mathrm{f}}^{\left(\frac{n_{\mathrm{f}}+2}{n_{\mathrm{f}}+1} - 0.46\right)} + qL_{\mathrm{iw}} + L_{\mathrm{ow}}\,[\mathrm{dB}] \quad \text{(A.6)}$$

UE inside another building:

$$L_{\mathrm{p}}\Big|_{\mathrm{dB}} = \max\left[\left(15.3 + 37.6\log\left(\frac{d}{\mathrm{m}}\right)\right), \left(38.46 + 20\log\left(\frac{d}{\mathrm{m}}\right)\right)\right] + 0.7\left(\frac{d_{\mathrm{i}}}{\mathrm{m}}\right) + 18.3 n_{\mathrm{f}}^{\left(\frac{n_{\mathrm{f}}+2}{n_{\mathrm{f}}+1} - 0.46\right)} + qL_{\mathrm{iw}} + 2L_{\mathrm{ow}}\,[\mathrm{dB}] \quad \text{(A.7)}$$

With the number of penetrated indoor walls q and n_{f} as the number of penetrated floors. d_{i} describes the indoor part of the distance between transmitter and receiver in meter. The penetration loss factor of an outer and indoor wall is denoted by L_{ow} and L_{iw}, respectively. To take care of the penetration loss inside an apartment the term $0.7 d_{\mathrm{i}}$ is introduced.

A.3 Throughput Calculation

The attenuated and truncated Shannon bound is used in the system-level simulator [82] with Shannon bound $S(\gamma) = \mathrm{ld}(1+\gamma\big|_{\mathrm{lin}}) = \mathrm{ld}(1+10^{\frac{\gamma|_{\mathrm{dB}}}{10}})$ in $\frac{\mathrm{bit/s}}{\mathrm{Hz}}$. For DL transmission the throughput per Hertz computes to:

$$\Upsilon'\left[\frac{\mathrm{bit/s}}{\mathrm{Hz}}\right] = \begin{cases} 0 & \text{for } \gamma < \gamma_{\min} = -10\mathrm{dB} \\ \alpha S(\gamma) & \text{for } \gamma_{\min} < \gamma < \gamma_{\max} = 23\mathrm{dB} \\ \Upsilon'_{\max} = 4.4\frac{\mathrm{bit/s}}{\mathrm{Hz}} & \text{for } \gamma > \gamma_{\max} = 23\mathrm{dB} \end{cases} \quad \text{(A.8)}$$

For $\gamma < \gamma_{\min} = -10\mathrm{dB}$ no reliable transmission is possible, and therefore zero throughput is present. α denotes the attenuation factor to account for implementation losses. The maximum $\Upsilon'_{\max} = 4.4\frac{\mathrm{bit/s}}{\mathrm{Hz}}$ is the limit due to the maximum MCS, whereas no further improvement

is possible even for higher SINR. The amount of data transmitted per RB computes as the product from throughput, bandwidth B_{RB} per RB, and time of a slot $T_{\mathrm{slot}} = 0.5\mathrm{ms}$. The overall throughput of a user computes from the product of data transmitted per resource block and the number of assigned RBs.

Bibliography

[1] Cisco, "Whitepaper: Cisco visual networking index: Global mobile data traffic forecast update 2016–2021," Cisco, Tech. Rep., 2017. [Online]. Available: http://www.cisco.com

[2] IDC, "Prepare for billions: The IoT 2020 IT infrastructure readiness indicator," International Data Corporation sponsored by Hewlett Packard, Tech. Rep., 2017.

[3] O. A. Sianaki, A. Yousefi, A. R. Tabesh, and M. Mahdavi, "Internet of everything and machine learning applications: Issues and challenges," in *32nd International Conference on Advanced Information Networking and Applications Workshops (WAINA)*, May 2018, pp. 704–708.

[4] A. Goldsmith, *Wireless Communications*. Cambridge University Press, 2005.

[5] C. Cox, *An introduction to LTE: LTE, LTE-Advanced, SAE, VoLTE and 4G mobile communications*, 2nd ed. Chichester: Wiley-VCH, 2014. [Online]. Available: https://onlinelibrary.wiley.com/doi/book/10.1002/9781118818046

[6] C. Gessner, A. Roessler, and M. Kottkamp, "White paper: UMTS long term evolution (LTE) - technology introduction," Rohde & Schwarz, Tech. Rep., 2012.

[7] *3GPP TR 25.892 V6.0.0 Feasibility Study for Orthogonal Frequency Division Multiplexing (OFDM) for UTRAN enhancement (Release 6)*, Technical Report, 3GPP Std., 2004.

[8] H. T. Friis, "A note on a simple transmission formula," *Proceedings of the IRE*, vol. 34, no. 5, pp. 254–256, May 1946.

[9] COST231, "Digital mobile radio: COST 231 view on the evolution towards 3rd generation systems," 1999.

[10] *3GPP TR 25.996 V15.0.0 Technical specification group radio access network; Spatial channel model for multiple input multiple output (MIMO) simulations (Release 15)*, Technical Report, 3GPP Std., 2018.

[11] M. Sauter, *Grundkurs Mobile Kommunikationssysteme: LTE-Advanced, UMTS, HSPA, GSM, GPRS, Wireless LAN und Bluetooth*, 6th ed. Wiesbaden: Springer

Vieweg, 2015. [Online]. Available: http://nbn-resolving.de/urn/resolver.pl?urn=10.1007/978-3-658-08342-7

[12] M. Sauter, Ed., *Grundkurs Mobile Kommunikationssysteme: LTE-Advanced Pro, UMTS, HSPA, GSM, GPRS, Wireless LAN und Bluetooth*, 7th ed., ser. SpringerLink : Bücher. Wiesbaden: Springer Vieweg, 2018. [Online]. Available: http://dx.doi.org/10.1007/978-3-658-21647-4

[13] A. Meylan, "3GPP TSG-RAN WG2 LTE radio layer 2, RRC and LTE radio layer 2, RRC and radio access network architecture," 2009. [Online]. Available: ftp://www.3gpp.org/Information/presentations/presentations_2010/2010_06_India/3GPP%20LTE%20Radio%20layer%202.pdf

[14] 3rd Generation Partnership Project, *3GPP TS 36.401 V15.0.0 Technical Specification Group Radio Access Network; Evolved Universal Terrestrial Radio Access Network; (E-UTRAN); Architecture description (Release 15)*, Technical Specification, 3GPP Std., 2017.

[15] E. Gutt, *LTE Long Term Evolution - Neue Dimension mobiler Breitbandnutzung - Eine technische Einführung*. LTEmobile, 2010. [Online]. Available: http://www.ltemobile.de

[16] *3GPP TR 36.133 V15.4.0 Evolved Universal Terrestrial Radio Access (E-UTRA); Requirements for support of radio resource management*, Technical Report, 3GPP Std., 2018.

[17] *3GPP TR 36.211 V15.2.0 Technical Specification Group Radio Access Network; Evolved Universal Terrestrial Radio Access (E-UTRA); Physical channels and modulation (Release 15)*, Technical Report, 3GPP Std., 2018.

[18] S. Parkvall, E. Dahlman, A. Furuskar, and M. Frenne, "NR: The new 5G radio access technology," *IEEE Communications Standards Magazine*, vol. 1, no. 4, pp. 24–30, Dec 2017.

[19] ETSI, *3GPP TS 38.212 V15.2.0 Technical Specification 5G; NR; Multiplexing and channel coding (Release 15)*, Technical Report, 3GPP Std., 2018.

[20] O. Iscan, D. Lentner, and W. Xu, "A comparison of channel coding schemes for 5G short message transmission," in *IEEE Globecom Workshops (GC Wkshps)*, Dec 2016, pp. 1–6.

[21] E. Telatar, "Capacity of multi-antenna gaussian channels," *European Transactions on Telecommunications*, vol. 10, no. 6, pp. 585–595, 1999. [Online]. Available: https://onlinelibrary.wiley.com/doi/abs/10.1002/ett.4460100604

[22] G. J. Foschini, "Layered space-time architecture for wireless communication in a fading environment when using multi-element antennas," *Bell Labs Technical Journal*, vol. 1, no. 2, pp. 41–59, Autumn 1996.

[23] J. Speidel, *Introduction to Digital Communications*, ser. Signals and Communication Technology. Springer International Publishing, 2019. [Online]. Available: https://doi.org/10.1007/978-3-030-00548-1

[24] E. Björnson, J. Hoydis, and L. Sanguinetti, "Massive MIMO networks: Spectral, energy, and hardware efficiency," *Foundations and Trends® in Signal Processing*, vol. 11, no. 3-4, pp. 154–655, 2017. [Online]. Available: http://dx.doi.org/10.1561/2000000093

[25] ——, "Massive MIMO has unlimited capacity," *IEEE Transactions on Wireless Communications*, vol. 17, no. 1, pp. 574–590, Jan 2018.

[26] S. Sesia, I. Toufik, and M. Baker, Eds., *LTE - The UMTS Long Term Evolution: From Theory to Practice*, 2nd ed. John Wiley & Sons, 2009.

[27] P. Frank, "Advanced transmission schemes for the 4th generation of mobile communication systems," Ph.D. dissertation, University of Stuttgart, Institute of Telecommunications, July 2011.

[28] W. Ajib and D. Haccoun, "An overview of scheduling algorithms in MIMO-based fourth-generation wireless systems," *IEEE Network*, vol. 19, no. 5, pp. 43–48, Sept 2005.

[29] A. Meylan, "LTE radio layer 2, RRC and radio access network radio access network architecture," Huawei, 2010. [Online]. Available: ftp://www.3gpp.org/Information/presentations/presentations_2010/2010_06_India/3GPP%20LTE%20Radio%20layer%202.pdf

[30] Alcatel-Lucent, "3GPP TSG-RAN1 LTE R1-071967, DL E-UTRA performance checkpoint," 2007.

[31] A. Durán, M. Toril, F. Ruiz, and A. Mendo, "Self-optimization algorithm for outer loop link adaptation in LTE," *IEEE Communications Letters*, vol. 19, no. 11, pp. 2005–2008, Nov 2015.

[32] Z. Hanzaz and H. D. Schotten, "Performance evaluation of link to system interface for long term evolution system," in *I7th International Wireless Communications and Mobile Computing Conference*, July 2011, pp. 2168–2173.

[33] F. L. Aguilar, G. R. Cidre, J. M. L. López, and J. R. Paris, "Mutual information effective SNR mapping algorithm for fast link adaptation model in 802.16e," in *Mobile Lightweight Wireless Systems*, P. Chatzimisios, C. Verikoukis, I. Santamaría, M. Laddomada, and O. Hoffmann, Eds. Berlin, Heidelberg:

Springer Berlin Heidelberg, 2010, pp. 356–367. [Online]. Available: https://link.springer.com/chapter/10.1007/978-3-642-16644-0_31#citeas

[34] S. ten Brink, "Communications," Institute of Telecommunications Lecture at the University of Stuttgart, 2018.

[35] J. Speidel, H. Droste, and P. Frank, "LTE-Advanced: Key Technologies for LTE-Advanced," Technology Radar Edition III/2010, Feature Paper Next Generation Mobile Networks, (R)evolution in Mobile Communications, 2010.

[36] J. Wannstrom. Carrier aggregation explained. 2013. [Online]. Available: http://www.3gpp.org/technologies/keywords-acronyms/101-carrier-aggregation-explained

[37] J. G. Andrews, "Seven ways that HetNets are a cellular paradigm shift," *IEEE Communications Magazine*, vol. 51, no. 3, pp. 136–144, March 2013.

[38] J. Wannstrom and K. Mallinson, "HetNet/Small Cells," Last visited: Dec 2018. [Online]. Available: http://www.3gpp.org/hetnet

[39] "ABI research anticipates in-building mobile data traffic to grow by more than 600% by 2020," 2016. [Online]. Available: https://www.abiresearch.com/press/abi-research-anticipates-building-mobile-data-traf/

[40] J. Belschner and Z. Bleicher, "Methods for interference coordination in LTE networks," in *ITG 5.2.4*, 2010.

[41] I. Shgluof, M. Ismail, and R. Nordin, "Efficient femtocell deployment under macrocell coverage in LTE-Advanced system," in *International Conference on Computing, Management and Telecommunications (ComManTel)*, Jan 2013, pp. 60–65.

[42] D. Lopez-Perez, I. Guvenc, G. de la Roche, M. Kountouris, T. Quek, and J. Zhang, "Enhanced intercell interference coordination challenges in heterogeneous networks," *IEEE Wireless Communications*, vol. 18, no. 3, pp. 22–30, June 2011.

[43] A. Yahya, *LTE-A Cellular Networks: Multi-hop Relay for Coverage, Capacity and Performance Enhancement*. Cham: Springer, 2017. [Online]. Available: http://dx.doi.org/10.1007/978-3-319-43304-2

[44] M. Iwamura, H. Takahashi, and S. Nagata, "Relay technology in LTE-Advanced," NTT DOCOMO Technical Journal Vol. 12 No. 2, Tech. Rep., 2010.

[45] A. Müller, "Analysis and optimization of wireless communication systems with regenerative relaying," Ph.D. dissertation, University of Stuttgart, Institute of Telecommunications, July 2011.

[46] S. Parkvall, A. Furuskär, and E. Dahlman, "Next generation LTE, LTE -Advanced," *Ericsson review*, 2010.

[47] D. Liu, L. Wang, Y. Chen, M. Elkashlan, K. K. Wong, R. Schober, and L. Hanzo, "User association in 5G networks: A survey and an outlook," *IEEE Communications Surveys & Tutorials*, vol. 18, no. 2, pp. 1018–1044, Second quarter 2016.

[48] T. Küstner, "Interferenzkoordination in heterogenen Mobilfunknetzen mit Picozellen," Studienarbeit, University of Stuttgart, 2011.

[49] D. Lopez-Perez, A. Valcarce, G. de la Roche, and J. Zhang, "OFDMA femtocells: A roadmap on interference avoidance," *IEEE Communications Magazine*, vol. 47, no. 9, pp. 41–48, September 2009.

[50] X. Chu, D. López-Pérez, Y. Yang, and F. Gunnarsson, *Heterogeneous Cellular Networks: Theory, Simulation and Deployment*. Cambridge University Press, 2013. [Online]. Available: https://doi.org/10.1017/CBO9781139149709

[51] J. G. Andrews, W. Choi, and R. W. Heath JR., "Overcoming interference in spatial multiplexing MIMO cellular networks," *IEEE Wireless Communications*, vol. 14, no. 6, pp. 95–104, December 2007.

[52] J. Heyman, "Intercell interference management in an OFDM-based downlink," Ph.D. dissertation, Linköping University, Department of Electrical Engineering, July 2006.

[53] A. Lodhi, A. Awad, T. Jeffries, and P. Nahi, "On re-use partitioning in LTE-FDD systems," in *IEEE 20th International Symposium on Personal, Indoor and Mobile Radio Communications*, Sept 2009, pp. 910–913.

[54] S. G. Kim, K. Cho, D. Yoon, Y.-J. Ko, and J. K. Kwon, "Performance analysis of downlink inter cell interference coordination in the LTE-Advanced system," in *ICDT Fourth International Conference on Digital Telecommunications*, July 2009, pp. 30–33.

[55] Y. S. Cho, J. Kim, W. Y. Yang, and C.-G. Kang., *MIMO-OFDM Wireless Communications with MATLAB*. Wiley, 2010.

[56] K. T. Kim and S. K. Oh, "An incremental frequency reuse scheme for an OFDMA cellular system and its performance," in *IEEE Vehicular Technology Conference Spring*, May 2008, pp. 1504–1508.

[57] S. W. Halpern, "Reuse partitioning in cellular systems," in *33rd IEEE Vehicular Technology Conference*, vol. 33, May 1983, pp. 322–327.

[58] S. Hämäläinen, H. Sanneck, and C. Sartori, *LTE Self-Organizing Networks (SON): Network Management Automation for Operational Efficiency*. Wiley, 2012. [Online]. Available: https://onlinelibrary.wiley.com/doi/book/10.1002/9781119961789

[59] ETSI, *3GPP TR 36.922 V13.0.0 Technical Report LTE Evolved Universal Terrestrial Radio Access (E-UTRA), TDD Home eNode B (HeNB) Radio Frequency (RF) requirements analysis (Release 13)*, Technical Report, 3GPP Std., 2016.

[60] S. P. Yeh, S. Talwar, G. Wu, N. Himayat, and K. Johnsson, "Capacity and coverage enhancement in heterogeneous networks," *IEEE Wireless Communications*, vol. 18, no. 3, pp. 32–38, June 2011.

[61] Y. Bai, J. Zhou, L. Liu, L. Chen, and H. Otsuka, "Resource coordination and interference mitigation between macrocell and femtocell," in *IEEE 20th International Symposium on Personal, Indoor and Mobile Radio Communications*, Sept 2009, pp. 1401–1405.

[62] O. Ramos-Cantor, J. Belschner, and M. Pesavento, "A cooperative power control scheme for interference management in LTE-Advanced based cognitive radio networks," in *6th International Symposium on Communications, Control and Signal Processing (ISCCSP)*, May 2014, pp. 530–533.

[63] S. U. Abdullahi, J. Liu, C. Huang, and X. Zhang, "Enhancing throughput performance in LTE-Advanced HetNets with buffered fractional frequency reuse," in *Eighth International Conference on Ubiquitous and Future Networks (ICUFN)*, July 2016, pp. 918–923.

[64] D. Hwang, S. Hong, C.-Y. Oh, and T.-J. Lee, "Resource allocation based on channel sensing and spatial spectrum reuse for cognitive femtocells," *Wireless Personal Communications*, vol. 97, no. 2, pp. 2249–2268, Nov 2017. [Online]. Available: https://doi.org/10.1007/s11277-017-4606-4

[65] M. I. Kamel and K. M. F. Elsayed, "ABSF offsetting and optimal resource partitioning for eICIC in LTE-Advanced: Proposal and analysis using a nash bargaining approach," in *2013 IEEE International Conference on Communications (ICC)*, June 2013, pp. 6240–6244.

[66] A. Paradisi, M. D. Yacoub, F. L. Figueiredo, and T. R. Tronco, *Long Term Evolution: 4G and Beyond*, 1st ed., A. Paradisi, M. D. Yacoub, F. L. Figueiredo, and T. R. Tronco, Eds. Cham: Springer, 2016. [Online]. Available: http://dx.doi.org/10.1007/978-3-319-23823-4

[67] M. Rosenberger, Z. Bleicher, P. Arnold, and J. Belschner, "Verfahren und Einrichtung zur Zuweisung von Funkressourcen in einem heterogenen Mobilfunknetz," German Patent 12 159 839.5, March 16, 2012.

[68] J. Ellenbeck, H. Al-Shatri, and C. Hartmann, "Performance of decentralized interference coordination in the LTE uplink," in *IEEE 70th Vehicular Technology Conference Fall*, 2009, pp. 1–5.

[69] J. Ellenbeck, C. Hartmann, and L. Berlemann, "Decentralized inter-cell interference coordination by autonomous spectral reuse decisions," in *14th European Wireless Conference*, June 2008, pp. 1–7.

[70] A. G. Alexiou, D. Bilios, and C. Bouras, "Power efficient group communication in small cell networks," in *International Conference on Selected Topics in Mobile and Wireless Networking, MoWNet 2014, Rome, Italy, September 8-9*, 2014, pp. 17–25.

[71] A. Waheed Ahmad, H. Yang, G. Shahzad, and C. Lee, "Macrocells-user protected interference-aware transmit power control for lte-a heterogeneous networks," *Mobile Information Systems*, vol. 2016, pp. 1–12, 05 2016.

[72] J. Zheng, Y. Wu, N. Zhang, H. Zhou, Y. Cai, and X. Shen, "Optimal power control in ultra-dense small cell networks: A game-theoretic approach," *IEEE Transactions on Wireless Communications*, vol. 16, no. 7, pp. 4139–4150, July 2017.

[73] *3GPP TS 25.814 V7.1.0 Physical layer aspects for evolved Universal Terrestrial Radio Access (UTRA) (Release 7)*, Technical Specification, 3GPP Std., 2006.

[74] 3GPP R4-092042, "Simulation assumptions and parameters for FDD HeNB RF requirements," San Francisco, May 2009.

[75] M. Simsek, T. Akbudak, B. Zhao, and A. Czylwik, "An LTE-femtocell dynamic system level simulator," in *International ITG Workshop on Smart Antennas (WSA)*, Feb 2010, pp. 66–71.

[76] F. Capozzi, G. Piro, L. A. Grieco, G. Boggia, and P. Camarda, "On accurate simulations of LTE femtocells using an open source simulator," *EURASIP Journal on Wireless Communications and Networking*, vol. 2012, no. 1, p. 328, Oct 2012. [Online]. Available: https://doi.org/10.1186/1687-1499-2012-328

[77] G. Merziger and T. Wirth, *Repetitorium der höheren Mathematik*, 6th ed. Barsinghausen: Binomi-Verl., 2010, uB Vaihingen.

[78] I. N. Bronštejn, K. A. Semendjaev, G. Musiol, and H. Mühlig, *Taschenbuch der Mathematik*, 10th ed. Haan-Gruiten: Verlag Europa-Lehrmittel Nourney, Vollmer GmbH & Co. KG, 2016. [Online]. Available: http://d-nb.info/1081907711/04

[79] *3GPP TR 36.814 V9.2.0 Evolved Universal Terrestrial Radio Access (E-UTRA); Further Advancements for E-UTRA Physical Layer Aspects (Release 9)*, Technical Report, 3GPP Std., 2017.

[80] M. Shalaby, M. Shokair, and N. W. Messiha, "System design and performance analysis of LTE cognitive femtocells," *Wireless Personal Communications*, vol. 85, no. 4, pp. 2463–2483, Dec 2015. [Online]. Available: https://doi.org/10.1007/s11277-015-2915-z

[81] R. A. Saeed, R. A. Saeed, B. S. Chaudhari, and R. A. Mokhtar, *Femtocell Communications and Technologies: Business Opportunities and Deployment Challenges*, 1st ed. Hershey, PA, USA: IGI Global, 2012.

[82] *3GPP TR 36.942 (V14.0.0) Evolved Universal Terrestrial Radio Access (E-UTRA); Radio Frequency (RF) system scenarios (Release 14)*, Technical Report, 3GPP Std., 2017.